THESIS FOR THE DEGREE OF DOCTOR OF PHILOSOPHY (Ph.D.)

Role of poly(ADP-ribose) polymerase-1 (PARP-1) in the regulation of transcription

by

Attila Brunyánszki

Supervisor: Dr. Péter Bai

UNIVERSITY OF DEBRECEN
DOCTORAL SCHOOL OF MOLECULAR MEDICINE

DEBRECEN, 2011

1. Table of Contents

2. Abbreviations

3-AB	3-amino-benzamide
8-OHdG	8-oxo-2'-deoxyguanosine
ACC	acetyl-CoA carboxylase
ACO	acyl-CoA oxidase
AP-1	activator protein-1
ARH3	ADP-ribosyl hydrolase-3
ATF-2	activating transcription factor
ATP5g1	ATP synthase lipid-binding protein
BAT	brown adipose tissue
BCL6	B-cell lymphoma 6 protein
B-Myb	Myb-related protein B
BRCT	breast cancer associated protein C-terminus
CHS	contact hypersensitivity reaction
COX17	cytochrome c oxidase or Complex IV
CPT1	carnitine palmitoyltransferase I
CXCL1	chemokine (CXC motif) ligand 1 (CXCL1)
Cyt C	cytochrome c
DAPI	4,6-diamidino-2-phenylindole
Dio	iodothyronine deiodinase
DTT	dithiothreitol
eNOS	endothelial nitric oxide synthase
ERR	estrogen-related receptor
E-selectin	endothelial selectin
FOXO	forkhead box O
G6Pase	glucose-6-phosphatase
GK	glucokinase
HEPES	4-(2-hydroxyethyl)-1-piperazineethanesulfonic acid
HNE	trans-4-hydroxy-2-nonenal
I-CAM	intercellular cell adhesion molecule
IL-1β	interleukin-1β
iNOS	inducible nitric oxide synthase

L-CAM	leukocyte cell adhesion molecule
MCAD	medium chain acetyl-CoA dehydrogenase
MCP-1	monocyte chemotactic protein-1
MEF	mouse embryonic fibroblast
MHC	myosine heavy chain
MIP	macrophage inflammatory protein
MKK	mitogen-activated protein kinase kinase
MMP	matrix metalloproteinase
MOPS	3-(N-morpholino) propanesulfonic acid
MPO	myeloperoxidase
NFAT	Nuclear factor of activated T-cells
NF-κB	nuclear factor kappa light-chain-enhancer of activated B cells
NOS	NO synthase
Oct-1	organic cation transporter member 1
OXA	oxazolone
PAR	poly(ADP-ribose)
PARP	poly(ADP-ribose) polymerase
PBS	phosphate buffered saline
PEPCK	phosphoenol pyruvate carboxykinase
PGC-1α	PPAR gamma coactivator 1-α
RNS	reactive nitrogen species
ROS	reactive oxygen species
Sp1	stimulating protein-1
SIRT	sirtuin
TFF-1	Trefoil factor 1
TIMP	tissue inhibitor of metalloproteinases
TNFα	tumor necrosis factor α
Trop	troponin
UCP	uncoupling protein
V-CAM	vascular cell adhesion molecule

3. Introduction

3.1. Enzymatic properties of poly(ADP-ribose) polymerase-1

Poly(ADP-ribose) polymerase-1 (PARP-1) belongs to the poly(ADP-ribose) polymerase (PARP) superfamily. This superfamily consists of 17 members sharing a similar catalytic domain (Ame *et al.*, 2004). PARP-1, the founding member of the superfamily, is a multidomain protein comprising a DNA binding domain at the N-terminus, an automodification domain, functioning as a target for direct covalent auto-modification (D'Amours *et al.*, 1999) and a catalytic domain at the carboxyl terminus that polymerizes ADP-ribose units (Fig. 1). The first two zinc finger motifs at the N-terminus facilitate tight binding of PARP-1 to DNA that promotes the activation of the catalytic domain at the C-terminus. The third zinc finger also plays an important role in the inter-domain interactions and is vital for PARP-1 enzymatic action (Langelier *et al.*, 2008). The automodification domain contains a BRCT motif that is involved in protein-protein interactions, which promote the recruitment of DNA repair enzymes to the site of DNA damage (El-Khamisy *et al.*, 2003; Masson *et al.*, 1998). The catalytic domain contains the NAD^+ acceptor sites and critical residues involved in the initiation, elongation and branching of poly(ADP-ribose) polymers (PAR).

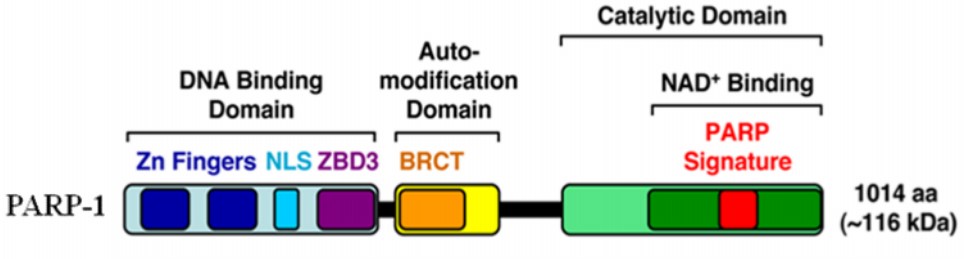

Figure 1. Domain architecture of human poly(ADP-ribose) polymerase-1.
NLS: nuclear localization signal; ZBD3: third zinc-binding domain; BRCT: BRCA1 C-terminus-like (BRCT) motif. Reproduced from (Kraus, 2008).

The catalytic function of PARP1 relates to its role as DNA-damage sensor and signalling molecule. The zinc fingers of PARP-1 recognize single- and double-stranded DNA breaks and PARP-1 subsequently forms homodimers and catalyses covalent binding of ADP-ribose units from donor NAD^+-molecules to a variety of target proteins resulting in linear or branched polymers of PAR as large as 200 units (D'Amours *et al.*,

1999) (Fig. 2). This covalent modification takes place at glutamate and less commonly at aspartate, or lysine resides of target molecules (D'Amours *et al.*, 1999; Rolli *et al.*, 1997).

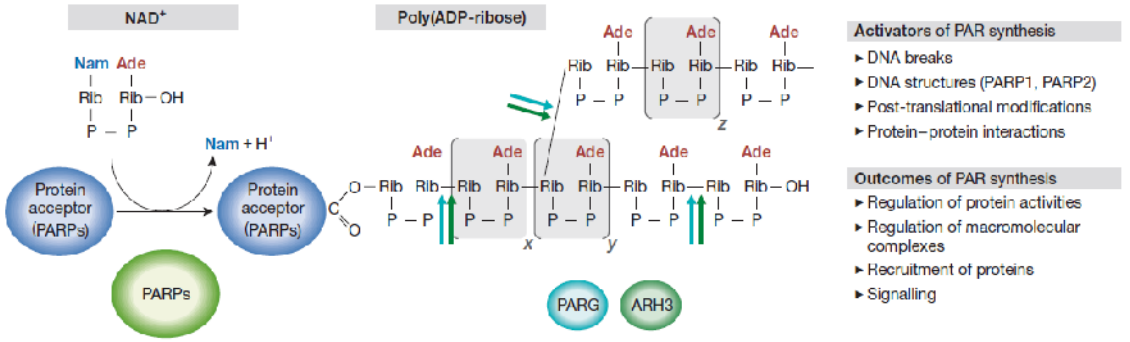

Figure 2. Biochemistry of poly(ADP-ribosyl)ation.

PARP hydrolyse NAD^+ and catalyze the successive addition of ADP-ribose units mainly to glutamate residues of either acceptor proteins (heteromodification) or themselves (automodification). PAR is heterogeneous in size and complexity, as indicated by the *x*, *y* and *z* labels that represent values from 0 to >200. PARG and ARH3 can both hydrolyse PAR at the indicated positions; activators and outcomes of PAR synthesis are indicated. Ade: adenine; Nam: nicotinamide; PAR: poly(ADP-ribose); PARP: poly(ADP-ribose) polymerase; Rib: ribose; ARH3: ADP-rybosil hydrolase-3;PARG: poly(ADP-ribose) glycohydrolase. Reproduced from (Hakme *et al.*, 2008b).

Under physiological conditions enzymatic activity of PARP-1 is very low, but it is stimulated dramatically in the presence of a variety of allosteric activators such as single- or double-strand breaks, crossovers, cruciforms, supercoils, some specific double-stranded sequences (Rolli *et al.*, 2000), nucleosomes, and a variety of protein-binding partners (D'Amours *et al.*, 1999; Kim *et al.*, 2004; Kun *et al.*, 2002; Oei and Shi, 2001). Moreover, a DNA damage independent PARP activation pathway has also been reported (Homburg *et al.*, 2000). The best-characterized activator of PARP-1 is DNA damage induced by free radicals that exert several effects in cells. Enhanced oxidative stress-provoked excessive PARP-1 activation may deplete cellular NAD^+/ATP stores blocking apoptosis and resulting in necrosis (Virag and Szabo, 2002). Moreover, reactive species can play a role in a series of other cell process such as cell signalling, genome integrity or transcription. To understand the role of PARP-1 in these processes, hereby we will overview the origin of reactive species.

3.1.1. Reactive species evoked oxidative stress: activators of PARP-1

Oxidative stress is an imbalance evoked by the excessive formation of ROS (**R**eactive **O**xygen **S**pecies, ROS) and/or RNS (**R**eactive **N**itrogen **S**pecies) and limited antioxidant defenses (Turrens, 2003). Molecules or elements bearing an unpaired electron are defined as free radicals, in chemistry. Free radicals are often regarded as reactive species formed *in vivo* in biology, of which numerous bear unpaired electrons (hence fall into the chemical category of true free radicals, e.g. superoxide anion). However, some reactive species possess reactive character although lack unpaired electrons (e.g. peroxynitrite). Free radicals and their derivatives can be classified as reactive oxygen species and reactive nitrogen species depending on the central atom. Various derivatives are formed at the same time and at the same place under oxidative stress, developing their biological impact on the cells together. Hence, in biology different free radicals and their derivatives are referred as reactive species representing their joint participation in specific biological process. The most frequent reactive species are summarized in Table 1.

Radicals	Name	Symbol
"true" free radicals	Oxygen (bi-radical)	$^{**}O_2$
	Superoxide anion	$^{*}O_2^-$
	Hydroxyl radical	*OH
	Peroxyl radical	ROO*
	Alkoxyl radical	RO*
	Nitric oxide	NO*
radicals without unpaired electrons	Hydrogen peroxide	H_2O_2
	Organic peroxide	ROOH
	Hypochlorous acid	HOCl
	Ozone	O_3
	Aldehydes	HCOR
	Peroxynitrite	$ONOO^-$

Table 1. List of important reactive species in biological systems.

The most reactive among these species are the hydroxyl radicals, hydrogen peroxide and peroxynitrite. Hydroxyl radicals are short lived (Halliwell and Gutteridge, 1999). Hydroxyl radical is a powerful oxidizing agent that can react at a high rate with most organic and inorganic molecules in the cell. In particular, hydrogen peroxide is not radical by definition but causes damage to the cell at a relatively low concentration (10 μM). Hydrogen peroxide is freely dissolved in aqueous solution and can easily penetrate biological membranes (Halliwell and Gutteridge, 1999). This is in contrast to superoxide radicals that are considered relatively stable and have constant, relatively low reaction rates with biological components. Superoxide can react with NO forming peroxynitrite:

$$*O_2^- + NO* \rightarrow ONOO^-$$

Peroxynitrite ($ONOO^-$) is a powerful oxidizing agent (Beckman and Koppenol, 1996) that - upon protonation - decomposes to hydroxyl radical and nitrogen dioxide. It causes the depletion of sulfhydryl (SH) groups and oxidation of a wide variety of molecules causing damage (Halliwell and Gutteridge, 1999).

3.1.2. Endogenous sources of reactive species

Cells are exposed to a large variety of ROS and RNS from both exogenous and endogenous sources. Although the exogenous exposure to ROS can also be significant, endogenous sources is much more important because it can be produced continuously during the life span of every cell (Kohen, 1999). Hereby we concentrate on the endogenous sources of reactive species.

Mitochondria The most prominent ROS producing organelle is the mitochondrium. Mitochondria are working continuously under the whole life span of a cell and represent the place of terminal oxidation and oxidative phosphorylation. Electrons are transfered from reducing equivalents (such as NADH and $FADH_2$) to molecular oxygen leading to the build up of a proton gradient across the inner mitochondrial membrane that is then used for ATP synthesis in terminal oxidation. Importantly, electrons may leak from the respiratory chain at complex I, complex III and reduce oxygen to superoxide (Fig. 3) instead of serving as substrates for the complete reduction of molecular oxygen to water as catalyzed by cytochrome c oxidase (complex IV).

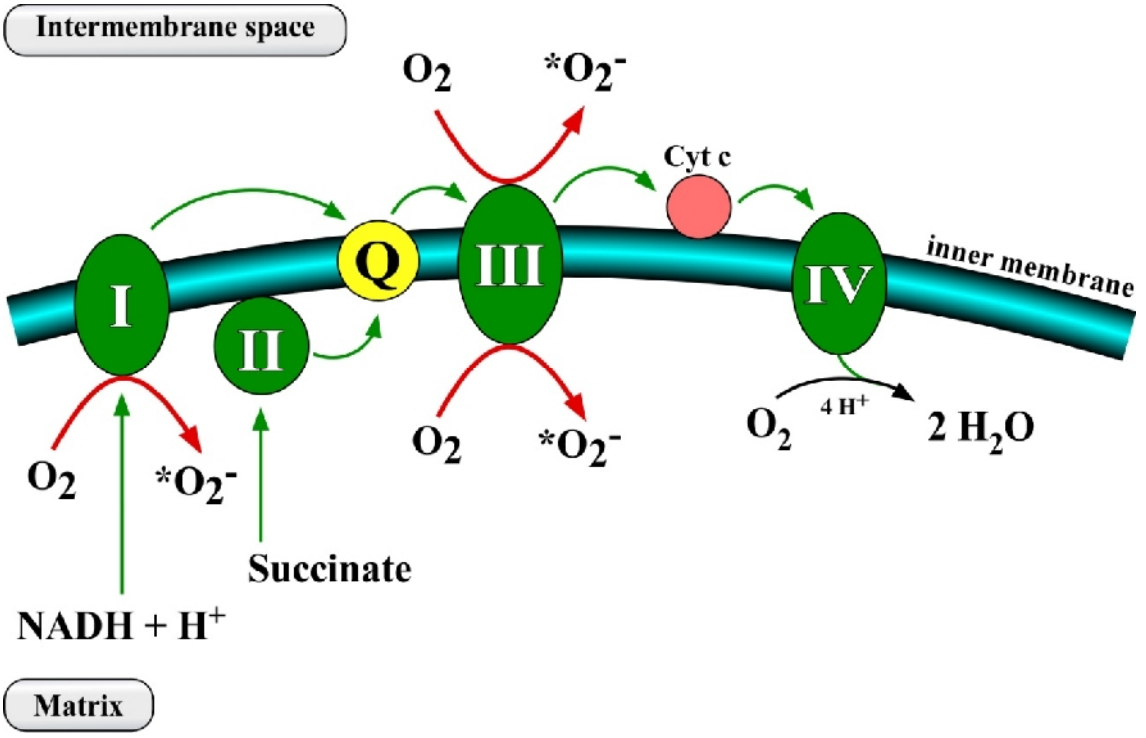

Figure 3. Generation of superoxide at the respiratory chain of the inner mitochondrial membrane.
Superoxide is formed by reduction of molecular oxygen by electrons leaking from complex I (NADH: ubiquinone oxidoreductase, also known as NADH dehydrogenase) as well as complex III (ubiquinol: cytochrome c oxidoreductase). Q: ubiquinone; Cyt c: cytochrome c. Reproduced from (Jacob and Winyard, 2009).

It has been estimated that up to 1% of all oxygen molecules used in respiration is only partially reduced and thus yield superoxide (Powers and Jackson, 2008). The respiratory complex I and complex III can leak electrons generating superoxide, but only complex III is capable of leaking electrons to the intermembrane space. As a result of this process, several different oxygen derivatives are formed (e.g. H_2O_2) (Ames BN, 1995; Bacon and Britton, 1989).

Peroxisomes Peroxisomes also possess ROS generating abilities (Schrader and Fahimi, 2006). The main metabolic processes contributing to the generation of H_2O_2 in peroxisomes are the β-oxidation of fatty acids and the enzymatic reactions of the flavin oxidases (Fig. 4.). Furthermore, transition metal ion complexes (e.g. iron and copper) are abundant in peroxisomes. Under certain conditions, these metal ions might be released (e.g. by xenobiotics) and catalyze the formation of *OH in the Fenton reaction:

$$Fe^{2+} + H_2O_2 \rightarrow Fe^{3+} + OH^- + {}^*OH$$

The occurrence of reactive species leads to lipid peroxidation, damage of the peroxisomal membrane and loss of peroxisomal functions (Bacon and Britton, 1989; Yokota et al., 2001).

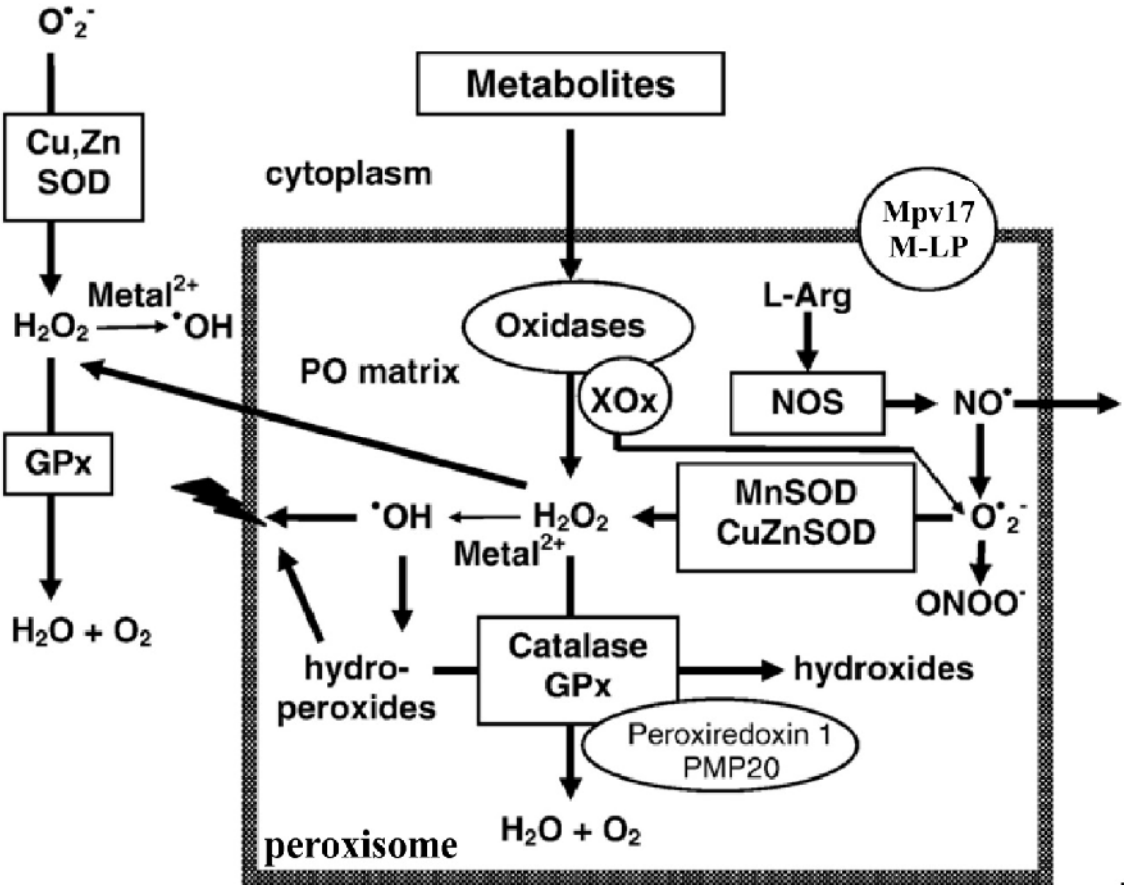

Figure 4. Schematic overview of peroxisomal enzymes that produce or degrade ROS.

H_2O_2 is produced by peroxisomal oxidases (e.g., acyl-CoA oxidase that is involved in the β-oxidation of fatty acids). H_2O_2 is decomposed by catalase and glutathione-peroxidase (GPx) or converted to hydroxyl radicals (*OH). Hydroperoxides formed in this process can be decomposed by catalase and glutathione-peroxidase. Superoxide anion ($*O_2^-$) are generated by peroxisomal oxidases (for example, xanthine oxidase (XOx)) Nitric oxide synthase (NOS) catalyses the oxidation of L-arginine (L-Arg) to nitric oxide (NO). H_2O_2 and NO can penetrate the peroxisomal membrane and act in cellular signalling. Protein Mpv17 (Mpv17) and Mpv17-like protein (M-LP) regulate the peroxisomal ROS production. SOD: superoxide dismutase. Reproduced from (Schrader and Fahimi, 2006).

Phagolysosomes In phagolysosomes exogenous invaders (e.g. invading bacteria) are destroyed by reactive species. Phagolysosomes are mainly present in certain white blood cells (granulocytes, monocytes and lymphocytes) (Forman and Torres, 2001; Yokota et al., 2001) and major producers of endogenous ROS during inflammatory processes (Ginsburg, 1998; Ginsburg and Kohen, 1995). Following stimulation, these cells undergo a respiratory burst (Babior et al., 2002). The consequence of the respiratory burst is that a number of reactive oxygen species are produced, which kill the engulfed bacteria. NADPH serves as a donor of electrons to an activated enzymatic complex in the plasma membrane. This NADPH-oxidase complex utilizes electrons to produce superoxide radicals from the oxygen molecule. Following dismutation, the production of H_2O_2 leads to the formation of *OH by the metal-mediated, Haber-Weiss reaction (Fig. 5A). The enzymatic activity of myeloperoxidase (the most abundantly in neutrophils) (Hawkins *et al.*, 2001; Male *et al.*, 2006; Rodrigues *et al.*, 2002) leads to the production of HOCl by interaction between hydrogen peroxides and chlorides (Fig. 5B) (Hawkins *et al.*, 2001).

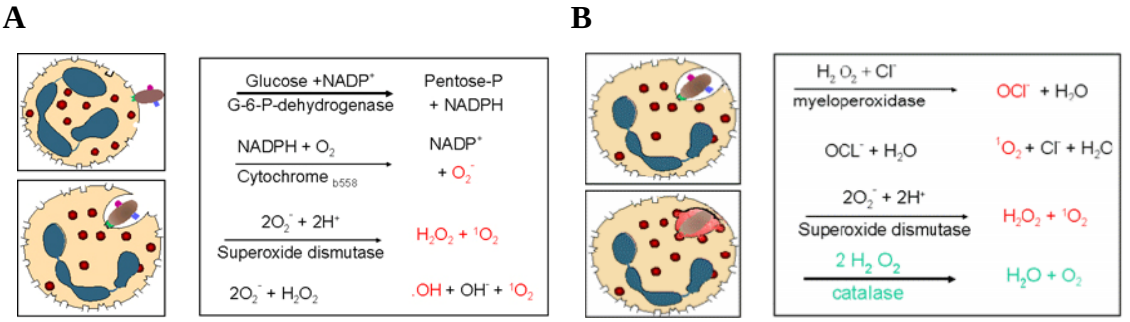

Figure 5. (A) Oxygen-dependent myeloperoxidase-independent and (B) myeloperoxidase-dependent intracellular killing in neutrophil granulocytes.
(A) The activated NADPH oxidase uses oxygen to oxidize NADPH. The result is the production of superoxide anion. Some of the superoxide anion is converted to H_2O_2 and singlet oxygen by superoxide dismutase. In addition, superoxide anion can react with H_2O_2 resulting in the formation of hydroxyl radical and more singlet oxygen. The result of all of these reactions is the production of the toxic oxygen compounds superoxide anion (O_2^-), H_2O_2, singlet oxygen ($^1O_2$) and hydroxyl radical (*OH). **(B)** Myeloperoxidase utilizes H_2O_2 and halide ions (usually Cl^-) to produce hypochlorite (OCl^-), a highly toxic substance. Some of the hypochlorite can spontaneously break down to yield singlet oxygen ($^1O_2$). Reproduced from (Male *et al.*, 2006).

Nitric oxide synthase enzymes Nitric oxide synthase (NOS) enzymes synthesize NO. NOS enzymes convert L-arginine to NO and L-citrulline via the intermediate N-

hydroxy-L-arginine (James, 1998; Moncada *et al.*, 1991; Nathan and Xie, 1994; Stuehr and Marletta, 1985) (Fig. 6). There are three NOS enzymes. Neuronal NOS (nNOS, NOS-1) was originally characterized in neurons and it is expressed in the central and peripheral neuronal tissue (Ignarro, 2000). Endothelial NOS (eNOS, NOS-3) was originally characterized in endothelial cells, it produces NO in blood vessels and regulates vascular function (Ignarro, 2000). The third type of NOS, described in the immune and cardiovascular system, is the inducible form of NOS (iNOS or NOS-2) (Ignarro, 2000). Activity of nNOS and eNOS is activated in response to a calcium signal, while iNOS activity is regulated at the level of expression. Expression of iNOS is induced by several agents including bacterial lipopolysaccharide or cytokines such as interferon-γ (IFNγ), IL-1 or tumor necrosis factor-α (TNFα). In contrast to nNOS and eNOS, iNOS generates high concentrations of NO and this level of synthesis is sustained for hours or days, depending on how long the enzyme is present in the cells or tissue. iNOS has an eminent role in inflammation-related "respiratory burst" (James, 1998; Moncada *et al.*, 1991).

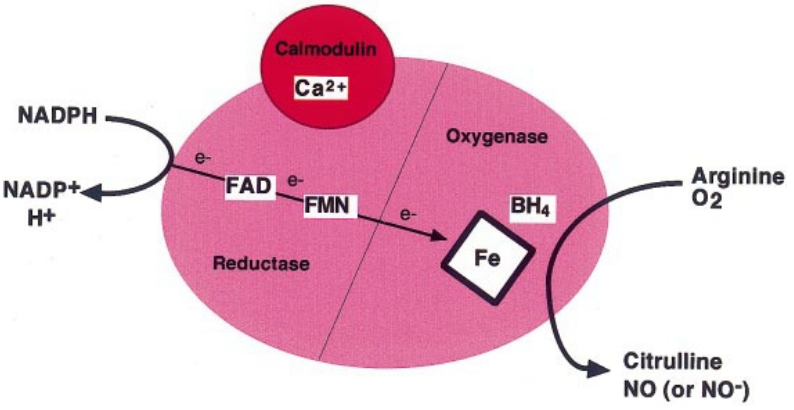

Figure 6. General reaction mechanism and cofactors of NOS enzymes.
Electrons are donated by NADPH to the reductase domain of the enzyme and transferred via FAD and FMN redox carriers to the oxygenase domain. There they interact with the hem iron and a cofactor (tetrahydrobiopterin BH_4)at the active site to catalyse the reaction of oxygen with L-arginine, generating citrulline and NO as end products. Electron flow through the reductase domain requires the binding of calmodulin to the reductase domain. Reproduced from (Alderton *et al.*, 2001).

3.1.3. The harmful effects of reactive species

Reactive species can damage vital cell components like polyunsaturated fatty acids, proteins, and nucleic acids.

Lipid peroxidation influences membrane phospholipids containing polyunsaturated fatty acids. Peroxidation of lipids can disturb membrane assembly causing changes in fluidity and permeability, alterations of ion transport and inhibition of metabolic processes. The products of this reaction are 4-hydroxy-2-nonenal (HNE) and acrolein (Esterbauer *et al.*, 1991; Niki, 2009; Parola *et al.*, 1999).

Predominantly hydroxyl, alkoxyl, and nitrogen-centred radicals cause protein damage. Proteins can undergo oxidation, damage to specific amino-acid residues (e.g. nitration of tyrosine yielding nitrotyrosine), or tertiary structure degradation and fragmentation. The consequence of protein damage is usually loss of enzymatic activity and altered cellular functions. Protein oxidation products are usually aldehydes, keto and carbonyl compounds (Berlett and Stadtman, 1997; Grune *et al.*, 1997; Levine and Stadtman, 2001).

Reactive species induce modifications of DNA such as modification of nucleotide bases, single- and double strand DNA breaks, loss of purines (apurinic sites), damage to deoxyribose, DNA-protein cross-linkage, and damage to the DNA repair system. Mainly the *OH can attack DNA bases for example at guanine site to yield an oxidation product, 8-hydroxy-2-deoxyguanosine (8-OHdG)(Cadet *et al.*, 2010; Cooke *et al.*, 2003; Poulsen *et al.*, 2000). The oxidative modifications evoked by reactive species are summarized on Fig. 7.

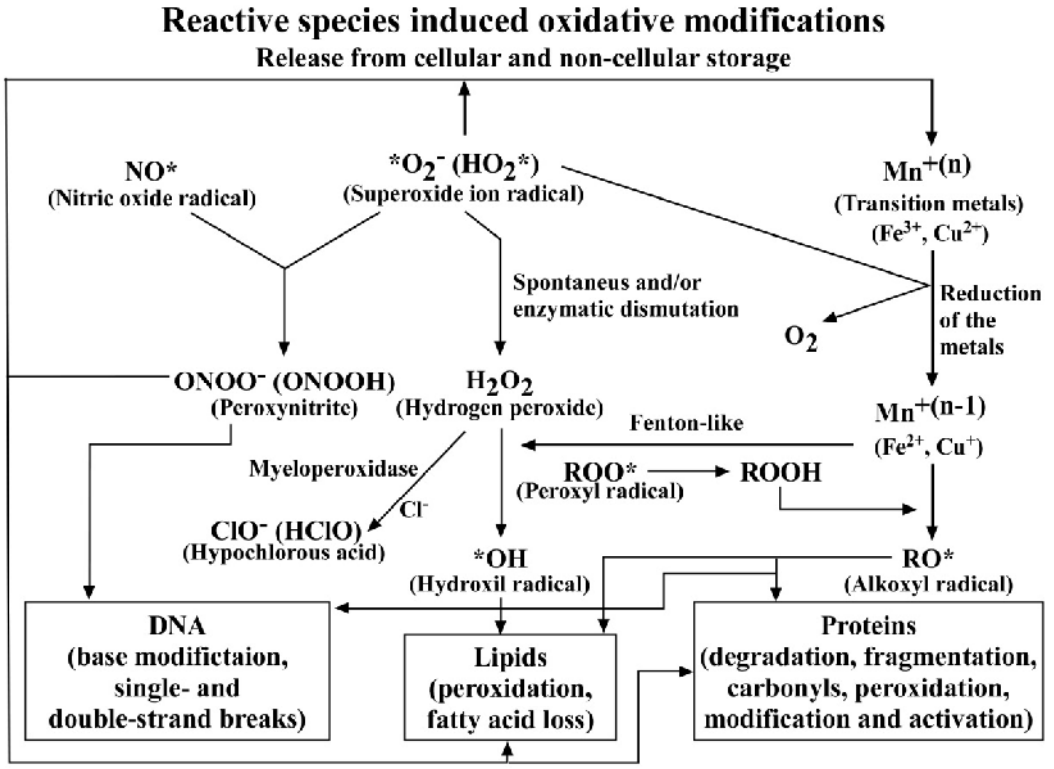

Figure 7. The overview of reactive species-induced oxidative modifications.

The continuous efflux of ROS from endogenous and exogenous sources results in continuous and accumulative oxidative damage to cellular components such as lipids, porteins and DNA. These alterations modify many cellular functions. Reproduced from (Kohen and Nyska, 2002).

These reactive species-induced oxidative modifications can also play role in redox signaling. Redox modifications lead to alterations of biomolecules that are the activators of diverse signaling pathways, initiating redox-sensitive regulation and redox-dependent signal transduction. These changes may modulate gene expression through redox-sensitive transcription factors (Haddad, 2002). There are numerous transcription factors that are described as redox-sensitive, such as NF-κB, AP-1. These transcription factors are known to interact with PARP-1, although in most cases the exact molecular background of the interaction is not yet defined. We will outline the consequence of these free radical-evoked processes in the following chapters.

3.2. Biological functions of PARP-1

As mentioned earlier, PARP-1 has diverse biological functions including DNA repair functions such as base excision repair (Dantzer *et al.*, 2000; Dantzer *et al.*, 1999) nucleotide excision repair and contributes to double strand break repair (Audebert *et al.*, 2004; Fisher *et al.*, 2007). PARP-1 also possesses non-repair functions such as regulation of cardiac remodelling (Xiao *et al.*, 2005), vasoconstriction (Albadawi *et al.*, 2006), astrocyte and microglial function (Chiarugi and Moskowitz, 2003), long term memory (Sung and Ambron, 2004), inflammation (Oliver *et al.*, 1999), aging (Burkle *et al.*, 2005), energy metabolism (Asher *et al.*, 2010) and transcription (Kraus and Lis, 2003).

3.2.1. Role of PARP-1 in the regulation of transcription

The regulation of gene expression requires a wide array of protein factors that can modulate chromatin structure, act at enhancers, function as transcriptional coregulators, or regulate insulator function. PARP-1 can regulate transcription as (a) a component of insulator, (b) a component of enhancer/promoter regulatory complexes, (c) a modulator of chromatin structure and (d) a transcriptional coregulator (Kraus, 2008) (Fig. 8.).

PARP-1 has been suggested to act as an insulator (Klenova and Ohlsson, 2005). Insulators are DNA elements that help to organize the genome into discrete regulatory units by limiting the effects of enhancers on promoters or by preventing the spreading of heterochromatin (Wallace and Felsenfeld, 2007). PARP-1-dependent PARylation of CCCTC-binding factor or 11-zinc finger protein (CTCF), an ubiquitous DNA-binding protein that functions at insulator sites have suggested to be crucial for the preservation of insulator function (Yu *et al.*, 2004; Yusufzai *et al.*, 2004) (Fig. 8A).

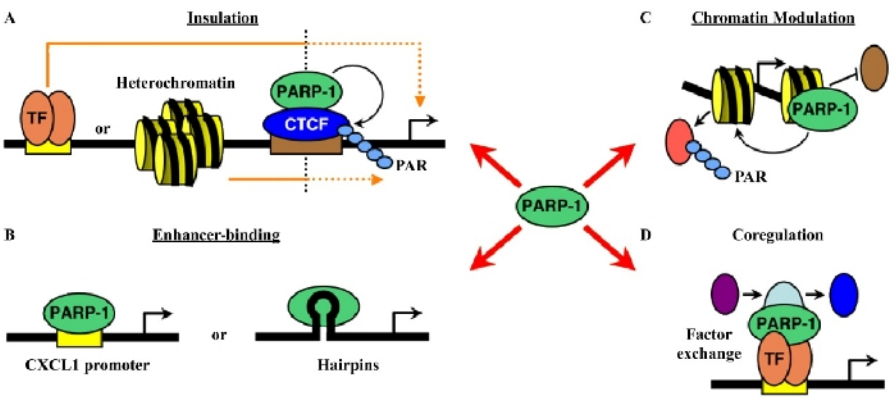

Figure 8. Modes of transcriptional regulation by PARP-1.
PARP-1 regulates transcription in four modes, as indicated. (A) PARP-1 can function as a component of insulators, (B) can act as an enhancer-binding factor, (C) can modulate chromatin structure and (D) can function as transcriptional coregulator in a manner similar to classical coactivators and corepressors. Reproduced from (Kraus, 2008).

The earliest characterized effects of PARP-1 on the genome were the modulation of chromatin structure and the PARylation of histones (D'Amours *et al.*, 1999; Huletsky *et al.*, 1989; Kraus and Lis, 2003; Malanga and Althaus, 2005; Poirier *et al.*, 1982) (Fig.8C). PARP-1 binding to nucleosomes in the absence of NAD^+ promotes the compaction of nucleosomal arrays into higher order structures (Wacker *et al.*, 2007). In the presence of NAD^+, PARP-1 undertakes its own automodification and dispatches from chromatin, leading to decompaction and restoration of transcription *in vitro* (Kim *et al.*, 2004) (Fig. 8C). PARP-1 can lead to more specific and elaborate changes in chromatin such as the exclusion of H1 from the promoters of some PARP-1 regulated genes (Krishnakumar *et al.*, 2008), possibly by PARylating nucleosomes or by competing with H1 for binding to nucleosomes (Huletsky *et al.*, 1989). Furthermore, in the case of estrogen-induced transcription of the trefoil factor 1 (TFF1) gene PARP-1 does not only promote the removal of H1, but also increases the levels of a chromatin architectural protein (HMGB1) that enhances transcription (Ju *et al.*, 2006). In addition, PARP-1-dependent PARylation of DEK, an abundant and ubiquitous architectural component of chromatin, promotes the release of DEK from chromatin, the loading of the Mediator coregulatory complex, and the enhancement of transcription (Gamble and Fisher, 2007).

Many of the early studies have described direct effects of PARP-1 on transcriptional regulation. In this action PARP-1 binds to specific DNA sequences or structures in the regulatory regions of genes where PARP-1 acts as a classical enhancer binding factor (Butler and Ordahl, 1999; Huang *et al.*, 2004; Nirodi *et al.*, 2001) (Fig. 8B). In fact, direct binding of PARP-1 to hairpins may underlie an autoregulatory mechanism governing the expression of the PARP-1 gene itself (Soldatenkov *et al.*, 2002). The best examples for such interaction are the promoters of chemokine (CXC motif) ligand 1 (CXCL1) (Amiri *et al.*, 2006) and B-cell lymphoma 6 protein (BCL6) (Ambrose *et al.*, 2007).

Finally, PARP-1 has been identified as promoter-specific coregulator (either a coactivator or a corepressor) for a number transcription factors, such as NF-κB, nuclear receptors, Myb-related protein B (B-Myb), organic cation transporter member 1 (Oct-1), stimulating protein-1 (Sp1), Nuclear factor of activated T-cells (NFAT) and others (Fig. 8D). PARP-1 can interact with enhancers and promoters of genes by a) direct sequence-specific binding, b) recruitment via DNA binding of transcription factors (e.g. NF-κB), c) direct binding to DNA structures and (d) binding to the dyad axis (Fig 9).

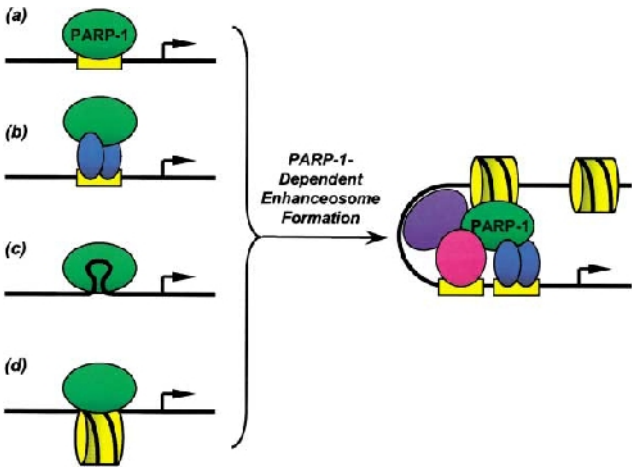

Figure 9. A Model for Activator/Coactivator Functions of PARP-1 at Enhancers and Promoters
PARP-1 can interact with enhancers and promoters of genes by (a) direct sequence-specific binding to enhancers, (b) recruitment via DNA binding transcription factors (e.g., NF-κB), and (c) direct binding to DNA structures (e.g., cruciform, curved, supercoiled, and crossover) and (d) to the dyad axis where DNA enters and exits the nucleosome. In many cases, PARP-1 may promote the binding of other factors to DNA, stimulating the formation of enhanceosomes and the activation of transcription in a manner independent of PARP-1 enzymatic activity.

The respective DNA-binding factors recruit PARP-1 to relevant target promoters, where in turn PARP-1 may promote the binding of further factors to DNA, stimulating the formation of enhanceosomes (also indicated as PARP-1 coactivator complex) and the activation of transcription. In some cases, enzymatic activity of PARP-1 is essential to form transcription complex with other transcription factors e.g. SP-1 and NFAT. DNA-binding factors or other components of the coregulatory complex are targets of PARP-1-dependent PARylation. PARP-1 was shown to promote the recruitment of topoisomerase IIβ to hormone-regulated promoters, leading to concomitant promoter DNA cleavage, factor exchange, and transcriptional activation (Ju *et al.*, 2006; Pavri *et al.*, 2005). Recruitment of the PARP-1 coactivator complex also promotes the release of histone H1, the recruitment of HMGB1/2, changes in chromatin architecture, and ultimately increased transcription of the gene (Ju *et al.*, 2006). Together, these studies highlight the diverse mechanisms of PARP-1 coregulator function, which are likely to vary in an activator-and gene-specific manner. The most important PARP-1 associated transcription factors are summarized in Table 2.

Transcription factor	Characteristics/functions	PARP-1 interaction
NF-κB	Inflammation, viral (HIV) activation, NO synthesis, cytokine release	(Oliver *et al.*, 1999)
AP-1	Cell proliferation, cell adhesion, GST regulation, multidrug resistance, inflammation	(Zingarelli *et al.*, 2004)
AP-2	Regulator of gene expression during embryogenesis	(Kannan *et al.*, 1999)
Sp-1	HIV, herpes simplex activation, myocyte differentiation, VEGF, hsp70, and HGH gene regulation	(Zaniolo *et al.*, 2005)
Oct-1	B cell–specific expression of immunoglobulins	(Tantin *et al.*, 2005)
B-MYB	Cell cycle regulation (required for S-phase entry), apoptosis, cancer	(Li and McDonnell, 2002)
TEF-1	High levels of gene expression in skeletal and cardiac muscles, transcriptional regulation of SV40 and papillomavirus, co-factors of the glucocorticoid receptor	(Maeda *et al.*, 2002)
Stat-1	Cell proliferation and apoptosis	(Levy and Darnell, 2002)
YY-1	Embryogenesis, growth, differentiations, proliferation and response to genotoxic stimuli	(Gordon *et al.*, 2006)
ATF-2	Inflammation, metabolic regulation, oncogenesis	(Maekawa *et al.*, 2010)
CREB	Inflammation, cell cycle regulation, cancer	(Ha, 2004)
p53	DNA repair, cell cycle regulation (G_1/S), apoptosis	(Sionov and Haupt, 1999)

Table 2. Transcription factors regulated by PARP-1

3.2.1.1. Transcriptional events in inflammation mediated by PARP-1

Studies performed with PARP-1 knockout mice revealed that genetic deletion of PARP-1 inhibits the propagation of inflammation which was later verified in a large number of diseases (reviewed in (Virag and Szabo, 2002)). The disregulation of different transcription factors represents the basis for the protection against inflammatory diseases. Some transcription factors involved in the regulation of inflammatory process are redox-sensitive and usually require the enzymatic activation of PARP-1. The dominant transcription factors activated during inflammation are NF-κB and AP-1.

NF-κB is a protein complex that controls the transcription from specific promoters. NF-κB exists in virtually all cell types and is involved in cellular responses to stimuli such as stress, cytokines or free radicals. NF-κB plays key role in regulating inflammatory processes. NF-κB family consists of multiple members such as c-Rel, RelA, RelB, NF-kB1 and NF-κB2. NF-κB consists of two protein subunits, p50 and p65, which are present in the cytosol of non-stimulated cells as homo- or heterodimers of the above proteins. The active transcription factor contains a nuclear localization signal, targeting it to the nucleus for DNA binding. In non-stimulated cells this signal is masked by the action of a monomeric inhibitor protein IκB, resulting in the cytoplasmic accumulation of the transcription factor. Cytokine stimulation induces a signal transduction cascade in which the key step is the phosphorylation of IκB by IκB kinase (IKK), which results in the release of NF-κB from IκB, followed by nuclear translocation and transcription of NF-κB-dependent genes. Several studies have been revealed the interaction between NF-κB and PARP-1 (Aguilar-Quesada *et al.*, 2007; Chiarugi and Moskowitz, 2003; Oliver *et al.*, 1999). PARP-1 may influence NFkB transactivation by several means. Primarily, upon the loss of PARP-1 NFkB binding to DNA is hampered (Oliver, 1999). It is under debate whether the enzymatic activation of PARP-1 is required or dispensable for NF-κB (Hassa and Hottiger, 2002; Oliver *et al.*, 1999). Finally, the PI3/Akt and MAP kinase signalling pathways may also modify NF-κB transactivation (Veres *et al.*, 2004).

The heterodimeric complex AP-1 is a basic leucine zipper protein formed by the dimerization of its components c-Fos, c-Jun or ATF-2. ATF-2 is a cAMP-responsive element-binding transcription factor (Livingstone *et al.*, 1995) that forms homomer

complex with c-Jun and binds to activator protein-1 sites (Reimold *et al.*, 2001). The genes regulating the cellular concentration of the transcription factor are induced by extracellular stress, linking AP-1 activity to the cell stress response. AP-1 can therefore be viewed as a critical intermedier in many signal transduction pathways. Under oxidative stress, activated $p38^{MAPK}$ rapidly translocates from the cytoplasm to the nucleus and phosphorylates its substrates such as transcription factors, e.g. cAMP-response element-binding protein (CREB), ATF-2 and c-Jun or other kinases, such as mitogen- and stress-activated protein kinase (Ha, 2004). The AP-1 transcription factor can bind to DNA and can start the transcription of inflammatory genes. ATF-2 has been shown to be regulated by PARP-1 (Ha, 2004). Genetic deletion of ATF-2 leads to impaired AP-1 activation and consequently to reduced expression of cytokines (TNF-α, IFN-γ, IL-1, IL-6, or MCP-1α) and adhesion factors (E-selectin and P-selectin) (Reimold et al., 2001). Deficient AP-1 activation upon PARP-1 ablation has already been described in a murine model of colitis to provide a protective phenotype (Zingarelli et al., 2004). PARP-1 can influence AP-1 transcription activity via MAP kinase phosphatase 1 (MKP-1) under oxidative stress conditions (Racz *et al.*, 2010) that is an attractive model to explain our findings on altered AP-1 transactivation in PARP-1 knockout mice. Namely, PARP-1 regulate transcription of MKP-1 which phosphorylate the $p38^{MAPK}$ and JNK/SAPK impacting on the phosphorilation of AP-1 subunits such as ATF-2 and c-Jun in the nucleus (Racz *et al.*, 2010).

Inflammatory cytokines such as TNFα, IL-1β are central regulators of the inflammatory process orchestrated by Th1 cells. These cytokines induce the expression of other cytokines and chemokines (chemoattractants), adhesion molecules, inducible nitric oxide synthase (iNOS), and cyclooxygenase-2 and matrix metalloproteinases. If PARP-1 is inhibited or knocked out, the expression of inflammatory cytokines is suppressed (MIP-1α, MIP-2, IL1β, TNFα, and MCP-1). These chemokines and cytokines were described to be NF-κB dependent (Espinoza *et al.*, 2007; Haddad *et al.*, 2006; Oliver *et al.*, 1999; Virag and Szabo, 2002). Therefore, the suppression of NF-κB activity provides a likely explanation for the reduced expression of these genes. Cytokines and chemokines possess central role in the propagation of inflammation. Changes in chemokine and cytokine expression represent a mechanism for reduced migration of inflammatory cells. Adherence, extravasation and migration of

inflammatory cells is facilitated by adhesion proteins, such as I-CAM, V-CAM, L-CAM, selectins expressed on the surface of endothelial. Inhibition of PARP-1 blocks the expression of these adhesion molecules and reduce cellular infiltration (Zingarelli *et al.*, 1999). Importantly, these genes are also regulated by NF-κB and AP-1 (Espinoza *et al.*, 2007; Haddad *et al.*, 2006).

Another important inflammatory gene regulated by PARP-1 is iNOS that is responsible for NO synthesis under inflammatory conditions (Lowenstein *et al.*, 1994; Moncada *et al.*, 1991). NO combines with superoxide to form peroxynitrite causing lipid peroxidation, protein oxidation and DNA strand breakage (Ischiropoulos *et al.*, 1992). iNOS is regulated via NF-κB activation, hence PARP inhibition markedly reduces iNOS expression and nitrosative stress (Haddad *et al.*, 2006).

MMPs are indispensable for tissular movement of cells. MMPs may be activated by free radical-induced structural changes (Le *et al.*, 2007). Several studies have shown that MMP activation during inflammation (e.g. MMP-9 activation in skin inflammation) can be prevented by knocking out PARP-1 or by pharmacological PARP-1 inhibition (Bai *et al.*, 2009; Kauppinen and Swanson, 2005; Koh *et al.*, 2005; Oumouna-Benachour *et al.*, 2007). Moreover, tissue inhibitors of MMPs (TIMPs) that reduce MMP activity are inversely regulated than MMPs upon inflammation (Bai *et al.*, 2009; Oumouna-Benachour *et al.*, 2007). PARP inhibition is capable of restoring the balance between MMPs and TIMPs (Bai *et al.*, 2009). It has not been determined as of yet whether these effects are related to direct gene expression changes or represent cellular invasion of tissues.

3.2.1.2. PARP-1 in the transcriptional control of oxidative energy metabolism

Sirtuins (SIRTs) – homologs of the yeast sir2 (silent mating-type information regulation 2) - are NAD^+-dependent class III histone deacetylases (HDAC III). Sirtuin protein family has seven members. Among these proteins, the nuclear protein SIRT1 is the closest homolog of yeast sir2. SIRT1 is induced by caloric restriction and have been implicated in influencing aging and regulating transcription, stress resistance, as well as energy efficiency (Guarente and Picard, 2005; Oberdoerffer *et al.*, 2008).

SIRT1 has a multiple role in the regulation of metabolism and can influence metabolism depending the level of nutrient availability. SIRT1 is capable of regulating

glucose and lipid metabolism in different metabolic tissues such as skeletal muscle, liver, brown adipose tissue (BAT), white adipose tissue and brain. In the pancreas SIRT1 activity regulates insulin secretion (Rodgers *et al.*, 2008). In these tissues, SIRT1 interacts PGC-1α and FOXO1 and upon activation it deacetylates and activates them (Feige and Auwerx, 2008; Lagouge *et al.*, 2006; Rodgers *et al.*, 2008). In this way, SIRT1 mediates the gene expression of mitochondrial biogenesis, fatty acid oxidations/syntheses, oxidative phosphorilation, adaptive thermogenesis, gluconeogenesis and glycolysis genes. Hence, SIRT1 can fine tune the energy homeostasis of the whole body (Fig. 10.).

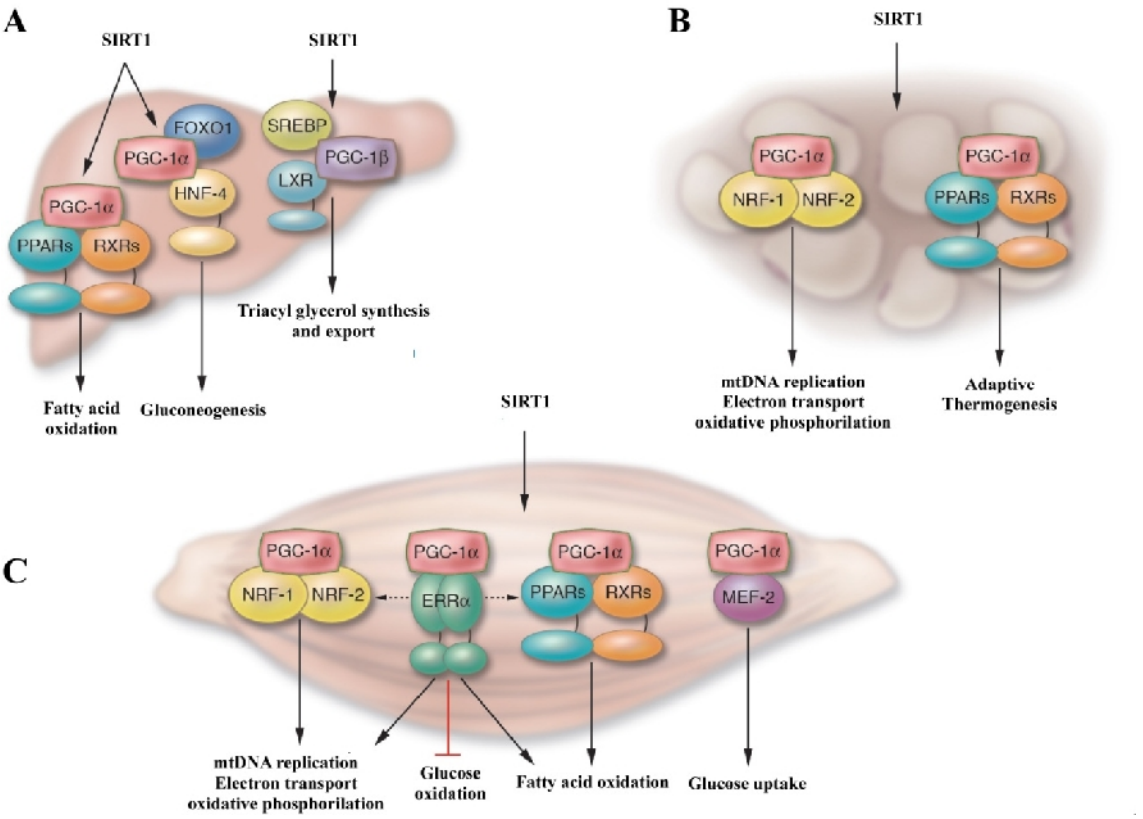

Figure 10. Summary of SIRT1 mediated metabolic pathway via PGC-1α and FOXO1.
By responding to metabolic alterations SIRT1 mediates key transcription factors of oxidative metabolism through which it translates energy status into gene expression programs in (A) liver, (B) BAT and (C) skeletal muscle. Reproduced from (Finck and Kelly, 2006).

SIRT1 can be activated by fasting (Rodgers *et al.*, 2005), exercise (Canto *et al.*, 2009) or low glucose availability (Fulco *et al.*, 2008). Under these conditions the level of glucose in blood decreases, while the intracellular NAD^+ levels is increased in the metabolic tissues: liver, skeletal muscle and BAT. SIRT1 is activated by increased NAD^+ level and deacetylates transcription factors PGC-1α and FOXO (Feige and Auwerx, 2008; Lagouge *et al.*, 2006; Rodgers *et al.*, 2005). Deacetylation activates these transcription factors, whereby they induce mitochondrial biogenesis mitochondrial biogenesis, fatty acid oxidation, oxidative phosphorilation in skeletal muscle (Gerhart-Hines *et al.*, 2007), adaptive thermogenesis in BAT (Uldry *et al.*, 2006) and moreover gluconeogenesis in liver (Finck and Kelly, 2006). At the same time the genes of fatty acid synthase are down-regulated in liver and skeletal muscle. Together these processes lead to fatty acid oxidation (ketone-body production) and glucose production in these tissues. Moreover, in skeletal muscle SIRT1 activation leads to muscle fiber type switch. Muscle fiber type switch elevates the quantity of type I (oxidative) fibers characterized by a higher mitochondrial content.

The dependence of SIRT1 on NAD links its enzymatic activity directly to the energy status of the cell via sensing cellular NAD^+/NADH ratio. PARP-1 can influence NAD^+ levels since its activation consumes cellular NAD^+ (Schraufstatter *et al.*, 1986). Moreover, PARP-1 is a faster and more efficient NAD^+ consumer than SIRT1 (Knight and Chambers, 2001; Malik *et al.*, 2009; Smith *et al.*, 2009). These data suggest that PARP-1 activity may impact on gene transcription through modulating SIRT1 activity. PARP-1 and -2 have a baseline PARP activity that is initiated by constant oxidative stress stemming from mitochondrial oxidative metabolism (Barja, 1992). Therefore, these PARP enzymes constantly turn over NAD^+ even under non-stressed conditions. Recent studies revealed that through modulating NAD^+ PARP-1 impacts on other NAD^+-dependent enzymes, such as SIRT1 (Cai *et al.*, 2006; Caito *et al.*, 2010; El Ramy *et al.*, 2009; Kolthur-Seetharam *et al.*, 2006; Rajamohan *et al.*, 2009). Moreover, it is important to note that NAD^+ is compartmentalized in cell, namely, nuclear, cytosolic and mitochondrial NAD^+ pools. NAD^+ between these pools cannot exchange (Houtkooper *et al.*, 2010). Since PARP-1 and SIRT1 are nuclear proteins their activity probably use only nuclear NAD^+ hence influencing gene expression in nucleus only.

4. Literary overview and aims

PARP-1 has been shown to influence transcription and oxidative stress at multiple levels. We set out to investigate the effects of PARP-1 depletion on transcription in different models. On one hand, we utilized a skin inflammation model, oxazolon-induced contact hypersensitivity. In this model we have already shown the prominent role of oxidative stress (Szabo *et al.*, 2001) and PARP activation (Bai *et al.*, 2009). However, the exact molecular mechanism though which PARP-1 or -2 influence inflammation is unknown. On the other hand, we set out to investigate how PARP-1 may act on SIRT1 and oxidative metabolism. As pointed out in the introduction, the interdependence of PARP-1 and SIRT1 have already been revealed (Cai *et al.*, 2006; Caito *et al.*, 2010; El Ramy *et al.*, 2009; Kolthur-Seetharam *et al.*, 2006; Rajamohan *et al.*, 2009), however the metabolic impact of their interplay and its molecular mechanism have not been studied yet.

Our aims were the following:

I. Investigation of the role of PARP-1 in oxazolone-induced contact hypersensitivity (CHS):

- Defining the respective role of PARP-1 in oxazolone-induced CHS.
- Characterization of oxidative stress in oxazolone-induced CHS.
- Characterization of transcriptional changes during oxazolone-induced CHS (proinflammatory cytokines, chemokines, adhesion molecules and transcription factors).

II. Characterization of gene expression changes after PARP-1 depletion or inhibition in

- skeletal muscle, BAT, liver
- murine embryonic fibroblasts
- pharmacology inhibition of PARP-1 with PJ34.

5. Materials and Methods

5.1. Methods

5.1.1. *In vivo* studies

All animal experiments were approved by the local ethical committee (9/2008/DE MÁB) and were performed according to EU and national guidelines.

In oxazolone-induced contact hypersensitivity reaction, homozygous PARP-1 (Menissier-de Murcia *et al.*, 1997) and PARP-2 knockout (KO) mice and their respective wild-type (WT) littermates on C57/Bl6 background were used. Female mice were randomized into four groups (WT non-sensitized, WT-sensitized, KO non-sensitized, KO sensitized) and were sensitized and challenged.

PMA–induced irritative dermatitis model was performed as described in (Bai *et al.*, 2009). Briefly, PMA (10 µl, 0.05% w/v) was smeared onto both sides of the ears of female mice (6 animals per group), ear swelling was determined together with all other biochemical measurements 24 hours later.

In metabolic studies, male PARP-$1^{+/+}$ and PARP-$1^{-/-}$ mice on a C57/Bl6 background were used. Mice were housed separately, had ad libitum access to water and standard rodent chow (10 kcal% of fat, Safe, Augy, France) and were kept under a 12 h dark-light cycle.

In case of PJ34 treatment, mice received each 12 h (at 7:00 and 19:00) 10 mg/kg PJ34 by intraperitoneal injection for 5 continuous days. In all studies animals were killed either CO_2 inhalation or cervical dislocation after 6 h of fasting (starting at 8:00), and tissues were collected each time (between 14:00 and 15:00) and processed as specified below.

5.1.2. Preparation of MEF cells

MEFs (primary mouse embryonic fibroblasts) were isolated by standard procedures (Isolation and handling of MEFs accompanying protocol to "Mouse embryonic stem (ES) cell culture - basic procedures" by Boris Gerber). After crossing heterozygous PARP-$1^{+/-}$ mice, we sacrificed the pregnant female at day 13 post coitum by cervical dislocation. Dissected out the uterine horns, briefly rinsed them in 70% (v/v) ethanol and placed into a petri dish containing PBS. We separated each embryo from its

placenta and surrounding membranes, cut away brain and dark red organs, washed with fresh PBS, to remove as much blood as possible. After it, we used a minimal amount of PBS and razor blades, finely minced the embryos until they became "pipettable", then suspended cells/tissue in several ml of trypsin-EDTA (Lonza) and incubated with gentle shaking at 37°C for 15 min. After incubation we transfered suspension to a 50 ml falcon tube and added about 2 volumes of fresh medium and we removed remaining pieces of tissue by low speed centrifugation (5 min, 1000 *g*) - resuspended the resulting cell pellet in warm MEF medium (Gibco) and plated out at 1 embryo equivalent per 10 cm dish. We changed medium on the following day. The fibroblasts were the only cells that attached to the dishes. Cells grew confluent within one or a few days.

5.1.3. Histology and microscopy

Haematoxylin-eosine (HE) histochemistry was performed as described earlier (Szabo *et al.*, 2001). Immunohistochemistry was performed on paraffin sections (7 µm) were treated with 0.3% hydrogen peroxide for 15 min to block endogenous peroxidase activity and then rinsed briefly in PBS. Non-specific binding was blocked by incubating the slides for 1 h in 2% goat serum (in PBS). To detect nitrotyrosine, rabbit polyclonal anti-nitrotyrosine antibody (Sigma) was applied for 2 h in a dilution of 1:1000 at room temperature. (Control sections were incubated with normal rabbit.) Following extensive washing (five times 5 min) with PBS, immunoreactivity was detected with a biotinylated goat anti-rabbit secondary antibody and the avidin-biotin-peroxidase complex (ABC), both supplied in the Vector Elite kit (Vector Laboratories, Burlingame, CA). Color was developed using nickel-DAB substrate. Sections were counterstained with nuclear fast red for 2 min, dehydrated, and mounted in Permount medium.In the case of neutrophil elastase (Santa Cruz, Santa Cruz, CA, USA) and anti-PAR murine monoclonal antibody (BD Biosciences, San Jose, CA, USA) were also used the above mentioned protocols.

5.1.4. Myeloperoxidase activity assay

The activity of myeloperoxidase (MPO), an indicator of neutrophil accumulation, was determined in tissue homogenates prepared in 0.5% hexa-decyl-trimethylammonium bromide in 10 mM MOPS buffer. The supernatants of the

homogenates were mixed with a solution of 1.6 mM tetramethylbenzidine and 1 mM hydrogen peroxide. Activity was measured spectrophotometrically as the change in absorbance at 650 nm at 37°C, using a Labsystems Multiskan MS plate reader (Analytical Instruments, Minneapolis, USA). MPO activity was expressed as the percentage of the MPO activity determined in the samples of WT non-sensitized animals.

5.1.5. MMP activity assay

Ears were homogenized in DQ buffer (50 mM Tris (pH 7.6), 150 mM NaCl, and 5 mM $CaCl_2$) by Ultra Turrax, and then homogenate was cleared by centrifugation. To 100 µl supernatant and 80 µl DQ buffer 20 µl of fluorescein-conjugated gelatine (DQ gelatine, Invitrogen, Carlsbad, CA, USA) was added, samples were incubated at room temperature 30 minutes and fluorescein fluorescence was determined using a Victor V3 fluorimeter (Beckton-Dickinson, Franklin Lakes, NJ, USA). Fluorescence values were normalized for protein content.

5.1.6. 8-oxo-2'-deoxyguanosine (8-OHdG) determination

8-OHdG determination was performed using a commercial kit from Cell Biolabs (San Diego, CA, USA) according to the manufacturer's instructions. After ear homogenisation by Ultra Turrax, we extracted DNA by standard phenol-chloroform methods from samples. Extracted DNA were dissolved in nuclease free water at 1-5 mg/mL. DNA samples were converted to single-stranded DNA by incubating the sample at 95ºC for 5 minutes and rapidly chilling on ice. DNA samples were digested by incubating the denatured DNA with 5-20 units of nuclease P1 for 2 hrs at 37 ºC in 20 mM sodium acetate, pH 5.2, and following with treatment of 10 units of alkaline phosphatase for 1 hr at 37 ^{o}C in 100 mM Tris, pH 7.5. The reaction mixture was centrifuged for 5 minutes at 6000 g and the supernatants were used for the 8-OHdG ELISA assay. Each 8-OHdG sample were measured in duplicate. 50 µL of unknown sample or 8-OHdG standard were added to the wells of the 8-OHdG conjugate coated plate. Plate was incubated at room temperature for 10 minutes on an orbital shaker. 50 µL of the diluted anti-8-OHdG antibody were added to each well, incubate at room temperature for 1 hour on an orbital shaker. After it we washed microwell strips 3 times

with PBS. After washing 100 µL of the diluted secondary antibody-enzyme conjugate were added to all wells. Incubate at room temperature for 1 hour on an orbital shaker and after washed again the plate warm 100 µL of substrate solution were added to each well and incubated at room temperature on an orbital shaker about 10 minutes. After stopping the enzyme reaction by adding 100 µL of stop solution into each well, results were read immediately on a spectrophotometer using 450 nm as the primary wavelength. We read off the data on standard curve and data were normalized to total DNA content represented in ng/mg DNA concentration.

5.1.7. Protein carbonyl assay

Protein carbanoylation was assessed using a commercial kit from Cayman Chemicals (Ann Harbour, MI, USA) according to the manufacturer's instructions.

We dissected 200-300 mg of tissue and rinsed with a PBS to remove any red blood cells or clots. The ears were homogenized in 2 ml of cold buffer (50 mM PBS, ph 6.7, 1 mM EDTA). Samples centrifuged at 10.000 x *g* for 15 minutes at 4 ^{o}C. The supernatant diluted to 10 µg/mL in 1X PBS. Each protein sample and BSA standard assayed in duplicate or triplicate. We pretreated lysate with nuclease to remove nucleid acids contaminantions followed by ammonium sulfate precipitation of high percentage saturation and removed precipitates by centrifuging at 6000 g for 10 minutes at 4ºC. 100 µL of 10 µg/mL protein samples, including reduced/oxidized BSA standards, were added to the 96-well protein binding plate. Plates were incubated at 37ºC for 2 hours and washed wells 3 times with 250 µL 1X PBS per well. After the last wash, we removed excess wash solution, added 100 µL of the DNPH working solution, and incubated for 45 minutes at room temperature in the dark. In the next step wells were washed with 250 µL of 1X PBS/Ethanol (1:1, v/v) and incubated on an orbital shaker for 5 minutes. After incubation we repeated washing a total of 5 times with 250 µL of 1X PBS. We added 200 µL of blocking solution per well and incubate for 2 hours at room temperature on an orbital shaker and wash again 3 times with 250 µL of 1X PBS. 100 µL of the diluted anti-DNP antibody were added to all wells and incubate for 1 hour at room temperature on an orbital shaker. The strip wells were washed 3 times with 1X PBS and added 100 µL of the diluted HRP conjugated secondary antibody to all wells and incubate for 1 hour at room temperature on an orbital shaker. In the next step after

repeated washing, warm substrate solution was added to each well and incubated at room temperature on an orbital shaker. Actual incubation time was 10 minutes. After stopping the enzyme reaction by adding 100 µL of stop solution to each well, results were read immediately. We used 450 nm as the primary wave length and calculated the average absorbance of each sample and control. We subtracted the average absorbance of the controls from the average absorbance of the samples (corrected absorbance: CA) and determined the concentration of the carbonyls by inserting the CA in the following equation:

Protein carbonyl (nmol/ml) = [(CA)/(0,011 uM-1)](500 ul/200 ul)

The calculated data then were normalized to protein content and represented in nmol/mg total protein concentration.

5.1.8. Lipid peroxidation assay

Lipid peroxidation was measured using a commercial kit to detect HNE-protein adducts from Cell Biolabs (San Diego, CA, USA) according to the manufacturer's instructions. After ear homogenised in cold 1X PBS by Ultra Turrax, we diluted unknown protein sample to 10 µg/mL in 1X PBS. Each protein sample and HNE-BSA standard were assayed in duplicate or triplicate. We added 100 µL of the 10 µg/mL protein samples or reduced/HNE-BSA standards to the 96-well protein binding plate and incubated at 37 ºC for at least 2 hours. After incubation wells were washed 2 times with 250 µL 1X PBS per well. After the last wash 200 µL of assay diluent was added to each well and incubated for 2 hours at room temperature on an orbital shaker. In next step we washed 3 times with 250 µL of 1X PBS with plate and added 100 µL of the diluted anti-HNE-His antibody to all wells and incubated for 1 hour at room temperature on an orbital shaker. After it plate was washed 3 times with 1X PBS and added 100 µL of the diluted secondary antibody-HRP conjugate to all wells and incubate for 1 hour at room temperature on an orbital shaker. After washing, warm 100 µL of substrate solution were added to each well and incubated it at room temperature on an orbital shaker. Actual incubation time was 10 minutes and stopped the enzyme reaction by adding 100 µL of stop solution to each well. Absorbance of each well was read immediately on a microplate reader using 450 nm as the primary wave length. Reduced BSA standard were absorbance blank. The exact value of each sample was

read off standard curve, normalized to protein, and represented them in mg/mg protein concentration.

5.1.9. Total RNA preparation, reverse transcription and qPCR

Total RNA was prepared using TRIzol (Invitrogen) according to the manufacturer's instructions. RNA was treated with DNase, and 2 µg of RNA was used for reverse transcription (RT). cDNA was purified on QIAquick PCR cleanup columns (Qiagen, Valencia, CA, USA). 10X diluted cDNA were used for quantitative PCR (qPCR) reactions. The qPCR reactions were performed using an ABI 7500 thermal cycler (Applied Biosciences, Foster City, CA, USA) and qPCR Supermix (Applied Bioscience) with the primers summarized in Table 3.

Gene names	Primers
18S	GGG AGC CTG AGA AAC GGC GGG TCG GGA GTG GGT AAT TTT
36B4	AGA TTC GGG ATA TGC TGT TGG AAA GCC TGG AAG AAG GAG GTC
ACC1	GAC AGA CTG ATC GCA GAG AAA G TGG AGA GCC CCA CAC ACA
ACC2	CCC AGC CGA GTT TGT CAC T GGC GAT GAG CAC CTT CTC TA
ACO	CCC AAC TGT GAC TTC CAT T GGC ATG TAA CCC GTA GCA CT
ATP5g1	GCT GCT TGA GAG ATG GGT TC AGT TGG TGT GGC TGG ATC A
COX17	CGT GAT GCG TGC ATC ATT GA CAT TCA CAA AGT AGG CCA CC
Cyclophyllin	TGG AGA GCA CCA AGA CAG ACA TGC CGG AGT CGA CAA TGAT
Cyt C	TCC ATC AGG GTA TCC TCT CC GGA GGC AAG CAT AAG ACT GG
Dio2	GCA CGT CTC CAA TCC TGA AT TGA ACC AAA GTT GAC CAC CA
eNOS	GCA ATC TTC GTT CAG CCA TCA C AGA GCT CAG TGA TCT CCA CGT TG
ERRα	ACT GCC ACT GCA GGA TGA G CAC AGC CTC AGC ATC TTC AA
E-Selectin	GGC AGA GTG AGA TTT GAA GGA TG GGA CTT CAG CGT CAC TTT GGT AG
G6Pase	CCG GAT CTA CCT TGC TGC TCA CTT T TAG CAG GTA GAA TCC AAG CGC GAA AC

GK	ACA TTG TGC GCC GTG CCT GTG AA AGC CTG CGC ACA CTG GCG TGA AA
I-CAM	CTT TCG ATC TTC CAG CTA CCA TC CTG CTG TTT GTG CTC TCC TG
IL-1β	CAA CCA ACA AGT GAT ATT CTC CAT G GAT CCA CAC TCT CCA GCT GCA
L-CAM	GGC AGA GTG AGA TTT GAA GGA TG GGA CTT CAG CGT CAC TTT GGT AG
iNOS	GAA GTG CAA AGT CTC AGA CAT GG GAT TCT GGA ACA TTC TGT GCT GTC
Malic enzyme	GCC GGC TCT ATC CTC CTT TG TTT GTA TGC ATC TTG CAC AAT CTT T
MCAD	GAT CGC AAT GGG TGC TTT TGA TAG AA AGC TGA TTG GCA ATG TCT CCA GCA AA
MCP-1	CTC AGC CAG ATG CAG TTA ACG CTC TCT CTT GAG CTT GGT GAC A
mCPT1	TTG CCC TAC AGC TGG CTC ATT TCC GCA CCC AGA TGA TTG GGA TAC TGT
MHCI	GAG TAG CTC TTG TGC TAC CCA GC AAT TGC TTT ATT CTG CTT CCA CC
MHCIIA	GCA AGA AGC AGA TCC AGA AAC GGT CTT CTT CTG TCT GGT AAG TAA GC
MHCIIX	GCA ACA GGA GAT TTC TGA CCT CAC CCA GAG ATG CCT CTG CTT C
MIP-1α	CTC TGC AAC CAA GTC TTC TCA GC AAG GCT GCT GGT TTC AAA ATA GTC
MIP-2	CTC CAG CCA CAC TTC AGC CTA G CGT CAC ACT CAA GCT CTG GAT G
MMP-9	CAT TCG CGT GGA TAA GGA GT ACC TGG TTC ACC TCA TGG TC
Myoglobin	CTG ACG AAG GCC ACT TTG CAC CTC TG GCA CAA GAT CCC GGT CAA GTA CCT GGA G
Ndufa2	GCA CAC ATT TCC CCA CAC TG CCC AAC CTG CCC ATT CTG AT
Ndufa3	TAC CAC AAA CGC AGC AAA CC AAG GGA CGC CAT TAG AAA CG
Ndufb5	CTT CGA ACT TCC TGC TCC TT GGC CCT GAA AAG AAC TAC G
PARP-1	GGA GCT GCT CAT CTT CAA CC GCA GTG ACA TCC CCA GTA CA
PEPCK	CCA CAG CTG CTG CAG AAC A GAA GGG TCG CAT GGC AAA
PGC-1α	AAG TGT GGA ACT CTC TGG AAC TG GGG TTA TCT TGG TTG GCT TTA TG
PPARα	CCT GAA CAT CGA GTG TCG AAT AT GGT TCT TCT TCT GAA TCT TGC AGC T

SREBP1	GGC CGA GAT GTG CGA ACT TTG TTG ATG AGC TGG AGC ATG T
TIMP-2	CGT TTC TTT GGG GTT TCT GA TTT ATC ACT AAC AAT ATA GAC AGC CAC TCT
TNFα	CAT CTT CTC AAA ATT CGA GTG ACA A TGG GAG TAG ACA AGG TAC AAC CC
Troponin I	CCA GCA CCT TCA GCT TCA GGT CCT TGA T TGC CGG AAG TTG AGA GGA AAT CCA AGA T
UCP1	GGC CCT TGT AAA CAA CAA AAT AC GGC AAC AAG AGC TGA CAG TAA AT
UCP2	TGG CAG GTA GCA CCA CAG G CAT CTG GTC TTG CAG CAA CTC T
UCP3	ACT CCA GCG TCG CCA TCA GGA TTC T TAA ACA GGT GAG ACT CCA GCA ACT T
V-Cam	TAC CAG CTC CCA AAA TCC TG TCT GCT AAT TCC AGC CTC GT

Table 3. List of primers

5.1.10. Transcription factor transactivation studies

Transfactor Extraction kit (Clontech, Mountain View, CA, USA) was used for nuclear protein extraction according to the manufacturer's instructions as described below. Ears were frozen in liquid nitrogen and were ground into fine powder in a mortar cooled in liquid nitrogen. All further procedures were performed on ice with ice-cold reagents and equipment. The powdered sample was re-suspended in a small volume of ice-cold PBS and was consequently centrifuged at 450 *g* for 5 min at 4 ^{o}C. The pellet was resuspended in lysis buffer (10 mM HEPES, pH 7.9), 1.5 mM $MgCl_2$, 10 mM KCl, 1 mM DTT and protease inhibitor cocktail, Roche) and was disrupted repeatedly pressing through a syringe fitted with a No. 26 gauge needle (obtained from 10 times each). The disrupted tissue lysate was then centrifuged at 11,000 *g* for 20 min, the supernatant removed and the nuclear pellet resuspended in extraction buffer (20 mM HEPES (pH 7.9), 1.5 mM $MgCl_2$, 0.42 M NaCl, 0.2 mM EDTA, 25% (v/v) glycerol, 1 mM DTT and protease inhibitor cocktail). The nuclei were then disrupted with a syringe fitted with a No. 26 gauge needle (10 times each) and centrifuged for 5 min at 21,000 *g*. Protein concentration of the supernatant (nuclear extract) was measured with Bradford protein assay. For the quantification of transcription factor transactivation, the TransFactor Inflammatory Profiling-1 kit was utilized (Clontech). The kit enables the colorimetric determination of the DNA binding of the active transcription factors using

an ELISA-based technique. 10 µg ear nuclear extract was loaded into each well and the measurement was performed according to the Manufacturer's instructions. The results are expressed as fold increase of the WT non-sensitized control samples.

5.1.11. mtDNA analysis

Select mouse tissues were homogenized and digested with Proteinase K overnight in a lysis buffer for DNA extraction by conventional phenol-chloroform method for direct analysis of liberated nucleic acids. Quantitative PCR was performed in duplicate, using 10 µM each primer (mtDNA specific PCR (16S rRNA), forward 5'- CCG CAA GGG AAA GAT GAA AGA C -3', reverse 5'- TCG TTT GGT TTC GGG GTT TC -3'; and nuclear specific PCR (hexokinase 2 gene, intron 9), forward 5'- GCC AGC CTC TCC TGA TTT TAG TGT -3', reverse 5'- GGG AAC ACA AAA GAC CTC TTC TGG -3') and LightCycler 480 SYBR Green I Master PCR Kit (Roche) in a LightCycler 480 Real-Time PCR system (Roche) with a program of 10 minutes at 95 °C, followed by 50 cycles of 15 seconds at 95 °C, 20 seconds at 60 °C. Single-product amplification was verified by an integrated post-run melting curve analysis. Exponential amplification efficiency was verified during each PCR run using a standard dilution series made from pooled samples. Results were calculated from the difference in threshold cycle (ΔC_T) values for mtDNA and nuclear specific amplification (Lagouge *et al.*, 2006).

5.1.12. Statistical analysis

Results were expressed as means ± SEM. Statistical significance between groups was determined by Student's t-test, $p<0.05$ was considered as significant. Error bars represent ± SEM.

6. Results

6.1. Role of PARP-1 in oxazolone-induced contact hypersensitivity

6.1.1. Characterization of the oxazolone-induced contact hypersensitivity reaction in PARP-1$^{-/-}$ mice

Ear swelling was determined 24 hours after OXA challenge. OXA challenge in PARP-1$^{+/+}$ mice caused twelve fold ear swelling compared to vehicle-sensitized animals (0,875 ± 0,07 μm vs. 10,5 ± 0,91 μm), while OXA-induced ear swelling was significantly reduced in the PARP-1$^{-/-}$ mice (1,4 ± 0,52 μm vs. 7,33 ± 1,23 μm) (Fig. 11A).

To assess immune cell infiltration, myeloperoxidase (MPO) activity was evaluated. MPO activity, indicative of the neutrophil infiltration, showed similar changes to ear swelling. PARP-1$^{-/-}$mice were protected against the OXA-evoked increase in MPO activity (Fig. 11B). The degree of protection provided by the PARP-1$^{-/-}$ phenotype was similar to the one previously observed in mice treated with the PARPinhibitor, PJ34 (Bai *et al.*, 2009).

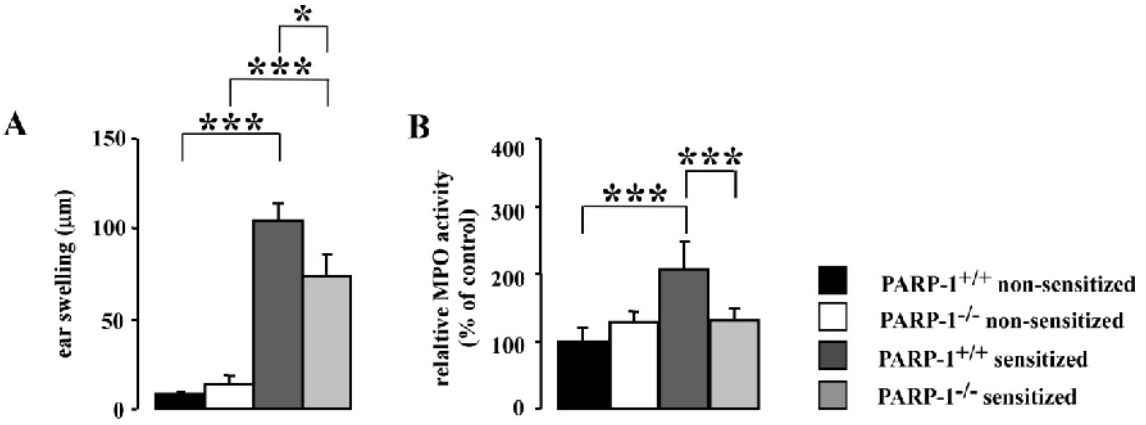

Figure 11. PARP-1$^{-/-}$ mice are protected against the oxazolon-induced CHS reaction.
(A) Oxazolon (10 μl, 0.5% w/v in acetone:olive oil mixture, 1:4 ratio) was spread on both sides of the ears of female mice PARP-1 (n=6 CTL PARP-1$^{+/+}$; n=6 OXA PARP-1$^{+/+}$; n=7 CTL PARP-1$^{-/-}$; n=9 OXA PARP-1$^{-/-}$, 12 weeks) one week after sensitization. Ear thickness was measured before and 24 hours after challenge by a calliper and was expressed as the difference of the values. **(B)** At 24 hours after OXA challenge, ears were removed and MPO activity was determined in the supernatants of ear homogenates spectrophotometrically at 650 nm 37 ^{o}C. Absorbance were normalized to protein and expressed as % of PARP-1$^{+/+}$ non-sensitized mice. Asterisks indicate significant difference between cohorts, where * p<0,05; *** p<0,001.

Oxazolone has strong irritative properties, therefore we set out to investigate whether PARP-1 might influence irritative dermatitis for which we applied a 12-O-tetradecanoyl-phorbol 13-acetate (PMA)-induced irritative dermatitis model. Similarly, to our previous observations with the PARP inhibitor compound PJ34, the PARP-$1^{-/-}$ phenotype also conferred partial protection against the PMA-induced irritative dermatitis both at the level of ear swelling (34,17 ± 0,73 μm vs. 30,63 ± 0,51 μm) and MPO activity (Fig. 12A, B). We detected marked cellular infiltration upon PMA-induction (Fig. 12D) in line with strong induction of matrix metalloproteinase (MMP) activity that was reduced in PARP-$1^{-/-}$ mice (Fig. 12C). Apparently, both the irritative and the immunological components are affected by the loss of PARP-1.

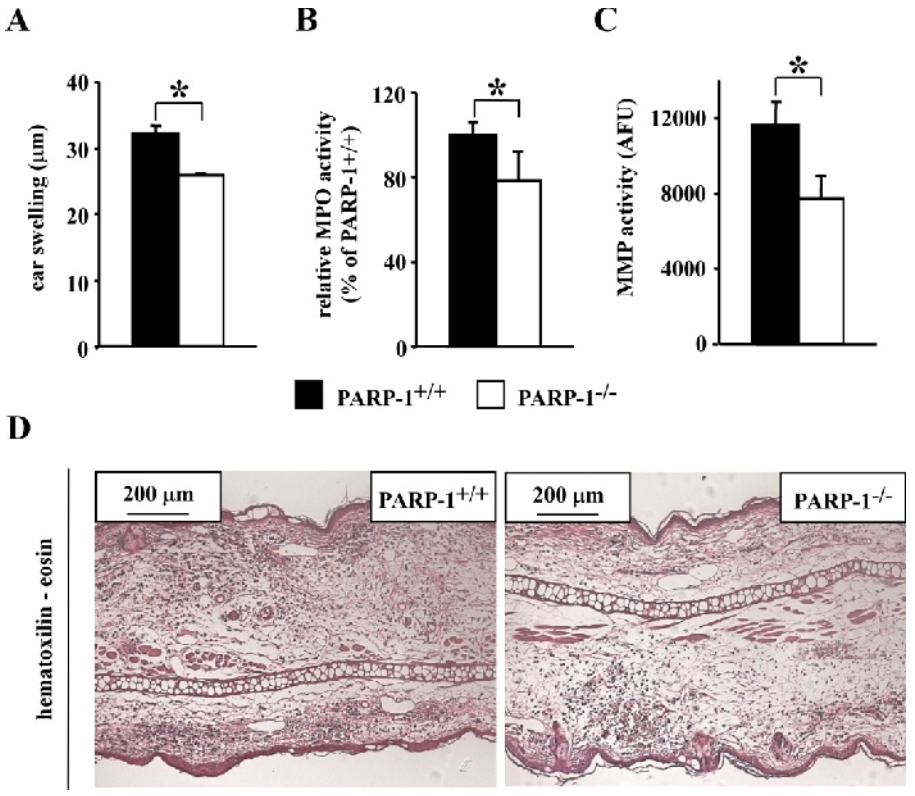

Figure 12. PARP-$1^{-/-}$ mice are protected against the PMA-induced irritative dermatitis.

PMA (10 μl, 0.05% w/v) was smeared onto both sides of the ears of female mice PARP-1 (n=6 CTL PARP-$1^{+/+}$; n=6 OXA PARP-$1^{+/+}$; n=7 CTL PARP-$1^{-/-}$; n=9 OXA PARP-$1^{-/-}$; 12 weeks) After 24 hours, **(A)** ear swelling and **(B)** MPO activity was determined. Absorbance were normalized to protein and expressed as % of PARP-$1^{+/+}$ non-sensitized mice. MMP activity **(C)** was measured in ear homogenates normalized for protein content. **(D)** Formalin-fixed, 7 μm paraffin-embedded tissue sections were stained with haematoxylin and eosin (HE).

Changes in MPO activity suggested similar changes in inflammatory cell infiltration therefore we investigated HE colored histology sections. Histology examination revealed inflammatory cell infiltration in the ear upon OXA challenge which was markedly reduced in the PARP-1$^{-/-}$ mice (Fig. 13A). This is in good correlation with ear swelling and MPO activity as presented on Fig 10. Using cell type-specific markers, we identified predominant neutrophil infiltration. In line with the suppressed inflammatory response, neutrophil infiltration was markedly reduced in the PARP-1$^{-/-}$ mice (Fig. 13B).

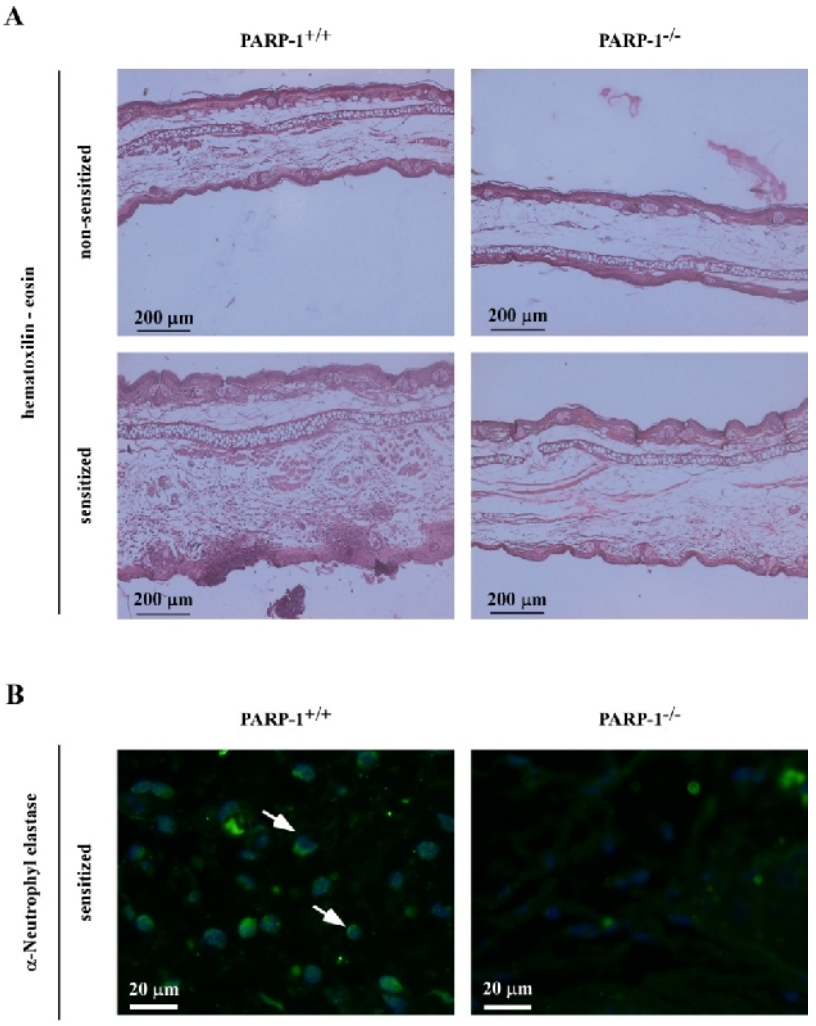

Figure 13. Genetic ablation of PARP-1 suppresses inflammatory cell immigration. **(A)** Formalin-fixed, 7 µm paraffin-embedded tissue sections were stained with HE and **(B)** for neutrophil elastase, with 4,6-diamidino-2-phenylindole (DAPI) nuclear counterstained as described in Materials and Methods. The arrows point at the neutrophil elastase-positive cells.

6.1.2. Lack of oxidative/nitrosative stress in PARP-1$^{-/-}$ mice

Leukocytic infiltration is usually accompanied by the production of reactive oxygen and nitrogen species, such as hydrogen peroxide and peroxynitrite. Moreover, these oxidants were shown to influence redox-sensitive transcription factors that prompted us to investigate oxidative stress and its related biochemical events in OXA-induced CHS.

As the endothelial and the inducible nitric oxide synthase enzymes (eNOS and iNOS, respectively) can be considered as the most important sources of NO in the ear under inflammatory conditions, their expression was assessed. Although eNOS expression was lower in the PARP-1$^{-/-}$ mice as compared to PARP-1$^{+/+}$, eNOS expression did not change upon OXA-treatment (Fig. 14A). Therefore eNOS is probably not the major source of NO under inflammatory conditions. Similarly to eNOS, iNOS expression was lower in the PARP-1$^{-/-}$ animals than in PARP-1$^{+/+}$ mice. Importantly, iNOS expression increased markedly upon OXA-challenge, while only mild induction was observed in the OXA-treated PARP-1$^{-/-}$ mice (Fig. 14A). Apparently, iNOS appears to be the major source of NO in our model system. This is in line with other findings obtained in different models of inflammation.

Nitrosative stress is indicated by the formation of protein tyrosine nitration, which could be observed in the ears of wild type but not that of PARP-1$^{-/-}$ mice (Fig. 14B). Nitrotyrosine staining could be detected in the infiltrating cells and in the keratinocytes with strongest immunopositivityseen in the microabscessi, where widespread keratinocyte death has previously been described.

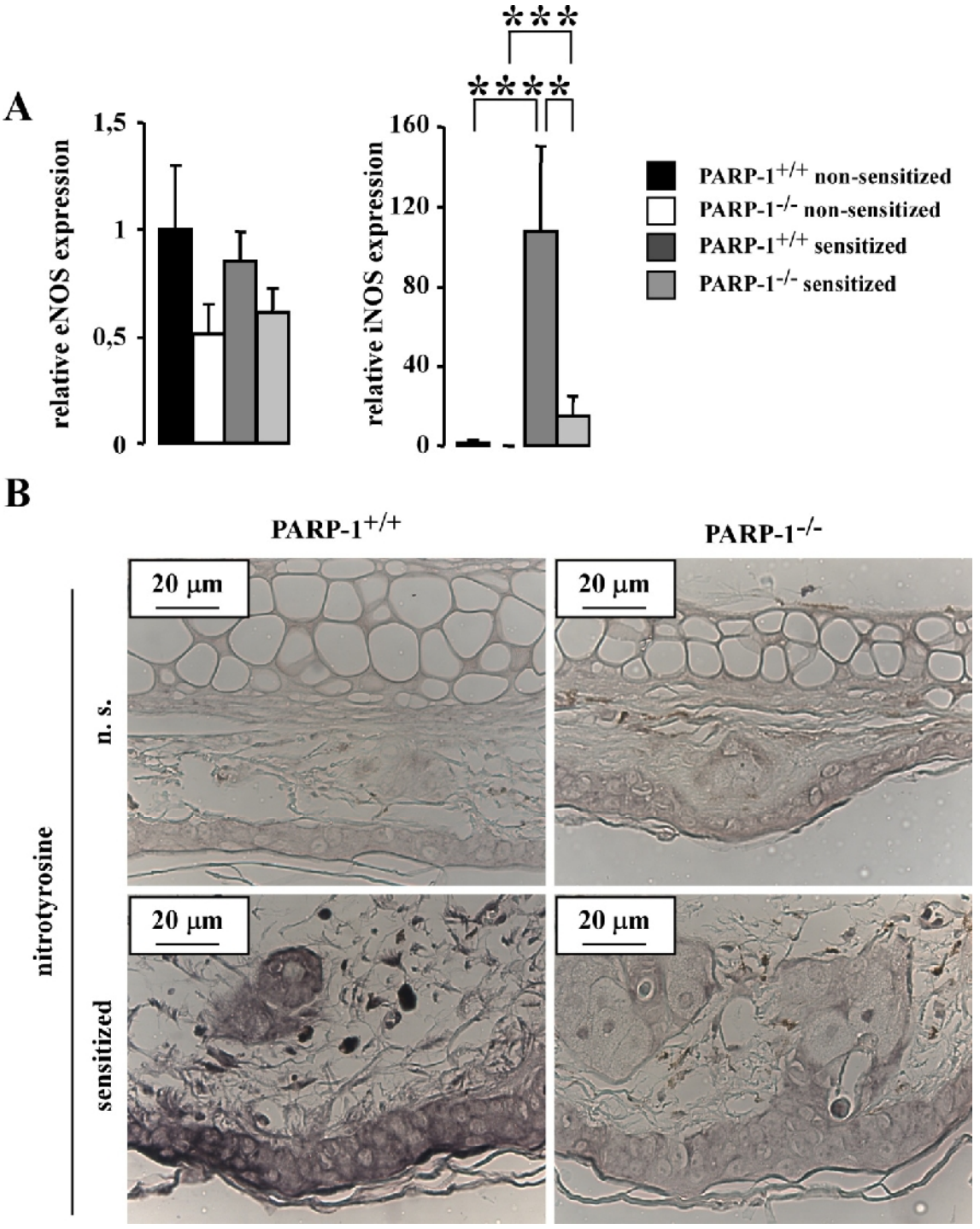

Figure 14. Reduced nitrosative stress in PARP-1$^{-/-}$ mice.
(A) Expression of eNOS and iNOS were determined by qRT-PCR (n=6 CTL PARP-1$^{+/+}$; n=6 OXA PARP-1$^{+/+}$; n=7 CTL PARP-1$^{-/-}$; n=9 OXA PARP-1$^{-/-}$; 12 weeks). Expression values were normalized to the geometric mean of 36B4, cyclophyllin and 18S expression then to the values of non-sensitized PARP-1$^{+/+}$ mice. **(B)** Nitrotyrosine immunohistochemistry was performed on formalin-fixed, 7 µm paraffin-embedded tissue sections as described in Materials and Methods. Asterisks indicate significant difference between cohorts, where * $p<0,05$; *** $p<0,001$.

Nitrosative stress is accompanied by the enhanced production of reactive oxygen species. In CHS, increased level of ROS was indicated by increased lipid, protein and DNA base oxidation (as shown by protein carbonylation (oxa PARP-$1^{+/+}$ 14,23 ± 3,06; oxa PARP-$1^{-/-}$ oxa 8,32 ± 2,90), protein-4-hydroxy-2-nonenal (HNE) adduct (oxa PARP-$1^{+/+}$ 12,42 ± 4,95; oxa PARP-$1^{-/-}$ 7,59 ± 0,97)and 8-OHdG (oxa PARP-$1^{+/+}$ 3,69 ± 0,21; oxa PARP-$1^{-/-}$ 2,31 ± 0,25) formation) that was all reduced in the PARP-$1^{-/-}$ mice (Fig. 15A-C).

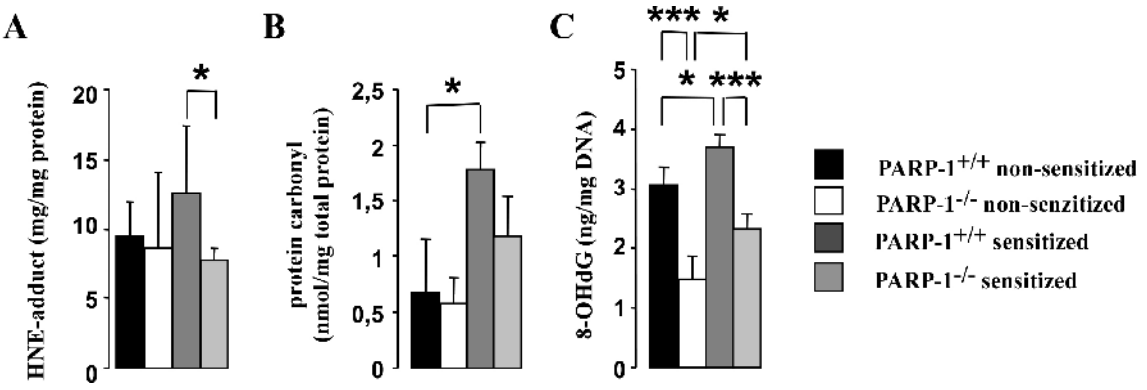

Figure 15. Reduced oxidative stress and DNA damage in PARP-$1^{-/-}$ mice
(A) HNE-adduct, **(B)** protein carbonyl and **(C)** 8-hydroxy-2'-deoxyguanosine (8-OHdG) were determined in the ear extracts of PARP-$1^{+/+}$ and PARP-$1^{-/-}$ mice (n=6 CTL PARP-$1^{+/+}$; n=6 OXA PARP-$1^{+/+}$; n=7 CTL PARP-$1^{-/-}$; n=9 OXA PARP-$1^{-/-}$; 12 weeks) as described in Materials and Methods. Asterisks indicate significant difference between cohorts, where *p< 0,05; ***p<0,001.

Oxidative and nitrosative stress can induce DNA breakage and PARP activation. Therefore, we set out to investigate DNA strand breakage by TUNEL assay. DNA strand breaks appeared in keratinocytes, endothelial cells and leukocytes (Fig. 16A) in PARP-$1^{+/+}$ mice. There were high number of TUNEL-positive cells in the microabscessi suggesting intense oxidative stress (Fig. 16A). The number of TUNEL-positive cells was reduced in the PARP-$1^{-/-}$ subjects. DNA strand breaks lead to PARP-1 activation resulting in the formation of PAR. A nuclear PAR signal could be detected in the PARP-$1^{+/+}$ mice which was absent in the PARP-$1^{-/-}$ animals (Fig. 16B). PAR was present in most cell types in the ear.

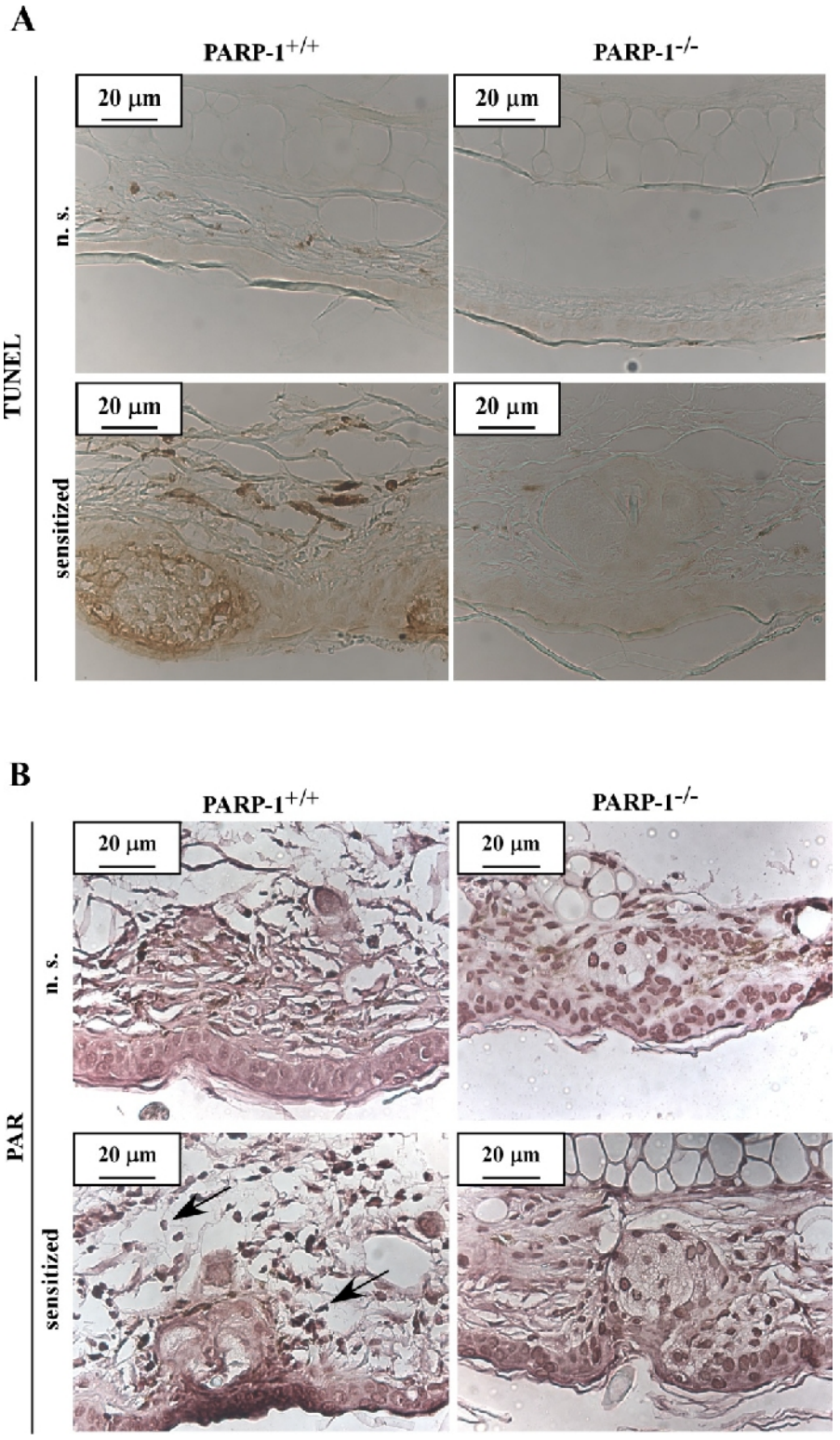

Figure 16. Poly(ADP-ribose) polymerase (PARP) activity is decreased in PARP-1 $^{-/-}$ mice.

(**A**)TUNEL assay and **(B)** PAR immunohistochemistry were performed on formalin-fixed, paraffin-embedded tissue sections as described in Materials and Methods. n.s.: non-sensitized. The arrows point at PAR-positive nuclei.

6.1.3. PARP-1 mediated gene expression in oxazolone-induced contact hypersensitivity

The infiltration and migration of polymorphonuclear leukocytes is facilitated by appearance of proinflammatory cytokines and chemokines. Therefore, we investigated their expression. On the course of the CHS reaction, we observed the induction of MIP-1α, MIP-2, IL-1β, MCP-1 and TNFα. A reduced expression of all of these cytokines/chemokines has been observed in the PARP-$1^{-/-}$ mice (Fig. 17A.).

Cellular extravasation and infiltration under inflammatory conditions require the concerted expression of different cell adhesion molecules such as I-CAM, L-CAM, V-CAM and E-Selectin. OXA challenge induced I-CAM, L-CAM, V-Cam and E-Selectin expression in the WT mice that was absent in the PARP-$1^{-/-}$ mice (Fig. 17B).

In addition to adhesion molecules, leukocytes also express MMPs in order to facilitate their movements in tissues. MMPs are secreted as zymogens that are subsequently activated by either proteolytic cleavage or free-radical-induced structural changes. We have observed the induction of MMP-9 upon OXA challenge in the PARP-$1^{+/+}$ mice. However, MMP-9 induction was impaired in the PARP-$1^{-/-}$ mice (Fig. 17C).

MMP activity is controlled by tissue inhibitors of metalloproteinases (TIMP1-4). Interestingly, TIMP2 was down-regulated in PARP-$1^{+/+}$ mice, which may support higher MMP-9 activity (Fig. 17C). On the contrary, TIMP2 expression was not reduced in PARP-$1^{-/-}$ mice.

PARP-1 interacts with a plethora of transcription factors and modulates their activity, hence gene expression. We hypothesized that the absence of PARP-1 protein and the consequent loss of PARP-1 activity may be the underlying mechanism for the altered expression of inflammatory mediators. We assessed the activation of a number of transcription factor in the ears. We have observed the strong activation of two redox-sensitive transcription factors, p65, a member of the NF-κB family and activating transcription factor-2 (ATF-2) upon OXA-sensitization in the PARP-$1^{+/+}$ mice (Fig. 17D). Interestingly, the activation of other members of the REL family such as p50 and c-Rel was not detectable. The activation of p65 was completely absent in the PARP-$1^{-/-}$ mice. ATF-2 showed a similar pattern to p65, though its activity was only partially reduced in the knockout mice (Fig.17D).

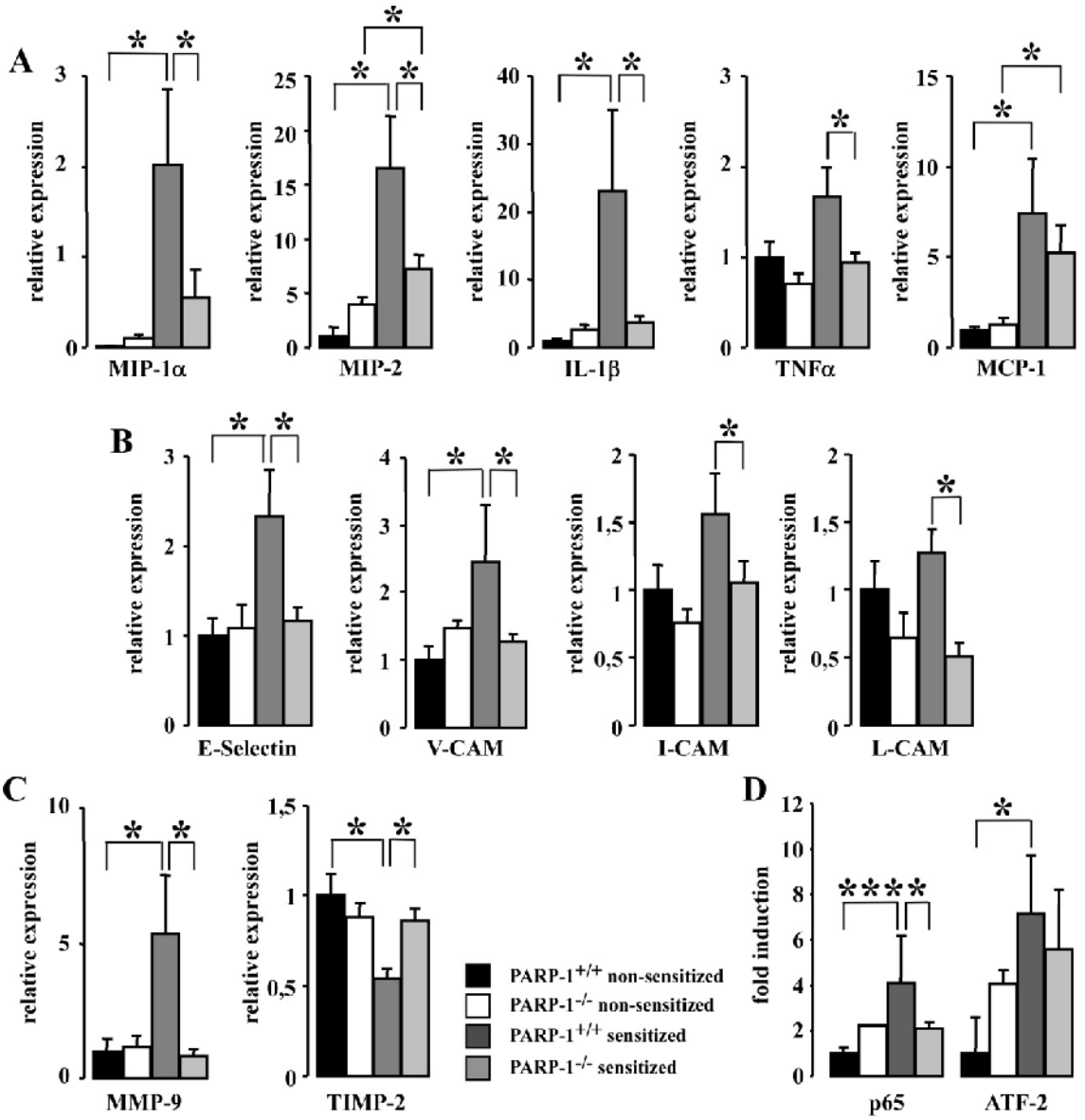

Figure 17. Expression of proinflammatory genes is suppressed in PARP-1$^{-/-}$ mice. Expression of **(A)** a set of a proinflammatory cytokines, **(B)** adhesion molecules, **(C)** MMP-9 and TIMP-2 were determined by qRT-PCR. **(D)** Transcription factor activation was determined using TransFactor kit (n=6 CTL PARP-1$^{+/+}$; n=6 OXA PARP-1 $^{+/+}$; n=7 CTL PARP-1$^{-/-}$; n=9 OXA PARP-1$^{-/-}$; 12 weeks). Expression values were normalized to the geometric mean of 36B4, cyclophyllin and 18S expression then to the values of non-sensitized PARP-1$^{+/+}$ mice. Asterisks indicate significant difference between cohorts, where * p<0,05; *** p<0,001. Abbreviations are in the text. Primer sequences are listed in primer Table 3.

6.2 Transcriptional changes affected by the PARP-1 SIRT1 interdependence

6.2.1. Brown adipose tissue and muscle, but not liver from PARP-1$^{-/-}$ mice have higher mitochondrial content

Large amount of literature data suggest (Cai *et al.*, 2006; Caito *et al.*, 2010; El Ramy *et al.*, 2009; Pillai *et al.*, 2005; Rajamohan *et al.*, 2009) that PARP-1 and SIRT1 interact and hence PARP-1 may interfere with transcriptional activities of SIRT1 which was further supported by the metabolic changes observed in skeletal muscle and BAT upon the genetic deletion of PARP-1. To gain insight into these changes we assessed the expression of genes responding to SIRT1 that was shown by assessing the acetylation level of PGC-1α (Fig. 2D and F in (Bai *et al.*, 2011)) in different *in vivo* and cellular models. First we investigated BAT with transmission electron microscopy that (Fig 1M in (Bai *et al.*, 2011)) revealed higher mitochondrial content in PARP-1$^{-/-}$ BAT, which was further corroborated by the increased mitochondrial DNA content (Fig. 18A). This higher mitochondrial DNA content in PARP-1$^{-/-}$ mice was in line with increased expression of genes involved in mitochondrial uncoupling (UCP1 and UCP3), fatty acid oxidation (MCAD) and respiration (Ndufa2, Ndufa3, Ndufb5, Cyt C, COX17) (Fig.18B). Additionally, the expression of Deiodinase-2 (Dio2) was higher in PARP-1$^{-/-}$ mice, suggesting increased thyroid hormone activation in the BAT (Fig. 18B). PARP-1$^{-/-}$ skeletal muscle we observed a switch towards a more oxidative profile. Succinate dehydrogenase (SDH) staining (Fig. 1P in (Bai *et al.*, 2011)) and the expression of muscle fiber isotype Troponin I (Trop I), Myosin heavy chain I (MHCI) (Fig. 18C) indicated an increase in the number of oxidative fibers, characterized by a higher mitochondrial content than glycolytic fibers.

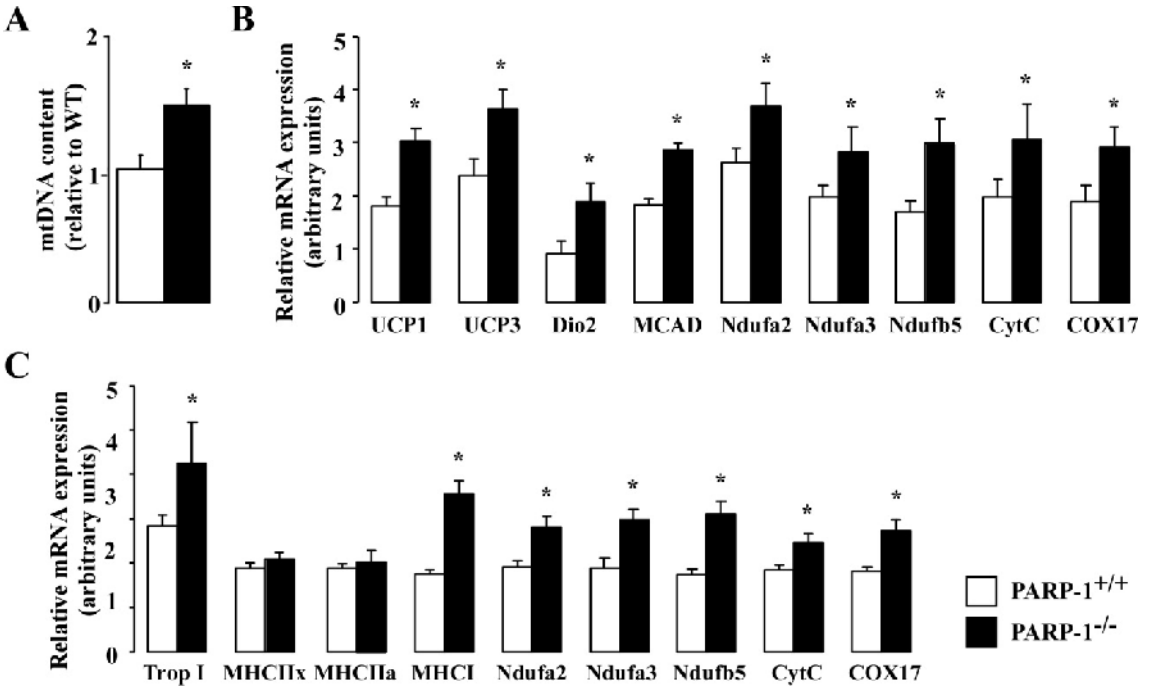

Figure 18. Increased mitochondrial mRNA expression in brown adipose tissue (BAT) and gastrocnemius muscle of PARP-1$^{-/-}$ mice.
(A) BAT mitochondrial DNA (mtDNA) and **(B)** mRNA levels of the indicated genes were determined by RT-qPCR in PARP-1$^{+/+}$ and $^{-/-}$ male mice (n=8/9; 46 weeks). **(C)** In gastrocnemius muscles, mRNA levels of the indicated genes were measured by RT-qPCR. Expression values were normalized to cyclophyllin expression. * indicates statistical difference vs. PARP-1$^{+/+}$ mice at $p<0.05$. Abbreviations can be found in the text. Primer sequences are listed in Table 3.

Another crucial tissue for whole body metabolism is the liver. We investigated the expression of a large set of genes, containing genes of the SIRT1 transcriptome, encoding for transcription factors: Estrogen receptor related-α (ERRα), Peroxisome proliferator activated receptor-γ (PPARγ), Peroxisome proliferator- activated receptor-gamma co-activator 1α (PGC-1α), Sterol regulatory element-binding protein (SREBP1) (Fig. 19A) and proteins involved in mitochondrial respiration (Ndufa2, Ndufa3, cyt c, ATP5g1), fatty acid oxidation (MCAD, ACO), fatty acid synthesis (ACC1, ACC2 and Malic enzyme) and glucose metabolism (PEPCK, GK, G6Pase) (Fig. 19B). The lack of significant changes in the expression of this metabolic gene set suggested that the absence of PARP-1 has only a minor metabolic impact in the liver, potentially explained by the very low expression of PARP-1 in the liver relative to skeletal muscle or BAT (Fig. 19C).

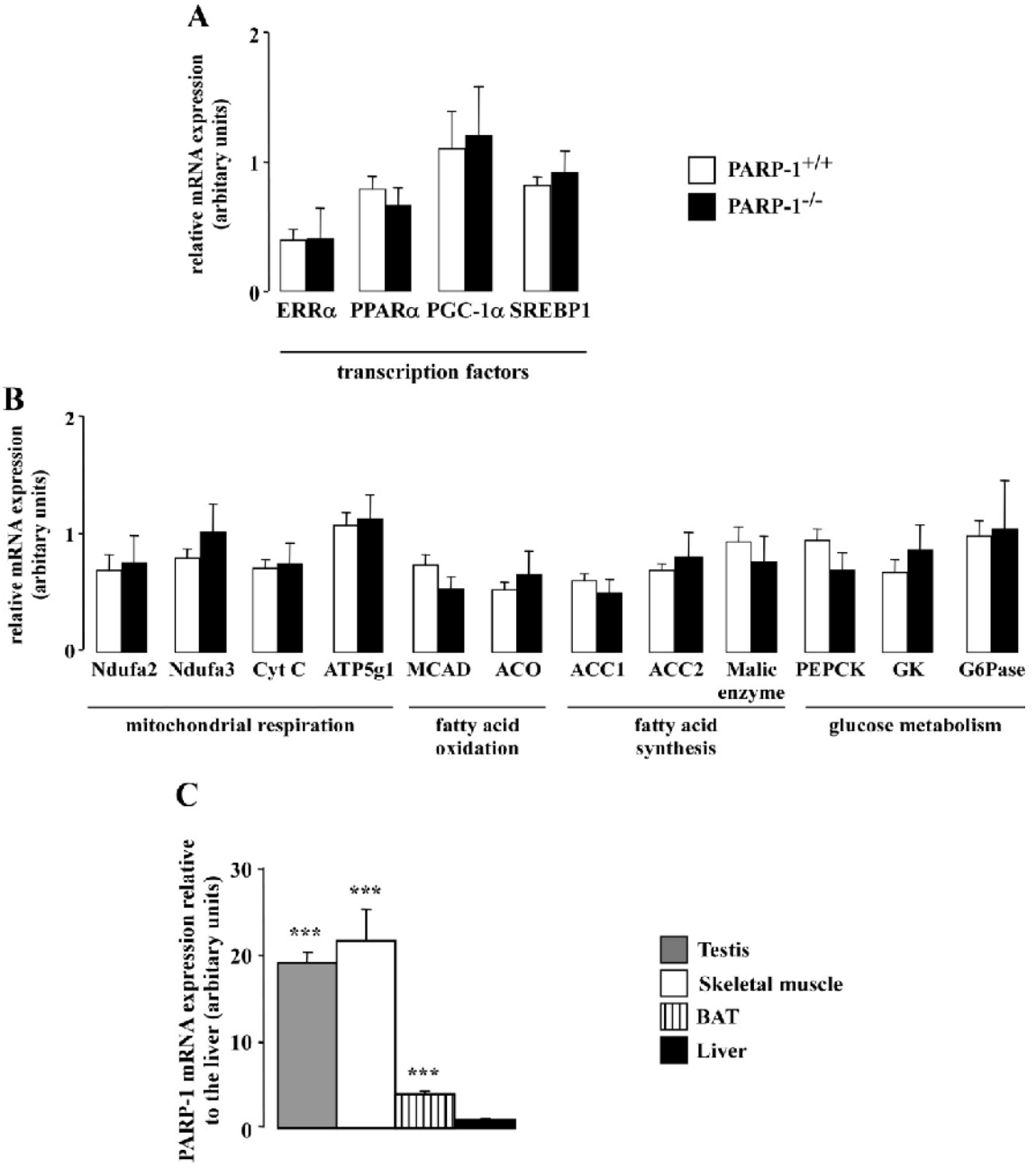

Figure 19. Gene expression pattern of different metabolic genes and Parp-1 in metabolic tissues.

(A); **(B)** mRNA expression levels of selected genes were quantified by RT-qPCR reactions in the liver of PARP-$1^{+/+}$ and $^{-/-}$ male mice (n=9/9; 46 weeks). **(C)** mRNA expression of PARP-1 were quantified in different metabolic tissues of C57/Bl6 male mice (n=5). Expression values were normalized to cyclophyllin expression. Asterisks indicate significant difference between the respective tissue and liver, where *** p<0,001. Abbreviations can be found in the text. Primer sequences are listed in Table 3.

6.2.2. Reduced PARP-1 activity in murine embryonic fibroblasts promotes oxidative metabolism.

Given the relation between PARP-1 and SIRT1 upon the somatic ablation of PARP-1 we next evaluated whether reducing PARP-1 activity in cells could equally bring about the improvement of energy metabolism. For this purpose, we used of MEF cells from PARP-$1^{+/+}$ and PARP-$1^{-/-}$ mice. The reduction of PARP activity in this cell model perfectly recapitulated all expression changes observed *in vivo* findings (Suppl. Fig. 3. in (Bai *et al.*, 2011)), such as higher expression of genes involved in mitochondrial function (e.g. PGC-1α, Ndufb5, Cyt C, COX17, UCP-2, mCPT-1, ACO) (Fig. 20B).

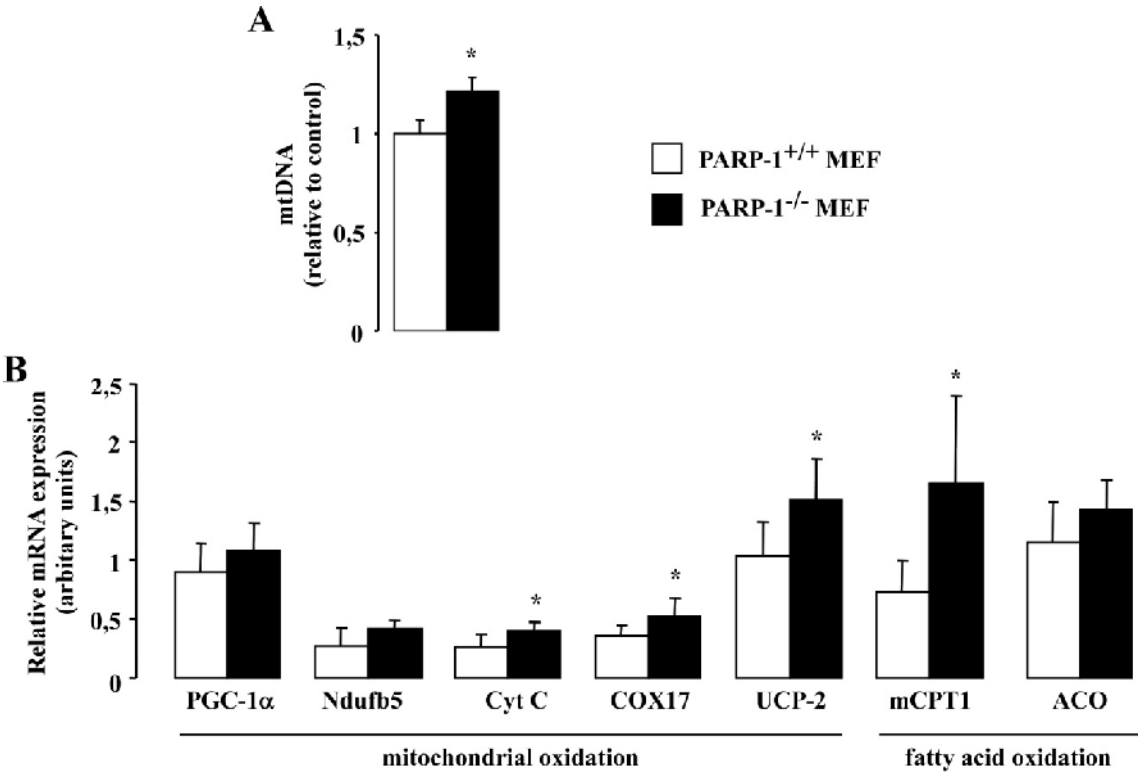

Figure 20. Assessment of mitochondrial expression in PARP-$1^{+/+}$ and $^{-/-}$ MEFs.
In PARP-$1^{+/+}$ and $^{-/-}$ primary MEFs (n=3/3) mitochondrial DNA content **(A)** and mRNA expression **(B)** was determined. Expression values were normalized to cyclophyllin expression. Abbreviations are listed in the text. Asterisks indicate significant difference between cohorts, where * $p<0,05$. Abbreviations can be found in the text. Primer sequences are listed in Table 3.

6.2.3. Pharmacological inhibition of PARP-1 activity enhances oxidative metabolism via SIRT1.

Since genetic ablation of PARP-1 increased the expression of SIRT1-related genes, we turned to investigate whether *in vivo* pharmacological inhibition of PARP-1 could have similar effects.

We injected mice with PJ34 (10 mg/kg) twice a day for 5 days. In muscle, the increase in mitochondrial gene expression (Ndufa2, Ndufb5, UCP2 and UCP3) induced by PJ34 was accompanied by an increase in myoglobin mRNA levels, which facilitate oxygen delivery into muscle fibers (Fig. 21). All of these data indicate that PJ34 treatment phenocopies also *in vivo* part of the oxidative features (Suppl. Fig. 4 in (Bai *et al.*, 2011)) induced by PARP-1 gene deletion.

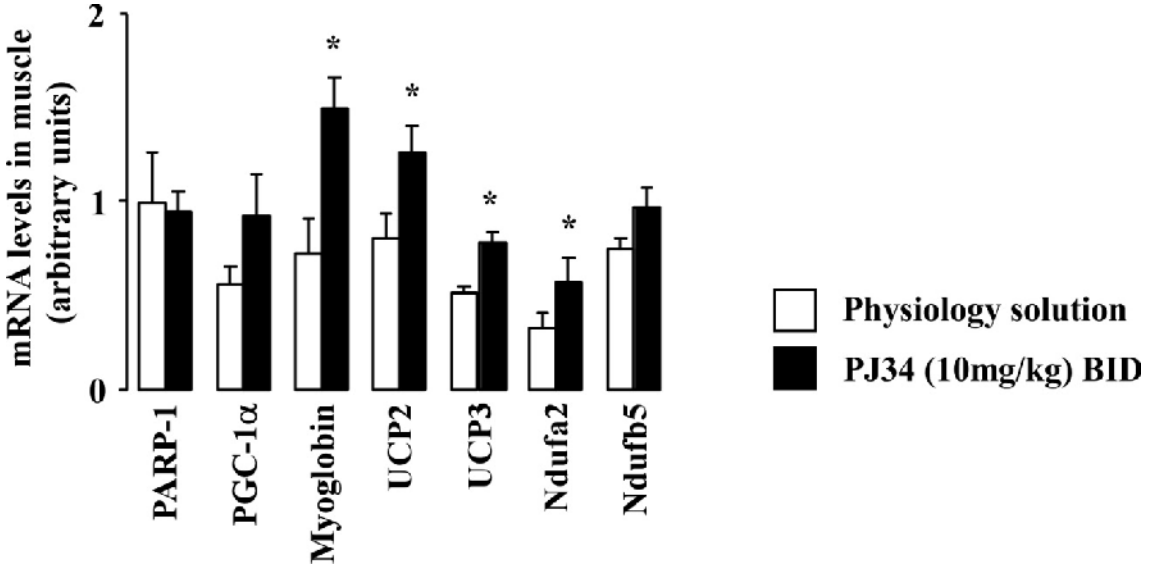

Figure 21. Pharmacological PARP-1 inhibition *in vivo* phenocopies SIRT1 activation.
C57/Bl6 male mice were injected with PJ34 (2 x 10 mg/kg/day i.p.) or saline (n=10/10; 12 weeks) and were sacrificed after 5 days of injections. Then mRNA expression levels of selected genes in gastrocnemius muscle were quantified by RT-qPCR reactions. Expression values were normalized to cyclophyllin expression. Abbreviations are listed in the text. * indicates statistical vs. vehicle-treated group at $p<0.05$. Abbreviations can be found in the text. Primer sequences are listed in Table 3.

7. Discussion

Several studies have proven the major role of PARP-1 in the regulation of transcription (Kraus and Lis, 2003). Our aim was to elucidate the transcriptional role of PARP-1 in relation to skin hypersensitivity inflammatory reaction and to SIRT1 mediated transcription.

7.1. Role of PARP-1 in oxazolone-induced contact hypersensitivity

Several research groups have suggested the importance of PARP-1 in numerous inflammatory processes including some skin inflammations (Virag *et al.*, 2002). The role of PARP activity in CHS has previously been demonstrated by our group (Bai *et al.*, 2009).

PARP inhibition decrease inflammation in mouse model of CHS, where PJ34, a PARP inhibitor, conferred protection (Bai *et al.*, 2009). PJ34 is a panPARP inhibitor and since both PARP-1 and PARP-2 are active members of the PARP family (Sims *et al.*, 1981), both are likely to regulate CHS. In the present work we identified PARP-1 as the main PARP enzyme mediating CHS, since the genetic ablation of PARP-1 proved to be protective against CHS. The level of protection provided by PARP-1 ablation suggests that PARP-1 is the sole PARP involved in CHS. However, there are other PARPs and PARG that exert immune functions (e.g. macroPARPs (Hakme *et al.*, 2008a) or PARG (Frizzell *et al.*, 2009)) that may have additional minor roles.

Oxazolone has strong irritative effect. The involvement of the irritative component was assessed in PMA-induced dermatitis, where PARP-1 provided partial protection. Apparently, the irritative component affects most PARP-1-mediated effects of CHS (MMP activation, infiltration).

It is an interesting notion that PARP-1 ablation did not fully block oedema formation, we observed reduction only by roughly 30%. Apparently the reduction in oedema formation correlated with lower immune function in PARP-$1^{-/-}$ mice, however we have no knowledge about the origin of the remaining 70% that seems PARP-1 independent. It is tempting to speculate whether neurogenic inflammation may account for that portion of ear swelling. Neurogenic inflammation may have important role in airway and skin inflammatory processes (Meggs, 1993). During certain inflammatory processes chemical sensitizers, such as oxazolone, has been described to induce

neurogenic inflammation (Richardson and Vasko, 2002). Therefore it is tempting to speculate that neurogenic inflammation may occur also in our model system.

Upon the induction of CHS we have observed neutrophil infiltration that was accompanied by increased oxidative stress as indicated by increased MPO activity, protein carbonyl production, HNE and 8-OHdG levels. Nitrosative stress was also elevated as illustrated by increased iNOS expression and nitrotyrosine staining similarly to previous findings (Szabo *et al.*, 2001). The high level of reactive species may lead to DNA breakage and PARP activation in keratinocytes, endothelial cells and leukocytes.

In order to characterize inflammatory processes we measured inflammatory molecules such as MIP-1α and-2, IL-1β, TNF-α, and MCP-1. They were induced in CHS and were reduced in PARP-$1^{-/-}$ mice. These chemokines/cytokines are known mediators of CHS (Olmos *et al.*, 2007; Saint-Mezard *et al.*, 2004) and are of different origin (dermal cells, mast cells, or Langerhans cells) possessing pleiotropic effects (Biedermann *et al.*, 2000) leading to the (1) upregulation of cellular adhesion molecules on the surface of the endothelium (McHale *et al.*, 1999); and (2) the recruitment, activation, and proliferation of inflammatory cells (Homey *et al.*, 1998; Lim *et al.*, 2008), culminating in enhanced inflammation.

Moreover, we found different adhesion molecules (I-CAM, L-CAM, V-CAM, and E-selectin) regulated by PARP-1 (Fuchs *et al.*, 2001; Kelly *et al.*, 2007). These molecules support the adherence of leukocytes onto the endothel. Consequently, decrease in the expression of adhesion molecules impairs infiltration of inflammatory cells, as we demonstrated in PARP-$1^{-/-}$ mice. Our observations correspond to the result of Zingerelli and co-workers showing that reduced PARP-1 levels diminish adhesion molecule expression, leading to decreased inflammatory infiltration in murine colitis (Zingarelli *et al.*, 1999). To facilitate diapedesis, leukocytes secrete MMPs in order to help their movements in tissues. MMPs are secreted as zymogens that are subsequently activated by either proteolytic cleavage or free radical-induced structural changes (Le *et al.*, 2007). It has been shown that upon PARP-1 inhibition, or depletion, the activity and protein levels of MMP-9 increases in oxazolone induced CHS (Bai *et al.*, 2009; Kauppinen and Swanson, 2005; Koh *et al.*, 2005). TIMP-1 - 4 regulate the activity of MMP. We have observed the downregulation of TIMP-2 upon OXA challenge, that further enhance MMP-9 activity. However, TIMP-2 downregulation did not take place

in PARP-1$^{-/-}$ mice. This pattern is in alignment with the effects of pharmacological PARP inhibition that also blocked TIMP-2 downregulation (Bai *et al.*, 2009; Oumouna-Benachour *et al.*, 2007).

The concerted changes of iNOS, chemokines, adhesion factors, MMP-9 and TIMP-2 suggest common roots at the level of gene transcription. PARP-1 interacts with numerous transcription factors and modulates their activity. Our hypothesis was that the absence of PARP-1 protein and loss of its activity may be responsible for the transcriptional alterations of inflammatory mediators. In CHS we have identified the activation of two redox-sensitive transcription factors, p65, a member of the NF-κB family and activating transcription factor-2 (ATF-2) from AP-1 family that were suppressed in PARP-1$^{-/-}$ mice.

The defective p65 activation is in line with the reduced expression of numerous NF-κB target genes such as iNOS, adhesion factors and cytokines (Oliver *et al.*, 1999). The direct molecular interaction between PARP-1 and NF-κB has already been described (Hassa and Hottiger, 1999; Oliver *et al.*, 1999). However, the exact molecular mechanism through which PARP-1 affects NF-κB, is not clear yet. It seems that PARP-1 affects DNA binding of NF-κB, but it is of question whether PARP-1 activation is crucial for NF-κB transcriptional activity.

Concerning the AP-1 pathway, PARP-1 can affect phosphorylation of ATF-2 and c-Jun through MKP-1 (Racz *et al.*, 2010). MKP-1 through phosphorylating p38^{MAPK} and JNK/SAPK can influence the activity of AP-1. Therefore the aforementioned changes in phosphorylation levels represent a likely model to explain how hampered ATF-2 activation lead to the repression of inflammation.

DNA breakage may also contribute to the transcriptional regulation through PARP-1. Estrogen receptor activation has been reported to lead to DNA nicking. These DNA nicks need to be repaired for the effective ER–related transcription. PARP-1 activation is crucial for the resolution of these nicks (Ju *et al.*, 2006). Therefore it is tempting to speculate that a similar mechanism may also participate in the activation of NF-κB or ATF-2.

PARP-1 has a central role in the control of oxidative stress in the elicitation phase of CHS (Fig. 22), and its inhibition or genetic deletion disrupts the self-

intensifying propagation of inflammation. Altogether, these results provide further support for the possible therapeutic applicability of PARP inhibitors in CHS.

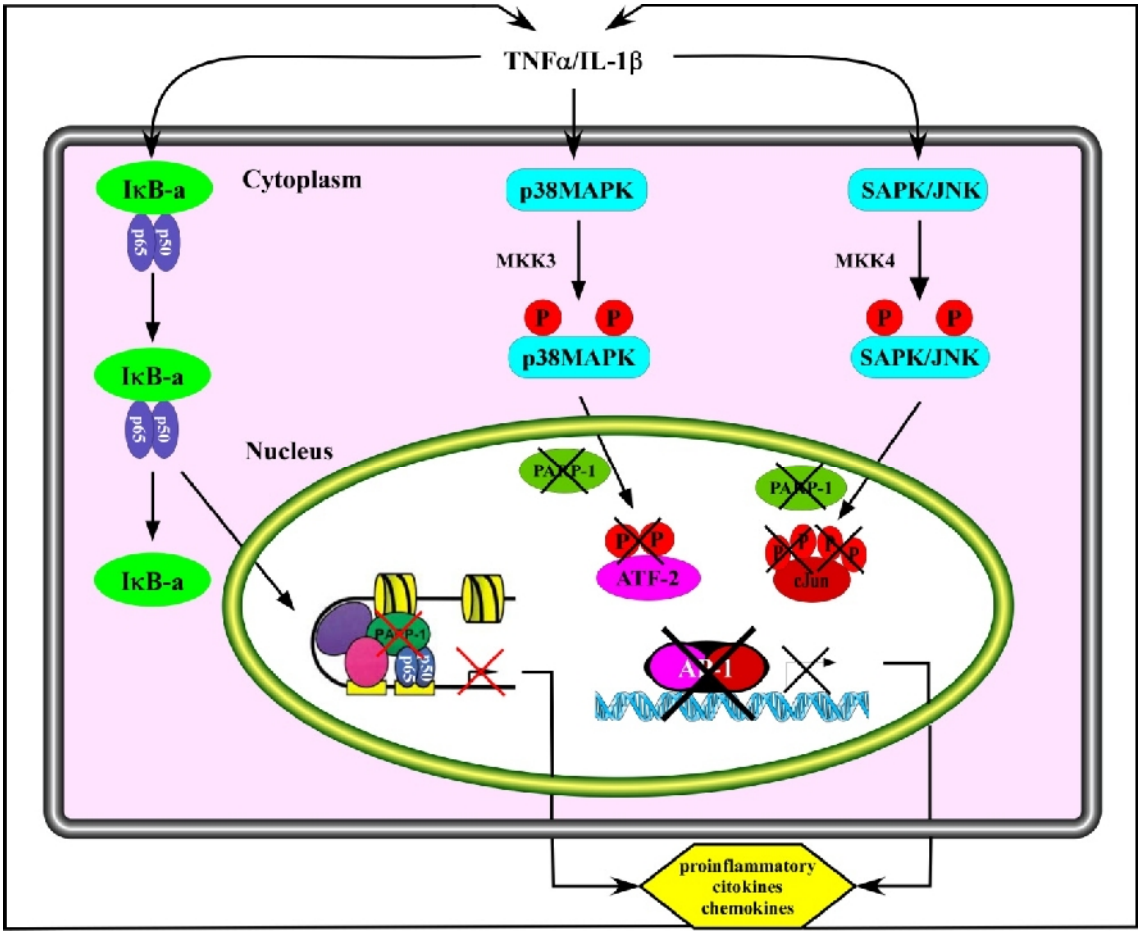

Figure 22. The possible signalling mechanism leading to NFkB or AP-1 – activation and rearrengment of inflammatory gene expression on the course of CHS reaction. NF-κB and AP-1 have crucial roles in the regulation of cytokine induced gene expression. Upon the depletion of PARP-1 NF-κB transactivation decrease hence inflammatory gene expression is quenched. The lack of PARP-1 may block the phosphorilation of ATF-2 or c-Jun thereby AP-1 cannot be formed in the nucleus, hampering gene experession.

7.2. Transcriptional effects of the PARP-1 SIRT1 interplay

Multiple groups have identified links between SIRT1 and PARP-1, where activation of SIRT1 suppresses PARP-1 activity (El Ramy *et al.*, 2009; Kolthur-Seetharam *et al.*, 2006; Pillai *et al.*, 2005; Rajamohan *et al.*, 2009). Physiological observations revealed that PARP-$1^{-/-}$ mice have less body fat than PARP-$1^{+/+}$ littermates. PARP-$1^{-/-}$ mice consumed more O_2 than PARP-$1^{+/+}$ mice. PARP-$1^{-/-}$ mice also maintained higher body temperature upon cold exposure, were more glucose tolerant and had a trend towards lower fasting blood glucose levels despite similar insulin levels. These observations were affirmed upon high fat feeding experiments where PARP-$1^{-/-}$ retained glucose tolerance and insulin sensitivity. In line with the amelioration of metabolic parameters, improved mitochondrial content and activity was observed.

As PARP-1 is a major NAD^+ consumer (Sims *et al.*, 1981), we speculated that the lack of PARP-1 activity might increase NAD^+-content, in turn activating SIRT1. Our group demonstrated that NAD^+-levels increased in BAT and muscle of PARP-1 knockout mice (Fig. 2B, 2C in (Bai *et al.*, 2011)). At the same time, increased PGC-1α and FOXO1 deacetylation and the induction of SIRT1-specific genes were revealed in BAT and muscle (Fig. 2D, 2E in (Bai *et al.*, 2011)), which is an indicator of enhanced SIRT1 activation. We observed similar increase of SIRT1 activity in PARP-1 depleted HEK293T and MEF cells where we encountered with similar gene expression changes as in PARP-$1^{-/-}$ mice. In both cases, mitochondrial content and oxidative metabolism was also enhanced. Furthermore, in mice treated with PJ34, PARP activity was suppressed and SIRT1 activity was induced by decreased PGC-1α acetylation and induction of genes of oxidative metabolism (Fig. 4H, 4I in (Bai *et al.*, 2011)). Importantly, most of the metabolic effects elicited by PARP-1 depletion were lost when SIRT1 was simultaneously knocked-down (Fig. 4J in (Bai *et al.*, 2011)).

It is possible that endogenous oxidants leaking out of mitochondra (in the BAT and muscle due to high oxidative metabolism (Barja, 1992) maintain a high basal PARP activity that leads to a constant NAD^+ turnover. Therefore, when NAD^+ degradation by PARP-1 is inhibited, it causes significant increases in cellular NAD^+. Our group demonstrated that attenuation of PARP-1 activity impacts on metabolic homeostasis by increasing intracellular NAD^+ content (Bai *et al.*, 2011) and SIRT1 activity (Bai *et al.*,

2011). SIRT1 activation then prompts the deacetylation and activation of key metabolic transcriptional regulators such as PGC-1α and FOXO1 (Bai *et al.*, 2011), and subsequently increases mitochondrial content and oxidative metabolism.

Technically, reciprocal regulation exists between PARP-1 and SIRT1, because they both may limit NAD^+ availability for each other. Moreover, due to differences in enzyme kinetics, PARP-1 limits NAD^+ availability for SIRT1. The K_M for NAD^+ of the purified enzymes is significantly lower for PARP-1 than for SIRT1 (Knight and Chambers, 2001; Malik *et al.*, 2009; Smith *et al.*, 2009). Similarly, PARP-1 has a much higher (~20-fold) $kcat/K_M$ for NAD^+ than SIRT1 (Smith *et al.*, 2009). It indicates that PARP-1 is a faster and more efficient NAD^+ consumer than SIRT1. Under basal conditions PARP-1 activity accounts for the most part of cellular NAD^+ consumption, which would maintain NAD^+ at limiting levels for SIRT1 activity. Supporting this notion, overactivation of PARP-1 is enough to deplete intracellular NAD^+ dramatically and hence decrease SIRT1 activity. The theoretical prediction that PARP-1 deletion would allow NAD^+ levels to increase and potentiate SIRT1 activation is supported by our experimental observations. Moreover, our results indicate that the interplay between both proteins could be exploited pharmacologically in metabolic diseases. Since several SIRT1 substrates, such as PGC-1α, FOXOs or p53, are crucial metabolic regulators, it is not surprising that the activation of SIRT1 by increased NAD^+ availability enhances mitochondrial biogenesis and oxidative metabolism (Canto and Auwerx, 2009; Gross *et al.*, 2008; Vousden and Ryan, 2009). In this manner PARP-1 plays an indirect role in the regulation of gene expression for cell energy homeostasis by controlling SIRT1 activation. Fig. 23 depicts the complexity of this regulatory circuitry.

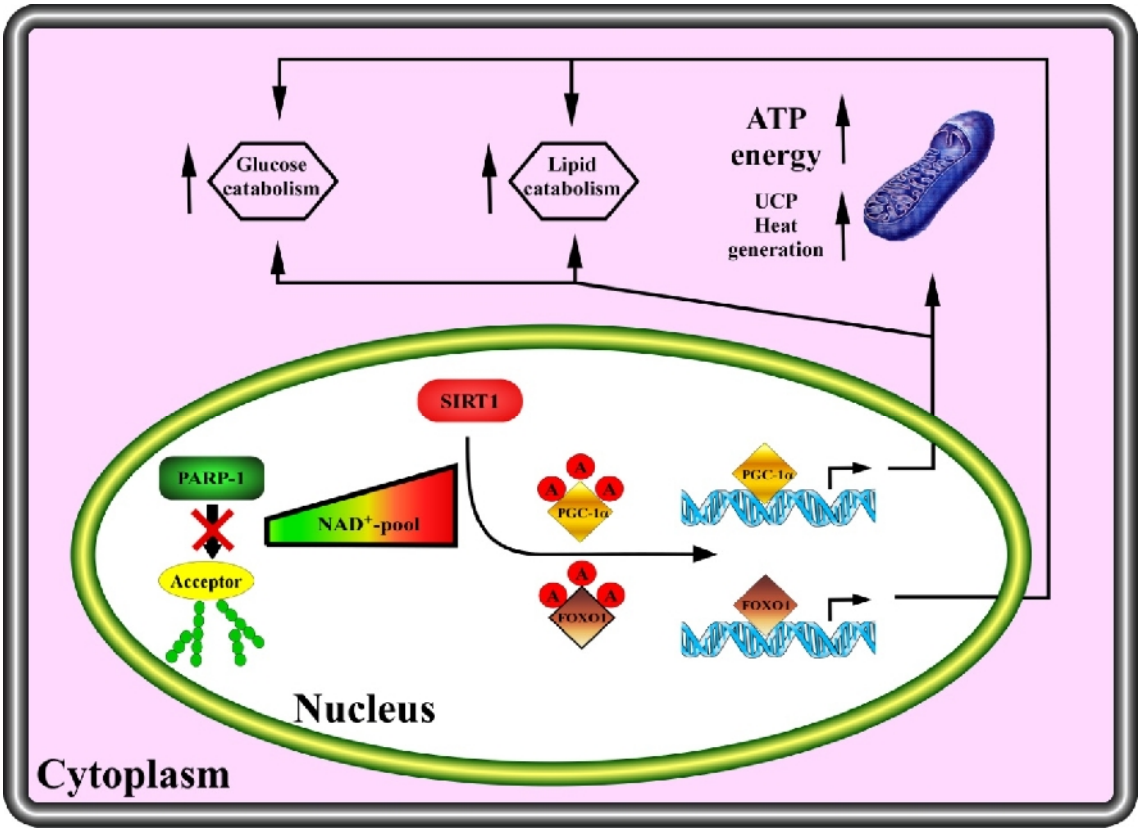

Figure 23. The regulation of genes of oxidative metabolism by PARP-1 via NAD^+ bioavailability of SIRT1.
PGC-1α and FOXO1 have crucial role in the regulation of oxidative metabolism through modulating gene expression. The lack of PARP-1 increase the NAD^+ content in cells, stimulating the activity of SIRT1. This leads to deacetilating of PGC-1α and FOXO1.These transcription factors increase the expression of oxidative metabolic genes leading to elevated metabolic rate and energy deliberation.

Despite the clear impact of PARP inhibition on SIRT1 activity and the involvement of SIRT1 in the phenotypes elicited by reductions in PARP activity, we cannot rule out the possibility that PARP inhibition also affects energy metabolism through SIRT1-independent mechanisms. Future research will have to clarify the nature of these SIRT1-independent effects of PARP inhibition on metabolism. Given the fact that PARP-1 is a nuclear protein, it will be particularly interesting to explore whether PARylation can directly modulate the activity of nuclear proteins and transcriptional regulators related to energy metabolism. It is of interest that the expression of the other PARP enzymes is unaltered in our PARP-$1^{-/-}$ mice indicating the lack of compensation upon the loss of PARP-1.

The utilization of PARP inhibitors raises the possibility of occurrence of adverse effects. The lack of PARP-1 has been associated with genomic instability upon serious DNA damage evoked by oxidative stress, γ-irradiation or alkylating agents (Bai *et al.*, 2007; Menissier-de Murcia *et al.*, 1997; Virag and Szabo, 2002). Therefore, prolonged PARP-1 inhibition may lead to the accumulation of DNA damage in the genome. However previous reports have shown (Allinson *et al.*, 2003), that despite the role of PARP-1 in DNA repair, no apparent DNA damage was observed in our PARP-$1^{-/-}$ mice under basal conditions. Moreover, PARP inhibitors were well tolerated in clinical trials (Fong *et al.*, 2009; Jagtap and Szabo, 2005). Together, this identifies PARP-1 as an attractive novel target to manage metabolic disease. Our work on one hand implicates the PARP-1 inhibition by riveting link between PARP-1 and SIRT1. The interplay between PARP-1 and SIRT1 might have implications in a number of additional areas, ranging from circadian rhythm, cellular proliferation and longevity, which warrant future investigation.

8. Summary

PARP-1 plays important roles in the regulation of transcription. It may act on chromatin condensation, transcription factors, or function as insulator. In these cases, PARP-1 directly controls gene expression via binding to other DNA-binding proteins (e.g. transcription factors) or PARylating them (e.g. histone proteins). However, several lines of evidence suggest that PARP-1 functions as a promoter-specific cofactor for transcription factor-dependent gene expression (e.g. NF-κB), or may indirectly control gene expression through modulating other NAD^+-dependent enzymes (e.g. SIRT1).

In the present work, we investigated the role of PARP-1 in the regulation of contact hypersensitivity reaction and in SIRT1-mediated mitochondrial alterations. Oxazolon-induced CHS was quenched in PARP-$1^{-/-}$ mice, as indicated by reduced neutrophil infiltration, oxidative and nitrosative stress. Under inflammation, cytokines, chemokines, adhesion molecules and matrix metalloproteinase-9 were induced, which was strongly suppressed in PAPR-$1^{-/-}$ mice. Furthermore, we identified two inflammatory transcription factors: p65 and ATF-2, which were induced in CHS but were suppressed in PARP-$1^{-/-}$ mice. p65 is the member of the NF-κB while ATF-2 is the member of the AP-1 family of transcription factors. Both transcription factors were described to be PARP-1-dependent, therefore the impaired activation of NF-κB and ATF-2 may explain the reduced inflammation in the PARP-$1^{-/-}$ mice.

In the other study, we investigated PARP-1 and SIRT1 interaction on energy metabolism and its impact on gene expression. We observed increased mitochondrial content and higher expression of oxidative metabolism genes (mitochondrial respiration, fatty acid oxidation, glucose metabolism) in BAT and skeletal muscle of PARP-$1^{-/-}$ mice. These observations were confirmed in PARP-$1^{-/-}$ MEF cells, where similar expression changes were observed. Moreover, pharmacological inhibition of PARP-1 has phenocopied the above gene expression alterations. Apparently, alterations in NAD^+ content and the consequent SIRT1 activation lay behind these alterations.

9. Összefoglalás

PARP-1 fontos faktora a transzkripció szabályozásának. Szerepet játszhat a kromatin kondenzációban, transzkripciós faktor aktivációjában, vagy mint insulator működhet. Ezekben az esetekben a PARP-1 közvetlenül szabályozza a génexpressziót más DNS-kötő fehérjékhez (pl.: transzkripciós faktorokhoz) való kapcsolódáson keresztül vagy PARiláció útján (pl.: hiszton fehérjéknél). Azonban több bizonyíték mutat arra, hogy a PARP-1 elsősorban promoter-specifikus kofaktorként működik közre a génexpresszió szabályozásában vagy közvetetten szabályozhatja a génexpressziót például egyéb NAD^+-függő enzimeken keresztül (SIRT1).

Jelen munkában a PARP-1 szerepét vizsgáltuk a kontakt hiperszenzitivitási reakció (CHS) és a SIRT1 által regulált mitokondriális metabolizmus szabályzásában. Az oxazolon által kiváltott CHS mértéke csökkent a PARP-$1^{-/-}$ egerekben, amit csökkent neutrofil infiltráció, oxidatív és nitrozatív stressz jelzett. A gyulladás során a citokinek, kemokinek, adhéziós molekulák és mátrix metalloproteináz-9 indukcióját figyeltük meg, amelyek erősen lecsökkentek a PARP-$1^{-/-}$ egerekben. Ezzel párhuzamosan gyulladásos transzkripciós faktorokról, a p65-ről és az ATF-2-ről kimutattuk, hogy gyulladás során PARP-1 függő módon aktiválódnak. A p65 az NF-κB, míg az ATF-2 az AP-1 család tagjai. Mindkét transzkripciós faktorról leírták, hogy PARP-1 függő ezért aktivációjuk megváltozása magyarázat lehet a gyulladás mértékének csökkenésére PARP-$1^{-/-}$ egerekben.

A PARP-1 SIRT-1 kölcsönhatás vizsgálata során a génexpresszió és a metabolikus egyensúly összefüggését vizsgáltuk. Modelljeinkben magasabb fokú mitokondriális biogenezist és az oxidatív metabolizmus génjeinek (mitokondriális légzési lánc, zsírsav oxidáció, glükóz metabolizmus) megnövekedett expresszióját figyeltük meg barna zsír szövetben és vázizomban. Ezeket a megfigyeléseinket megerősítettük PARP-$1^{-/-}$ MEF sejtekben, ahol szintén hasonló expressziós változásokat kaptunk. Továbbá a PARP-1 farmakológiai gátlása a fentiekkel azonos expressziós változásokat indukált. Úgy tűnik, hogy a NAD^+ koncentráció és a SIRT1 aktiváció változása felelős ezekért a jelenségekért.

10. References

Aguilar-Quesada R, Munoz-Gamez JA, Martin-Oliva D, Peralta-Leal A, Quiles-Perez R, Rodriguez-Vargas JM, *et al.* (2007) Modulation of transcription by PARP-1: consequences in carcinogenesis and inflammation. *Curr Med Chem* 14:1179-1187.

Albadawi H, Crawford RS, Atkins MD, Watkins MT (2006) Role of poly(ADP-ribose) polymerase during vascular reconstruction. *Vascular* 14:362-365.

Alderton WK, Cooper CE, Knowles RG (2001) Nitric oxide synthases: structure, function and inhibition. *Biochem J* 357:593-615.

Allinson SL, Dianova, II, Dianov GL (2003) Poly(ADP-ribose) polymerase in base excision repair: always engaged, but not essential for DNA damage processing. *Acta Biochim Pol* 50:169-179.

Ambrose HE, Papadopoulou V, Beswick RW, Wagner SD (2007) Poly-(ADP-ribose) polymerase-1 (Parp-1) binds in a sequence-specific manner at the Bcl-6 locus and contributes to the regulation of Bcl-6 transcription. *Oncogene* 26:6244-6252.

Ame JC, Spenlehauer C, de Murcia G (2004) The PARP superfamily. *Bioessays* 26:882-893.

Ames BN SM, Hagen TM (1995) Mitochondrial decay in aging. *Biochim Biophys Acta* 1271.

Amiri KI, Ha HC, Smulson ME, Richmond A (2006) Differential regulation of CXC ligand 1 transcription in melanoma cell lines by poly(ADP-ribose) polymerase-1. *Oncogene* 25:7714-7722.

Asher G, Reinke H, Altmeyer M, Gutierrez-Arcelus M, Hottiger MO, Schibler U (2010) Poly(ADP-ribose) polymerase 1 participates in the phase entrainment of circadian clocks to feeding. *Cell* 142:943-953.

Audebert M, Salles B, Calsou P (2004) Involvement of poly(ADP-ribose) polymerase-1 and XRCC1/DNA ligase III in an alternative route for DNA double-strand breaks rejoining. *J Biol Chem* 279:55117-55126.

Babior BM, Lambeth JD, Nauseef W (2002) The neutrophil NADPH oxidase. *Arch Biochem Biophys* 397:342-344.

Bacon BR, Britton RS (1989) Hepatic injury in chronic iron overload. Role of lipid peroxidation. *Chem Biol Interact* 70:183-226.

Bai P, Canto C, Oudart H, Brunyanszki A, Cen Y, Thomas C, *et al.* (2011) PARP-1 Inhibition Increases Mitochondrial Metabolism through SIRT1 Activation. *Cell Metab* 13:461-468.

Bai P, Hegedus C, Erdelyi K, Szabo E, Bakondi E, Gergely S, *et al.* (2007) Protein tyrosine nitration and poly(ADP-ribose) polymerase activation in N-methyl-N-nitro-N-nitrosoguanidine-treated thymocytes: implication for cytotoxicity. *ToxicolLett* 170:203-213.

Bai P, Hegedus C, Szabo E, Gyure L, Bakondi E, Brunyanszki A, *et al.* (2009) Poly(ADP-ribose) polymerase mediates inflammation in a mouse model of contact hypersensitivity. *J Invest Dermatol* 129:234-238. Epub 2008 Jul 2017.

Barja QG (1992) Brown fat thermogenesis and exercise: two examples of physiological oxidative stress? *Free Radical Bio Med* 13:325-340.

Beckman JS, Koppenol WH (1996) Nitric oxide, superoxide, and peroxynitrite: the good, the bad, and ugly. *American Journal of Physiology* 271:1424-C1437.

Berlett BS, Stadtman ER (1997) Protein oxidation in aging, disease, and oxidative stress. *J Biol Chem* 272:20313-20316.

Biedermann T, Kneilling M, Mailhammer R, Maier K, Sander CA, Kollias G, *et al.* (2000) Mast cells control neutrophil recruitment during T cell-mediated delayed-type hypersensitivity reactions through tumor necrosis factor and macrophage inflammatory protein 2. *J Exp Med* 192:1441-1452.

Burkle A, Diefenbach J, Brabeck C, Beneke S (2005) Ageing and PARP. *Pharmacological Research* 52:93-99.

Butler AJ, Ordahl CP (1999) Poly(ADP-ribose) polymerase binds with transcription enhancer factor 1 to MCAT1 elements to regulate muscle-specific transcription. *Molecular and Cellular Biology* 19:296-306.

Cadet J, Douki T, Ravanat JL (2010) Oxidatively generated base damage to cellular DNA. *Free Radic Biol Med* 49:9-21.

Cai AL, Zipfel GJ, Sheline CT (2006) Zinc neurotoxicity is dependent on intracellular NAD levels and the sirtuin pathway. *Eur J Neurosci* 24:2169-2176.

Caito S, Hwang JW, Chung S, Yao H, Sundar IK, Rahman I (2010) PARP-1 inhibition does not restore oxidant-mediated reduction in SIRT1 activity. *Biochem Biophys Res Commun* 392:264-270.

Canto C, Auwerx J (2009) PGC-1alpha, SIRT1 and AMPK, an energy sensing network that controls energy expenditure. *Curr Opin Lipidol* 20:98-105.

Canto C, Gerhart-Hines Z, Feige JN, Lagouge M, Noriega L, Milne JC, *et al.* (2009) AMPK regulates energy expenditure by modulating NAD+ metabolism and SIRT1 activity. *Nature* 458:1056-1060.

Chiarugi A, Moskowitz MA (2003) Poly(ADP-ribose) polymerase-1 activity promotes NF-kappaB-driven transcription and microglial activation: implication for neurodegenerative disorders. *J Neurochem* 85:306-317.

Cooke MS, Evans MD, Dizdaroglu M, Lunec J (2003) Oxidative DNA damage: mechanisms, mutation, and disease. *Faseb J* 17:1195-1214.

D'Amours D, Desnoyers S, D'Silva I, Poirier GG (1999) Poly(ADP-ribosyl)ation reactions in the regulation of nuclear functions. *Biochem J* 342 (Pt 2):249-268.

Dantzer F, de La RG, Menissier-de Murcia J, Hostomsky Z, de Murcia G, Schreiber V (2000) Base excision repair is impaired in mammalian cells lacking Poly(ADP-ribose) polymerase-1. *Biochemistry* 39:7559-7569.

Dantzer F, Schreiber V, Niedergang C, Trucco C, Flatter E, De La Rubia G, *et al.* (1999) Involvement of poly(ADP-ribose) polymerase in base excision repair. *Biochimie* 81:69-75.

El-Khamisy SF, Masutani M, Suzuki H, Caldecott KW (2003) A requirement for PARP-1 for the assembly or stability of XRCC1 nuclear foci at sites of oxidative DNA damage. *Nucleic Acids Res* 31:5526-5533.

El Ramy R, Magroun N, Messadecq N, Gauthier LR, Boussin FD, Kolthur-Seetharam U, *et al.* (2009) Functional interplay between Parp-1 and SirT1 in genome integrity and chromatin-based processes. *Cell Mol Life Sci* 66:3219-3234.

Espinoza LA, Smulson ME, Chen Z (2007) Prolonged poly(ADP-ribose) polymerase-1 activity regulates JP-8-induced sustained cytokine expression in alveolar macrophages. *Free Radic Biol Med* 42:1430-1440.

Esterbauer H, Schaur RJ, Zollner H (1991) Chemistry and biochemistry of 4-hydroxynonenal, malonaldehyde and related aldehydes. *Free Radic Biol Med* 11:81-128.

Feige JN, Auwerx J (2008) Transcriptional targets of sirtuins in the coordination of mammalian physiology. *Curr Opin Cell Biol* 20:303-309.

Finck BN, Kelly DP (2006) PGC-1 coactivators: inducible regulators of energy metabolism in health and disease. *J Clin Invest* 116:615-622.

Fisher AE, Hochegger H, Takeda S, Caldecott KW (2007) Poly(ADP-ribose) polymerase 1 accelerates single-strand break repair in concert with poly(ADP-ribose) glycohydrolase. *Mol Cell Biol* 27:5597-5605.

Fong PC, Boss DS, Yap TA, Tutt A, Wu P, Mergui-Roelvink M, *et al.* (2009) Inhibition of Poly(ADP-Ribose) Polymerase in Tumors from BRCA Mutation Carriers. *N Engl J Med* 361(2):123-134.

Forman HJ, Torres M (2001) Redox signaling in macrophages. *Mol Aspects Med* 22:189-216.

Frizzell KM, Gamble MJ, Berrocal JG, Zhang T, Krishnakumar R, Cen Y, *et al.* (2009) Global analysis of transcriptional regulation by poly(ADP-ribose) polymerase-1 and poly(ADP-ribose) glycohydrolase in MCF-7 human breast cancer cells. *J Biol Chem* 284:33926-33938.

Fuchs J, Zollner TM, Kaufmann R, Podda M (2001) Redox-modulated pathways in inflammatory skin diseases. *Free Radic Biol Med* 30:337-353.

Fulco M, Cen Y, Zhao P, Hoffman EP, McBurney MW, Sauve AA, *et al.* (2008) Glucose restriction inhibits skeletal myoblast differentiation by activating SIRT1 through AMPK-mediated regulation of Nampt. *Dev Cell* 14:661-673.

Gamble MJ, Fisher RP (2007) SET and PARP1 remove DEK from chromatin to permit access by the transcription machinery. *Nat Struct Mol Biol* 14:548-555.

Gerhart-Hines Z, Rodgers JT, Bare O, Lerin C, Kim SH, Mostoslavsky R, *et al.* (2007) Metabolic control of muscle mitochondrial function and fatty acid oxidation through SIRT1/PGC-1alpha. *EMBO J* 26:1913-1923.

Ginsburg (1998) Could synergistic interactions among reactive oxygen species, proteinases, membrane-perforating enzymes, hydrolases, microbial hemolysins and cytokines be the main cause of tissue damage in infectious and inflammatory conditions? *Medical Hypotheses* 51:337-346.

Ginsburg I, Kohen R (1995) Synergistic effects among oxidants, membrane-damaging agents, fatty acids, proteinases, and xenobiotics: killing of epithelial cells and release of arachidonic acid. *Inflammation* 19:101-118.

Gordon S, Akopyan G, Garban H, Bonavida B (2006) Transcription factor YY1: structure, function, and therapeutic implications in cancer biology. *Oncogene* 25:1125-1142.

Gross DN, van den Heuvel AP, Birnbaum MJ (2008) The role of FoxO in the regulation of metabolism. *Oncogene* 27:2320-2336.

Grune T, Reinheckel T, Davies KJ (1997) Degradation of oxidized proteins in mammalian cells. *Faseb J* 11:526-534.

Guarente L, Picard F (2005) Calorie restriction--the SIR2 connection. *Cell* 120:473-482.

Ha HC (2004) Defective transcription factor activation for proinflammatory gene expression in poly(ADP-ribose) polymerase 1-deficient glia. *Proc Natl Acad Sci USA* 101:5087-5092.

Haddad JJ (2002) Science review: Redox and oxygen-sensitive transcription factors in the regulation of oxidant-mediated lung injury: role for nuclear factor-kappaB. *Crit Care* 6:481-490.

Haddad M, Rhinn H, Bloquel C, Coqueran B, Szabo C, Plotkine M, *et al.* (2006) Anti-inflammatory effects of PJ34, a poly(ADP-ribose) polymerase inhibitor, in transient focal cerebral ischemia in mice. *Br J Pharmacol* 149:23-30.

Hakme A, Huber A, Dolle P, Schreiber V (2008a) The macroPARP genes Parp-9 and Parp-14 are developmentally and differentially regulated in mouse tissues. *Dev Dyn* 237:209-215.

Hakme A, Wong HK, Dantzer F, Schreiber V (2008b) The expanding field of poly(ADP-ribosyl)ation reactions. 'Protein Modifications: Beyond the Usual Suspects' Review Series. *EMBO Rep* 9:1094-1100.

Halliwell, Gutteridge *Free Radicals in Biology and Medicine (third edition)*. Oxford University Press, 1999.

Hassa PO, Hottiger MO (1999) A role of poly (ADP-ribose) polymerase in NF-kappaB transcriptional activation. *BiolChem* 380:953-959.

Hassa PO, Hottiger MO (2002) The functional role of poly(ADP-ribose)polymerase 1 as novel coactivator of NF-kappaB in inflammatory disorders. *Cell Mol Life Sci* 59:1534-1553.

Hawkins C, Brown B, Davies M (2001) Hypochlorite- and hypochlorite-mediated radical formation and its role in cell lysis. *Arch Biochem Biophys Res Commun* 395.

Homburg S, Visochek L, Moran N, Dantzer F, Priel E, Asculai E, *et al.* (2000) A fast signal-induced activation of Poly(ADP-ribose) polymerase: a novel downstream target of phospholipase c. *J Cell Biol* 150:293-307.

Homey B, Assmann T, Vohr HW, Ulrich P, Lauerma AI, Ruzicka T, *et al.* (1998) Topical FK506 suppresses cytokine and costimulatory molecule expression in epidermal and local draining lymph node cells during primary skin immune responses. *J Immunol* 160:5331-5340.

Houtkooper RH, Canto C, Wanders RJ, Auwerx J (2010) The secret life of NAD+: an old metabolite controlling new metabolic signaling pathways. *Endocr Rev* 31:194-223.

Huang K, Tidyman WE, Le KU, Kirsten E, Kun E, Ordahl CP (2004) Analysis of nucleotide sequence-dependent DNA binding of poly(ADP-ribose) polymerase in a purified system. *Biochemistry* 43:217-223.

Huletsky A, de MG, Muller S, Hengartner M, Menard L, Lamarre D, *et al.* (1989) The effect of poly(ADP-ribosyl)ation on native and H1-depleted chromatin. A role of poly(ADP-ribosyl)ation on core nucleosome structure. *J Biol Chem* 264:8878-8886.

Ignarro LJ *Nitric oxide: biology and pathobiology*. Academic Press: Orlando, 2000.

Ischiropoulos H, Zhu L, Beckman JS, Chen J, Tsai M, Martin JC, *et al.* (1992) Peroxynitrite-mediated tyrosine nitration catalyzed by superoxide dismutase. *Arch Biochem Biophys* 298:446-451.

Jacob C, Winyard PG *Redox signalling and regulation in Biology and Medcine*. Wiley-Vch Verlag Gmbh, 2009, 514pp.

Jagtap P, Szabo C (2005) Poly(ADP-ribose) polymerase and the therapeutic effects of its inhibitors. *Nat Rev Drug Discov* 4:421-440.

James SL (1998) Nitric oxide in health and disease. *Parasitol Today* 14:504.

Ju BG, Lunyak VV, Perissi V, Garcia-Bassets I, Rose DW, Glass CK, *et al.* (2006) A topoisomerase IIbeta-mediated dsDNA break required for regulated transcription. *Science* 312:1798-1802.

Kannan P, Yu Y, Wankhade S, Tainsky MA (1999) PolyADP-ribose polymerase is a coactivator for AP-2-mediated transcriptional activation. *Nucleic Acids Res* 27:866-874.

Kauppinen TM, Swanson RA (2005) Poly(ADP-ribose) polymerase-1 promotes microglial activation, proliferation, and matrix metalloproteinase-9-mediated neuron death. *J Immunol* 174:2288-2296.

Kelly M, Hwang JM, Kubes P (2007) Modulating leukocyte recruitment in inflammation. *J Allergy Clin Immunol* 120:3-10. Epub 2007 Jun 2007.

Kim MY, Mauro S, Gevry N, Lis JT, Kraus WL (2004) NAD+-dependent modulation of chromatin structure and transcription by nucleosome binding properties of PARP-1. *Cell* 119:803-814.

Klenova E, Ohlsson R (2005) Poly(ADP-ribosyl)ation and epigenetics. Is CTCF PARt of the plot? *Cell Cycle* 4:96-101.

Knight MI, Chambers PJ (2001) Production, extraction, and purification of human poly(ADP-ribose) polymerase-1 (PARP-1) with high specific activity. *Protein Expr Purif* 23:453-458.

Koh SH, Chang DI, Kim HT, Kim J, Kim MH, Kim KS, *et al.* (2005) Effect of 3-aminobenzamide, PARP inhibitor, on matrix metalloproteinase-9 level in plasma and brain of ischemic stroke model. *Toxicology* 214:131-139.

Kohen R (1999) Skin antioxidants: their role in aging and in oxidative stress--new approaches for their evaluation. *Biomed Pharmacother* 53:181-192.

Kohen R, Nyska A (2002) Oxidation of biological systems: oxidative stress phenomena, antioxidants, redox reactions, and methods for their quantification. *Toxicol Pathol* 30:620-650.

Kolthur-Seetharam U, Dantzer F, McBurney MW, de Murcia G, Sassone-Corsi P (2006) Control of AIF-mediated cell death by the functional interplay of SIRT1 and PARP-1 in response to DNA damage. *Cell Cycle* 5:873-877.

Kraus WL (2008) Transcriptional control by PARP-1: chromatin modulation, enhancer-binding, coregulation, and insulation. *Curr Opin Cell Biol* 20:294-302.

Kraus WL, Lis JT (2003) PARP goes transcription. *Cell* 113:677-683.

Krishnakumar R, Gamble MJ, Frizzell KM, Berrocal JG, Kininis M, Kraus WL (2008) Reciprocal binding of PARP-1 and histone H1 at promoters specifies transcriptional outcomes. *Science* 319:819-821.

Kun E, Kirsten E, Ordahl CP (2002) Coenzymatic activity of randomly broken or intact double-stranded DNAs in auto and histone H1 trans-poly(ADP-ribosylation), catalyzed by poly(ADP-ribose) polymerase (PARP I). *J Biol Chem* 277:39066-39069.

Lagouge M, Argmann C, Gerhart-Hines Z, Meziane H, Lerin C, Daussin F, *et al.* (2006) Resveratrol Improves Mitochondrial Function and Protects against Metabolic Disease by Activating SIRT1 and PGC-1alpha. *Cell* 127:1109-1122.

Langelier, Servent, Rogers, Pascal (2008) A third zinc-binding domain of human poly(ADPribose) polymerase-1 coordinates DNA-dependent enzyme activation. *J Biol Chem* 283.

Le NT, Xue M, Castelnoble LA, Jackson CJ (2007) The dual personalities of matrix metalloproteinases in inflammation. *Front Biosci* 12:1475-87.:1475-1487.

Levine RL, Stadtman ER (2001) Oxidative modification of proteins during aging. *Exp Gerontol* 36:1495-1502.

Levy DE, Darnell JE, Jr. (2002) Stats: transcriptional control and biological impact. *Nat Rev Mol Cell Biol* 3:651-662.

Li X, McDonnell DP (2002) The transcription factor B-Myb is maintained in an inhibited state in target cells through its interaction with the nuclear corepressors N-CoR and SMRT. *Mol Cell Biol* 22:3663-3673.

Lim YM, Moon SJ, An SS, Lee SJ, Kim SY, Chang IS, *et al.* (2008) Suitability of macrophage inflammatory protein-1beta production by THP-1 cells in differentiating skin sensitizers from irritant chemicals. *Contact Dermatitis* 58:193-198.

Livingstone C, Patel G, Jones N (1995) ATF-2 contains a phosphorylation-dependent transcriptional activation domain. *EMBO J* 14:1785-1797.

Lowenstein CJ, Dinerman JL, Snyder SH (1994) Nitric oxide: a physiologic messenger. *Ann Intern Med* 120:227-237.

Maeda T, Maeda M, Stewart AF (2002) TEF-1 transcription factors regulate activity of the mouse mammary tumor virus LTR. *Biochem Biophys Res Commun* 296:1279-1285.

Maekawa T, Jin W, Ishii S (2010) The role of ATF-2 family transcription factors in adipocyte differentiation: antiobesity effects of p38 inhibitors. *Mol Cell Biol* 30:613-625.

Malanga M, Althaus FR (2005) The role of poly(ADP-ribose) in the DNA damage signaling network. *Biochem Cell Biol* 83:354-364.

Male D, Brostoff J, Roth D, Roitt I (2006) Immunology, 7th Edition. (

Malik R, Kashyap A, Bansal K, Sharma P, Rayasam GV, Davis JA, *et al.* (2009) Comparative deacetylase activity of wild type and mutants of SIRT1. *Biochem Biophys Res Commun* 391:739-743.

Masson M, Niedergang C, Schreiber V, Muller S, Menissier-de MJ, de MG (1998) XRCC1 is specifically associated with poly(ADP-ribose) polymerase and negatively regulates its activity following DNA damage. *Mol Cell Biol* 18:3563-3571.

McHale JF, Harari OA, Marshall D, Haskard DO (1999) Vascular endothelial cell expression of ICAM-1 and VCAM-1 at the onset of eliciting contact hypersensitivity in mice: evidence for a dominant role of TNF-alpha. *J Immunol* 162:1648-1655.

Meggs WJ (1993) Neurogenic inflammation and sensitivity to environmental chemicals. *Environ Health Perspect* 101:234-238.

Menissier-de Murcia J, Niedergang C, Trucco C, Ricoul M, Dutrillaux B, Mark M, *et al.* (1997) Requirement of poly(ADP-ribose) polymerase in recovery from DNA damage in mice and in cells. *Proc Natl Acad Sci USA* 94:7303-7307.

Moncada S, Palmer RM, Higgs EA (1991) Nitric oxide: physiology, pathophysiology, and pharmacology. *Pharmacol Rev* 43:109-142.

Nathan C, Xie QW (1994) Nitric oxide synthases: roles, tolls, and controls. *Cell* 78:915-918.

Niki E (2009) Lipid peroxidation: physiological levels and dual biological effects. *Free Radic Biol Med* 47:469-484.

Nirodi C, NagDas S, Gygi SP, Olson G, Aebersold R, Richmond A (2001) A role for poly(ADP-ribose) polymerase in the transcriptional regulation of the melanoma growth stimulatory activity (CXCL1) gene expression. *J Biol Chem* 276:9366-9374.

Oberdoerffer P, Michan S, McVay M, Mostoslavsky R, Vann J, Park SK, *et al.* (2008) SIRT1 redistribution on chromatin promotes genomic stability but alters gene expression during aging. *Cell* 135:907-918.

Oei SL, Shi Y (2001) Transcription factor Yin Yang 1 stimulates poly(ADP-ribosyl)ation and DNA repair. *Biochem Biophys Res Commun* 284:450-454.

Oliver FJ, Menissier-de Murcia J, Nacci C, Decker P, Andriantsitohaina R, Muller S, *et al.* (1999) Resistance to endotoxic shock as a consequence of defective NF-kappaB activation in poly (ADP-ribose) polymerase-1 deficient mice. *EMBO J* 18:4446-4454.

Olmos A, Giner RM, Recio MC, Rios JL, Cerda-Nicolas JM, Manez S (2007) Effects of plant alkylphenols on cytokine production, tyrosine nitration and inflammatory damage in the efferent phase of contact hypersensitivity. *Br J Pharmacol* 152:366-373.

Oumouna-Benachour K, Hans CP, Suzuki Y, Naura A, Datta R, Belmadani S, *et al.* (2007) Poly(ADP-ribose) polymerase inhibition reduces atherosclerotic plaque size and promotes factors of plaque stability in apolipoprotein E-deficient mice: effects on macrophage recruitment, nuclear factor-kappaB nuclear translocation, and foam cell death. *Circulation* 115:2442-2450.

Parola M, Bellomo G, Robino G, Barrera G, Dianzani MU (1999) 4-Hydroxynonenal as a biological signal: molecular basis and pathophysiological implications. *Antioxid Redox Signal* 1:255-284.

Pavri R, Lewis B, Kim TK, Dilworth FJ, Erdjument-Bromage H, Tempst P, *et al.* (2005) PARP-1 determines specificity in a retinoid signaling pathway via direct modulation of mediator. *Mol Cell* 18:83-96.

Pillai JB, Isbatan A, Imai S, Gupta MP (2005) Poly(ADP-ribose) polymerase-1-dependent cardiac myocyte cell death during heart failure is mediated by NAD+ depletion and reduced Sir2alpha deacetylase activity. *J Biol Chem* 280:43121-43130.

Poirier GG, de Murcia G, Jongstra-Bilen J, Niedergang C, Mandel P (1982) Poly(ADP-ribosyl)ation of polynucleosomes causes relaxation of chromatin structure. *Proc Natl Acad Sci USA* 79:3423-3427.

Poulsen HE, Jensen BR, Weimann A, Jensen SA, Sorensen M, Loft S (2000) Antioxidants, DNA damage and gene expression. *Free Radic Res* 33 Suppl:S33-39.

Powers SK, Jackson MJ (2008) Exercise-induced oxidative stress: cellular mechanisms and impact on muscle force production. *Physiol Rev* 88:1243-1276.

Racz B, Hanto K, Tapodi A, Solti I, Kalman N, Jakus P, *et al.* (2010) Regulation of MKP-1 expression and MAPK activation by PARP-1 in oxidative stress: a new mechanism for the cytoplasmic effect of PARP-1 activation. *Free Radic Biol Med* 49:1978-1988.

Rajamohan SB, Pillai VB, Gupta M, Sundaresan NR, Konstatin B, Samant S, *et al.* (2009) SIRT1 promotes cell survival under stress by deacetylation-dependent deactivation of poly (ADP-ribose) polymerase 1. *Mol Cell Biol* 26:26.

Reimold AM, Kim J, Finberg R, Glimcher LH (2001) Decreased immediate inflammatory gene induction in activating transcription factor-2 mutant mice. *Int Immunol* 13:241-248.

Richardson JD, Vasko MR (2002) Cellular mechanisms of neurogenic inflammation. *J Pharmacol Exp Ther* 302:839-845.

Rodgers JT, Lerin C, Gerhart-Hines Z, Puigserver P (2008) Metabolic adaptations through the PGC-1 alpha and SIRT1 pathways. *FEBS Lett* 582:46-53.

Rodgers JT, Lerin C, Haas W, Gygi SP, Spiegelman BM, Puigserver P (2005) Nutrient control of glucose homeostasis through a complex of PGC-1alpha and SIRT1. *Nature* 434:113-118.

Rodrigues MR, Rodriguez D, Russo M, Campa A (2002) Macrophage activation includes high intracellular myeloperoxidase activity. *Biochem Biophys Res Commun* 292:869-873.

Rolli V, O'Farrell M, Menissier-de MJ, de MG (1997) Random mutagenesis of the poly(ADP-ribose) polymerase catalytic domain reveals amino acids involved in polymer branching. *Biochemistry* 36:12147-12154.

Rolli V, Ruf A, Augustin A, Schulz GE, Ménissier-de Murcia J, de Murcia G *Poly(ADP-ribose) polymerase: Structure and function. In From DNA damage and stress signalling to cell death: Poly ADP-ribosylation reactions.* Oxford University Press: New York, 2000.

Saint-Mezard P, Rosieres A, Krasteva M, Berard F, Dubois B, Kaiserlian D, *et al.* (2004) Allergic contact dermatitis. *Eur J Dermatol* 14:284-295.

Schrader M, Fahimi HD (2006) Peroxisomes and oxidative stress. *Biochim Biophys Acta* 1763:1755-1766.

Schraufstatter IU, Hinshaw DB, Hyslop PA, Spragg RG, Cochrane CG (1986) Oxidant injury of cells. DNA strand-breaks activate polyadenosine diphosphate-ribose polymerase and lead to depletion of nicotinamide adenine dinucleotide. *J Clin Invest* 77:1312-1320.

Sims JL, Berger SJ, Berger NA (1981) Effects of nicotinamide on NAD and poly(ADP-ribose) metabolism in DNA-damaged human lymphocytes. *J Supramol Struct Cell Biochem* 16:281-288.

Sionov RV, Haupt Y (1999) The cellular response to p53: the decision between life and death. *Oncogene* 18:6145-6157.

Smith BC, Hallows WC, Denu JM (2009) A continuous microplate assay for sirtuins and nicotinamide-producing enzymes. *Anal Biochem* 394:101-109.

Soldatenkov VA, Chasovskikh S, Potaman VN, Trofimova I, Smulson ME, Dritschilo A (2002) Transcriptional repression by binding of poly(ADP-ribose) polymerase to promoter sequences. *J Biol Chem* 277:665-670.

Stuehr DJ, Marletta MA (1985) Mammalian nitrate biosynthesis: mouse macrophages produce nitrite and nitrate in response to Escherichia coli lipopolysaccharide. *Proc Natl Acad Sci USA* 82:7738-7742.

Sung YJ, Ambron RT (2004) PolyADP-ribose polymerase-1 (PARP-1) and the evolution of learning and memory. *Bioessays* 26:1268-1271.

Szabo E, Virag L, Bakondi E, Gyure L, Hasko G, Bai P, *et al.* (2001) Peroxynitrite production, DNA breakage, and poly(ADP-ribose) polymerase activation in a mouse model of oxazolone-induced contact hypersensitivity. *J Invest Dermatol* 117:74-80.

Tantin D, Schild-Poulter C, Wang V, Hache RJ, Sharp PA (2005) The octamer binding transcription factor Oct-1 is a stress sensor. *Cancer Res* 65:10750-10758.

Turrens JF (2003) Mitochondrial formation of reactive oxygen species. *J Physiol* 552:335-344.

Uldry M, Yang W, St-Pierre J, Lin J, Seale P, Spiegelman BM (2006) Complementary action of the PGC-1 coactivators in mitochondrial biogenesis and brown fat differentiation. *Cell Metab* 3:333-341.

Veres B, Radnai B, Gallyas F, Jr., Varbiro G, Berente Z, Osz E, *et al.* (2004) Regulation of kinase cascades and transcription factors by a poly(ADP-ribose) polymerase-1 inhibitor, 4-hydroxyquinazoline, in lipopolysaccharide-induced inflammation in mice. *J Pharmacol Exp Ther* 310:247-255.

Virag L, Szabo C (2002) The therapeutic potential of poly(ADP-ribose) polymerase inhibitors. *Pharmacol Rev* 54:375-429.

Virag L, Szabo E, Bakondi E, Bai P, Gergely P, Hunyadi J, *et al.* (2002) Nitric oxide-peroxynitrite-poly(ADP-ribose) polymerase pathway in the skin. *Exp Dermatol* 11:189-202.

Vousden KH, Ryan KM (2009) p53 and metabolism. *Nat Rev Cancer* 9:691-700.

Wacker DA, Ruhl DD, Balagamwala EH, Hope KM, Zhang T, Kraus WL (2007) The DNA binding and catalytic domains of poly(ADP-ribose) polymerase 1 cooperate in the regulation of chromatin structure and transcription. *Mol Cell Biol* 27:7475-7485.

Wallace J, Felsenfeld G (2007) We gather together: insulators and genome organization. *Current Opinion in Genetics & Development* 17:400-407.

Xiao CY, Chen M, Zsengeller Z, Li H, Kiss L, Kollai M, *et al.* (2005) Poly(ADP-Ribose) polymerase promotes cardiac remodeling, contractile failure, and translocation

of apoptosis-inducing factor in a murine experimental model of aortic banding and heart failure. *J Pharmacol Exp Ther* 312:891-898.

Yokota S, Oda T, Fahimi HD (2001) The role of 15-lipoxygenase in disruption of the peroxisomal membrane and in programmed degradation of peroxisomes in normal rat liver. *J Histochem Cytochem* 49:613-622.

Yu W, Ginjala V, Pant V, Chernukhin I, Whitehead J, Docquier F, *et al.* (2004) Poly(ADP-ribosyl)ation regulates CTCF-dependent chromatin insulation. *Nat Genet* 36:1105-1110.

Yusufzai TM, Tagami H, Nakatani Y, Felsenfeld G (2004) CTCF tethers an insulator to subnuclear sites, suggesting shared insulator mechanisms across species. *Mol Cell* 13:291-298.

Zaniolo K, Rufiange A, Leclerc S, Desnoyers S, Guerin SL (2005) Regulation of the poly(ADP-ribose) polymerase-1 gene expression by the transcription factors Sp1 and Sp3 is under the influence of cell density in primary cultured cells. *Biochem J* 389:423-433.

Zingarelli B, Hake PW, Burroughs TJ, Piraino G, O'Connor M, Denenberg A (2004) Activator protein-1 signalling pathway and apoptosis are modulated by poly(ADP-ribose) polymerase-1 in experimental colitis. *Immunology* 113:509-517.

Zingarelli B, Szabo C, Salzman AL (1999) Blockade of Poly(ADP-ribose) synthetase inhibits neutrophil recruitment, oxidant generation, and mucosal injury in murine colitis. *Gastroenterology* 116:335-345.

Register Number: DEENKÉTK /55/2011.
Item Number:
Subject: Ph.D. List of Publications

Candidate: Attila Brunyánszki

Neptun ID: I0MOPN

Doctoral School: Doctoral School of Molecular Medicine

List of publications related to the dissertation

1. Bai, P., Cantó, C., Oudart, H., **Brunyánszki, A.**, Cen, Y., Thomas, C., Yamamoto, H., Huber, A., Kiss, B., Houtkooper, R.H., Schoonjans, K., Schreiber, V., Sauve, A.A., Menissier-de, M.J., Auwerx, J.: PARP-1 inhibition increases mitochondrial metabolism through SIRT1 activation.
   Cell Metab. Accepted by Publisher, 38.p., 2011.
   IF:17.35 (2009)

2. **Brunyánszki, A.,** Hegedűs, C., Szántó, M., Erdélyi, K., Kovács, K., Schreiber, V., Gergely, S., Kiss, B., Szabó, É., Virág, L., Bai, P.: Genetic ablation of PARP-1 protects against oxazolone-induced contact hypersensitivity by modulating oxidative stress.
   J. Investigative Dermatology. 130 (11), 2629-2637, 2010.
   DOI: http://dx.doi.org/10.1038/jid.2010.190
   IF:5.543 (2009)

List of other publications

3. Bai, P., Hegedűs, C., Szabó, É., Gyüre, L., Bakondi, E., **Brunyánszki, A.**, Gergely, S., Szabó, C., Virág, L.: Poly(ADP-ribose) polymerase mediates inflammation in a mouse model of contact hypersensitivity.
   J. Invest. Dermatol. 129 (1), 234-238, 2009.
   DOI: http://dx.doi.org/10.1038/jid.2008.196
   IF:5.543

4. Juhász, L., Docsa, T., **Brunyánszki, A.**, Gergely, P., Antus, S.: Synthesis and glycogen phosphorylase inhibitor activity of 2,3-dihydrobenzo[1,4]dioxin derivatives.

Bioorg. Med. Chem. 15 (12), 4048-4056, 2007.
DOI: http://dx.doi.org/10.1016/j.bmc.2007.03.084
IF:2.662

5. Benltifa, M., Vidal, S., Fenet, B., Msaddek, M., Goekjian, P.G., Praly, J.P., **Brunyánszki, A.**, Docsa, T., Gergely, P.: In search of glycogen phosphorylase inhibitors:5-substituted 3-C-glucopyranosyl-1,2,4-oxadiazoles from beta-D-glucopyranosyl cyanides upon cyclization of O-acylamidoxime intermediates.
European J. Org. Chem. 2006 (18), 4242-4256, 2006.
DOI: http://dx.doi.org/10.1002/ejoc.200600073
IF:2.769

6. Györgydeák, Z., Hadady, Z., Felföldi, N., Krakomperger, A., Nagy, V., Tóth, M., **Brunyánszki, A.**, Docsa, T., Gergely, P., Somsák, L.: Synthesis of N-(beta-D-glucopyranosyl)- and N-(2-acetamido-2-deoxy-beta-D-glucopyranosyl) amides as inhibitors of glycogen phosphorylase.
Bioorg. Med. Chem. 12 (18), 4861-4870, 2004.
DOI: http://dx.doi.org/10.1016/j.bmc.2004.07.013
IF:2.018

The Candidate's publication data submitted to the Publication Database of the University of Debrecen have been validated by Kenezy Life Sciences Library on the basis of Web of Science, Scopus and Journal Citation Report (Impact Factor) databases.

04 April, 2011

11. Keywords

Inflammation, oxidative stress, redox-sensitive transcription factors, PARP-1 SIRT1, NAD^+, PGC-1α, FOXO1, NF-κB, ATF-2

12. Acknowledgement

I wish to thank my supervisor Dr. Péter Bai for helping and guiding my work during my Ph.D study.

I would like to thank Prof. Pál Gergely, head of Department of Medical Chemistry and Prof. László Virág, head of laboratory for giving all the support for my work.

Many thanks to all the people in the Department of Medical Chemistry, especially our group: Magdolna Szántó, Dr. Katalin Erdélyi, Dr. Csaba Hegedűs, Petra Lakatos and Katalin Kovács for their scientific and personal support. I greatly appreciate the excellent technical assistance of Ms. Erzsébet Herbály, Ms. Julianna Hunyadi and Ms. Anita Jeney Szabó.

I am much obliged to Prof. Johan Auwerx and Dr. Carles Cantó for their help and support.

I would like to thank Dr. Valerié Schreiber for donating the PARP-1 and PARP-2 knockout strains.

I am very grateful for Ms Erzsébet Herbály who processed tissue blocks and performed histochemistry and immunohsitochemistry, Dr. Csaba Hegedűs who helped me by CHS and irritative dermatitis models. I would like thank to my family for encouragement and support.

13. Appendix

This thesis is built on the following publications:

Brunyánszki A, Hegedűs Cs, Szántó M, Erdélyi K, Kovács K, Schreiber V, Gergely Sz, Kiss B, Szabó É, Virág L, Bai P. Genetic ablation of PARP-1 protects against oxazolone-induced contact hypersensitivity by modulating oxidative stress. J Invest Dermatol. 2010; 130, 2629-2637
IF: 5,543

Bai P., Cantó C., Oudart H., **Attila Brunyánszki**, Cen Y., Thomas C., Yamamoto H., Huber A., Kiss B., Houtkooper H. R., Schoonjans K., Schreiber V., Sauve A. A., Menissier-de Murcia J. and Auwerx J. PARP-1 Inhibition Increases Mitochondrial Metabolism through SIRT1 Activation. Cell Metabolism. 2011; 13, 4, 461-468
IF: 17,35

Genetic Ablation of PARP-1 Protects Against Oxazolone-Induced Contact Hypersensitivity by Modulating Oxidative Stress

Attila Brunyánszki[1], Csaba Hegedűs[1,2], Magdolna Szántó[1], Katalin Erdélyi[1,2], Katalin Kovács[1], Valérie Schreiber[3], Szabolcs Gergely[4], Borbála Kiss[5], Éva Szabó[5], László Virág[1,2] and Péter Bai[1,2]

Contact hypersensitivity (CHS) reaction is a form of delayed-type of hypersensitivity caused by contact allergens such as oxazolone (OXA). In previous studies it has been shown that poly(ADP-ribose) polymerase (PARP) inhibition reduces the extent of inflammation in CHS. We aimed to shed light on the molecular events causing the protective effect of PARP inhibitors. PARP-1 and -2 knockout mice were sensitized by abdominal delivery of OXA, and a week later CHS was induced by applying OXA on the ears of the mice. PARP-$1^{-/-}$ mice were protected against OXA-induced CHS in contrast to PARP-$2^{-/-}$ mice. In PARP-$1^{-/-}$ mice, neutrophil infiltration was reduced in line with the suppressed expression of proinflammatory cytokines, cell adhesion factors, and matrix metalloproteinase-9, which is likely because of impaired activation of NF-κB p65 and activating transcription factor-2, the two redox-sensitive transcription factors. Moreover, reduced nitrosative and oxidative stress was observed under inflammatory conditions in the PARP-$1^{-/-}$ mice when compared with PARP-$1^{+/+}$. In conclusion, PARP-1 activation is necessary for proinflammatory gene expression through which PARP-1 enhances neutrophil infiltration and hence oxidative/nitrosative stress, forming a vicious circle, and further aggravating the inflammatory process. Our data identify PARP-1 as a possible target in CHS.

Journal of Investigative Dermatology advance online publication, 8 July 2010; doi:10.1038/jid.2010.190

INTRODUCTION

The poly(ADP-ribose) polymerase (PARP) superfamily consists of 17 members, with some of them implicated in the regulation of the immune response. PARP-1 and PARP-2 belong to the subgroup that can be activated *in vivo* by DNA single-strand breaks or *in vitro* by DNase I-treated DNA or aberrant DNA forms (de Murcia and Menissier-de Murcia, 1994; Ame *et al.*, 1999). Because of its abundance and high catalytic activity, PARP-1 is responsible for most of the cellular PARP activity after DNA damage (Shieh *et al.*, 1998). PARP-1 activation results in the cleavage of NAD^+ substrate and the synthesis and attachment of poly(ADP-ribose) (PAR) polymers to different acceptor proteins (Schraufstatter *et al.*, 1986; Schreiber *et al.*, 2006).

Both PARP-1 and PARP-2 have been described to influence inflammatory processes through modulating numerous transcription factors (Hassa and Hottiger, 2008; Yelamos *et al.*, 2008). PARP-1 interacts with a large number of proinflammatory transcription factors, and the beneficial effects of PARP-1 ablation on inflammatory damage have been shown in multiple disease models such as colitis, arthritis, uveitis, and pancreatitis (Virag and Szabo, 2002). Recent data suggest that PARP-2 may also affect immune functions. PARP-$2^{-/-}$ mice suffer compromised thymopoesis that leads to impaired survival of $CD4^+$ $CD8^+$ double-positive thymocytes and consequently to weaker systemic T-cell functions (Yelamos *et al.*, 2006). In addition, PARP-2 associates with transcription factors (such as thyroid transcription factor-1 and peroxisome proliferator activated receptor-γ) and with protein factors influencing the histone code, pointing toward a plethora of possible alterations in gene expression (Bai *et al.*, 2007; Quenet *et al.*, 2008; Yelamos *et al.*, 2008).

Contact hypersensitivity (CHS) is a form of T cell-mediated delayed type of hypersensitivity reaction caused by small-molecular-weight molecules (haptens) that bind to host proteins to form a complete allergen (Grabbe and Schwarz, 1998). The CHS reaction can be divided into the sensitization and elicitation phase. In the elicitation phase, proinflammatory cytokines and chemokines recruit different inflammatory

[1]*Department of Medical Chemistry, University of Debrecen, Medical and Health Science Center, Debrecen, Hungary;* [2]*Cell Biology and Signaling Research Group of the Hungarian Academy of Sciences, Debrecen, Hungary;* [3]*FRE3211 IREBS, CNRS, Université de Strasbourg, ESBS, Illkirch, France;* [4]*Department of Cardiology, Medical and Health Science Center, University of Debrecen, Debrecen, Hungary and* [5]*Department of Dermatology, Medical and Health Science Center, University of Debrecen, Debrecen, Hungary*

Correspondence: Péter Bai, Department of Medical Chemistry, University of Debrecen, Nagyerdei krt 98, Pf. 7. H-4032, Debrecen, Hungary. E-mail: baip@dote.hu

Abbreviations: ATF-2, activating transcription factor-2; CHS, contact hypersensitivity; eNOS, endothelial nitric oxide synthase; iNOS, inducible nitric oxide synthase; MMP, matrix metalloproteinase; MPO, myeloperoxidase; NOS, NO synthase; OXA, oxazolone; PAR, poly(ADP-ribose); PARP, poly(ADP-ribose) polymerase; WT, wild type

Received 23 February 2010; revised 30 April 2010; accepted 20 May 2010

© 2010 The Society for Investigative Dermatology

cells (e.g., neutrophil granulocytes) (Olmos *et al.*, 2007). Infiltration is accompanied by oxidative stress due to the formation of superoxide, hydrogen peroxide, nitric oxide, peroxynitrite, and further reactive species (Morita *et al.*, 1996; Rowe *et al.*, 1997; Olmos *et al.*, 2007; Korkina and Pastore, 2009), leading to DNA breakage and PARP activation (Szabo *et al.*, 2001). Recently, we showed that the inhibition of PARP activation has beneficial effects during the CHS reaction (Bai *et al.*, 2009). In this study we set out to identify the PARP isoform mediating CHS and to characterize the molecular events during the elicitation phase of the CHS reaction.

RESULTS AND DISCUSSION

PARP-1$^{-/-}$, but not PARP-2$^{-/-}$, mice are protected against OXA challenge

We evaluated the ear swelling, as a measure of inflammatory edema, 24 hours after oxazolone (OXA) challenge. OXA challenge in wild-type (WT) mice caused a 4- to 5-fold ear swelling compared with vehicle-sensitized animals, whereas ear swelling was significantly reduced in the PARP-1$^{-/-}$ mice. In contrast, there was no significant difference between the OXA-sensitized PARP-2$^{+/+}$ and the OXA-sensitized PARP-2$^{-/-}$ mice (Figure 1a).

The myeloperoxidase (MPO) activity, indicative of the neutrophil infiltration, showed similar changes to ear swelling. PARP-1$^{-/-}$, but not PARP-2$^{-/-}$, mice were protected against the OXA-evoked increase in MPO activity (Figure 1b). The degree of protection provided by the PARP-1$^{-/-}$ phenotype was similar to the one previously observed in mice treated with the PARP inhibitor, PJ34 (Bai *et al.*, 2009).

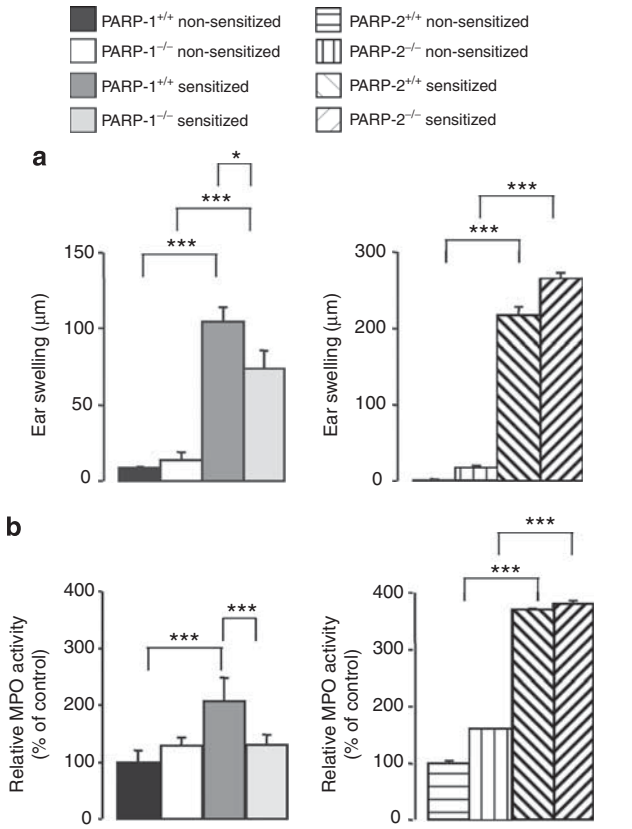

Figure 1. PARP-1$^{-/-}$, but not PARP-2$^{-/-}$, mice are protected against the oxazolone-induced CHS reaction. (**a**) Ear thickness was measured before and 24 hours after challenge by a caliper, and ear swelling was expressed as the difference of the two values. (**b**) At 24 hours after OXA challenge, ears were removed and relative MPO activity was determined. *$P<0.05$; ***$P<0.001$, significant difference between cohorts. CHS, contact hypersensitivity; MPO, myeloperoxidase; OXA, oxazolone; PARP, poly(ADP-ribose) polymerase.

PARP-1$^{-/-}$, but not PARP-2$^{-/-}$, mice are protected against the irritative component of CHS

In addition to the antigen-specific reaction, an irritative component is usually also present in contact allergies (Grabbe *et al.*, 1996). Therefore, we applied a 12-*O*-tetradecanoyl-phorbol 13-acetate-induced irritative dermatitis model (Bai *et al.*, 2009) to investigate whether the antigen-specific and/or the nonspecific irritant response is affected by PARP-1 and -2. Similar to our previous observations with the PARP inhibitor compound PJ34 (Bai *et al.*, 2009), the PARP-1$^{-/-}$ phenotype also conferred partial protection against the 12-*O*-tetradecanoyl-phorbol 13-acetate-induced irritative dermatitis, both at the level of ear swelling and MPO activity (Figure 2a and b). In contrast, genetic ablation of PARP-2 did not affect irritative dermatitis. We detected marked cellular infiltration upon 12-*O*-tetradecanoyl-phorbol 13-acetate induction (Figure 2d), in line with strong induction of matrix metalloproteinase (MMP) activity that was reduced in PARP-1$^{-/-}$ mice (Figure 2c). As our data indicate that PARP-2 has no functional role in CHS or in irritative dermatitis, we focused our mechanistic investigation on the role of PARP-1 and omitted the PARP-2 knockout strain from all further studies.

Genetic ablation of PARP-1 suppresses inflammatory cell immigration in CHS reaction

Histology examination revealed a marked infiltration of the ear with inflammatory cells upon OXA challenge that was reduced in the PARP-1$^{-/-}$ mice (Figure 3a). This is in good correlation with ear swelling and MPO activity as presented in Figure 1.

CHS is characterized by a mixed infiltration of polymorphonuclear leukocytes, monocytes (Olmos *et al.*, 2007), and T cells. Staining for cell type-specific markers revealed predominant neutrophil infiltration in the connective tissue. In line with the suppressed inflammatory response, neutrophil infiltration was markedly reduced in the PARP-1$^{-/-}$ mice (Figure 3b).

We went on to investigate the expression of proinflammatory cytokines and chemokines. On the course of the allergic inflammation, we observed the induction of macrophage inflammatory protein-1α and-2, IL-1β, tumor necrosis factor-α, and monocyte chemotactic protein-1. A reduced expression of all of these cytokines/chemokines has been observed in the PARP-1$^{-/-}$ mice (Figure 4a). These chemokines/cytokines are known mediators of CHS (Saint-Mezard *et al.*, 2004; Olmos *et al.*, 2007) and are of different origin (dermal cells, mast cells, or Langerhans cells) possessing pleiotropic

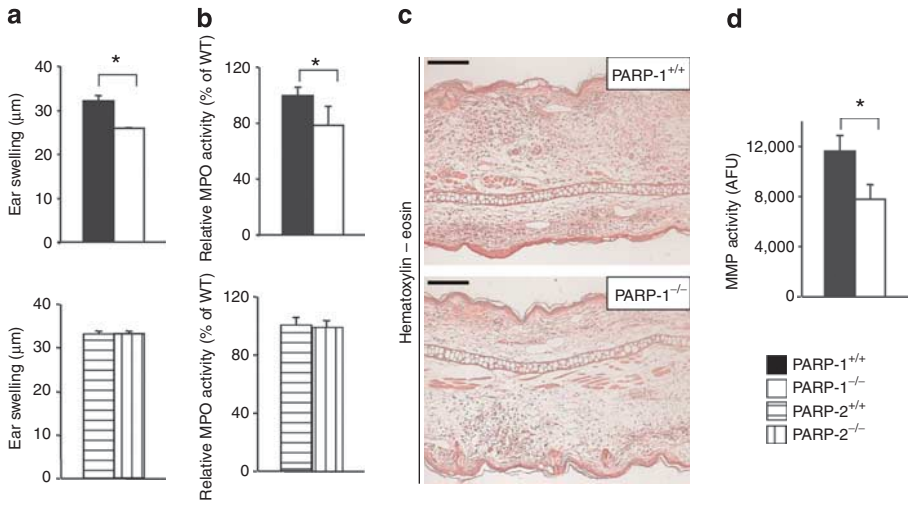

Figure 2. PARP-1$^{-/-}$, but not PARP-2$^{-/-}$, mice are protected against the PMA-induced irritative dermatitis. PMA (10 μl, 0.05% w/v) was smeared onto both sides of the ears of female mice (six animals per group). After 24 hours, (**a**) ear swelling, (**b**) MPO, and (**d**) MMP activities were determined. (**c**) Formalin-fixed, paraffin-embedded tissue sections were stained with HE. Scale bar = 200 μm. HE, hematoxylin and eosin; MMP, matrix metalloproteinase; MPO, myeloperoxidase; PARP, poly(ADP-ribose) polymerase; PMA, 12-*O*-tetradecanoyl-phorbol 13-acetate.

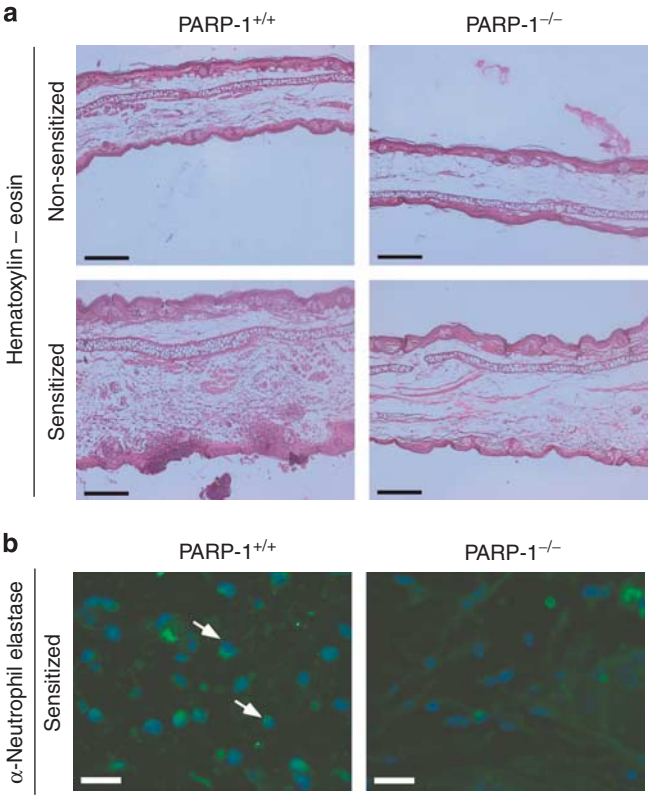

Figure 3. Genetic ablation of poly(ADP-ribose) polymerase-1 (PARP-1) suppresses inflammatory cell immigration. Formalin-fixed, paraffin-embedded tissue sections were stained with (**a**) hematoxylin and eosin (HE) and, (**b**) for neutrophil elastase, with 4,6-diamidino-2-phenylindole (DAPI) counterstain. The arrows point at the neutrophil elastase-positive cells (linear contrast adjustment was applied on image **b**). Scale bars = 200 μm for **a** and 20 μm for **b**.

effects (Biedermann *et al.*, 2000) leading to the (1) upregulation of cellular adhesion molecules on the surface of the endothelium (McHale *et al.*, 1999a, b); and (2) the recruitment, activation, and proliferation of inflammatory cells (Homey *et al.*, 1998; Lim *et al.*, 2008), culminating in inflammation.

As cellular extravasation and infiltration under inflammatory conditions require the concerted expression of different cell adhesion molecules such as I-CAM, L-CAM, V-CAM, and E-selectin (Fuchs *et al.*, 2001; Kelly *et al.*, 2007), we examined their expression. As expected, OXA challenge induced I-CAM, L-CAM, V-Cam, and E-selectin expression in the WT mice that was absent in the PARP-1$^{-/-}$ mice (Figure 4b). Similar observations have previously been made in several oxidative stress-related pathologies, in which inhibition or genetic ablation of PARP-1 reduced the expression of these adhesion molecules, leading to decreased inflammatory infiltration (Zingarelli *et al.*, 1999). Importantly, there is a strong correlation between the expression of the above-mentioned chemokines/cytokines (e.g., monocyte chemotactic protein-1 and tumor necrosis factor-α) and cellular adhesion molecules as all rely on NF-κB activation (Oliver *et al.*, 1999; Virag and Szabo, 2002; Haddad *et al.*, 2006; Espinoza *et al.*, 2007).

In addition to adhesion molecules, leukocytes also secrete MMPs to facilitate their movements in tissues. MMPs are expressed as zymogens that are subsequently activated either by proteolytic cleavage or free radical-induced structural changes (Le *et al.*, 2007). We have observed the induction of MMP-9 upon OXA challenge in the PARP-1$^{+/+}$ mice. However, MMP-9 induction was impaired in the PARP-1$^{-/-}$ mice (Figure 4c). Our observation is in line with other models of inflammation, in which MMP-9 expression was found to be reduced on pharmacological PARP inhibition or by treatment with small interfering RNA against PARP-1 (Kauppinen and Swanson, 2005; Koh *et al.*, 2005). MMP activity is controlled by tissue inhibitors of metalloproteinases 1–4. Interestingly, tissue inhibitor of metalloproteinase-2 was downregulated in PARP-1$^{+/+}$ mice, which may explain

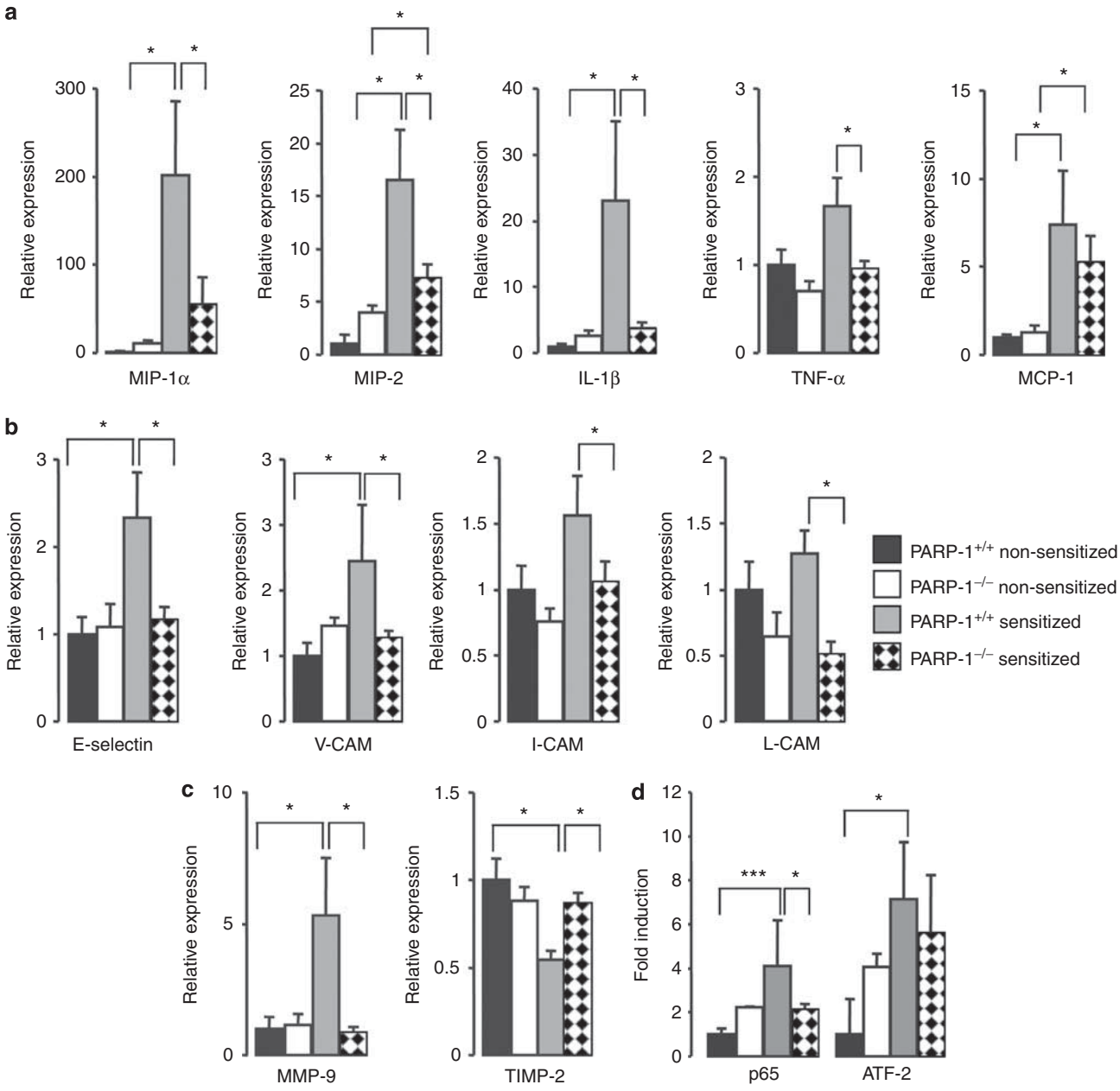

Figure 4. Expression of proinflammatory genes is suppressed in the PARP-1$^{-/-}$ mice. Expression of (**a**) a set of proinflammatory cytokines, (**b**) adhesion molecules, (**c**) MMP-9 and TIMP-2 were determined with qRT-PCR. (**d**) Transcription factor activation was determined using the TransFactor kit. *$P<0.05$; ***$P<0.001$, significant difference between cohorts. ATF-2, activating transcription factor-2; MCP-1, monocyte chemotactic protein-1; MIP, macrophage inflammatory protein; MMP, matrix metalloproteinase; PARP, poly(ADP-ribose) polymerase; qRT-PCR, quantitative real-time reverse transcriptase-PCR; TIMP-2, tissue inhibitor of metalloproteinase-2; TNF-α; tumor necrosis factor-α.

MMP-9 activation (Figure 4c). On the contrary, its expression was not reduced in PARP-1$^{-/-}$ mice. It is noteworthy that pharmacological PARP inhibition has previously also been found to prevent downregulation of this tissue inhibitor (Oumouna-Benachour *et al.*, 2007; Bai *et al.*, 2009).

PARP-1 interacts with a plethora of transcription factors and modulates their activity, and hence gene expression. Therefore, we hypothesized that the absence of PARP-1 protein and the consequent loss of PARP-1 activity may be the underlying mechanism for the altered expression of inflammatory mediators. We assessed the activation of a number of transcription factor in the ears. We have observed the strong activation of two redox-sensitive transcription factors, p65, a member of the NF-κB family and activating transcription factor-2 (ATF-2), on OXA sensitization in the PARP-1$^{+/+}$ mice (Figure 4d). Interestingly, the activation of other members of the REL family, p50 and c-Rel, was not detectable. The activation of p65 was completely absent in

the PARP-1$^{-/-}$ mice. ATF-2 showed a similar pattern to p65, although its activity was only partially reduced in the knockout mice (Figure 4d).

The defective p65 activation is in line with the reduced expression of numerous NF-κB target genes such as inducible nitric oxide synthase (iNOS), adhesion factors, and cytokines (Haddad *et al.*, 2006; Espinoza *et al.*, 2007). The direct molecular interaction between PARP-1 and NF-κB has already been described (Hassa and Hottiger, 1999; Oliver *et al.*, 1999). ATF-2 is a cAMP-responsive element-binding transcription factor that forms complex with c-Jun or itself and binds to activator protein-1 sites (Reimold *et al.*, 2001). ATF-2 has been shown to be regulated by PARP-1 (Ha, 2004). Genetic deletion of ATF-2 leads to impaired activator protein-1 activation and consequently to reduced expression of cytokines (tumor necrosis factor-α, IFN-γ, IL-1, IL-6, or monocyte chemotactic protein-1α) and adhesion factors (E-selectin and P-selectin) (Reimold *et al.*, 2001). Deficient activator protein-1 activation upon PARP-1 ablation has already been described in a murine model of colitis providing a protective phenotype (Zingarelli *et al.*, 2004). Apparently, the combined effects of PARP knockout on ATF-2 and NF-κB may culminate in the changes described in this study.

The lack of oxidative/nitrosative stress in the PARP-1$^{-/-}$ mice

Leukocytic infiltration is usually accompanied by the production of reactive oxygen and nitrogen species, such as hydrogen peroxide and peroxynitrite, a reactive nitrogen species, formed in the reaction of nitric oxide and superoxide (Beckman and Koppenol, 1996).

In the ear, the endothelial NOS (eNOS) and iNOS enzymes can be considered as the most important sources of nitric oxide under inflammatory conditions; therefore, we assessed their expression. Although eNOS expression was lower in the PARP-1$^{-/-}$ mice when compared with PARP-1$^{+/+}$, it did not change upon OXA challenge (Figure 5a). Therefore, eNOS cannot be considered as the major source of nitric oxide under inflammatory conditions. Similar to eNOS, iNOS expression was lower in the PARP-1$^{-/-}$ animals than in PARP-1$^{+/+}$ mice under normal conditions. Importantly, iNOS expression increased markedly upon OXA challenge, whereas only mild induction was observed in the OXA-treated PARP-1$^{-/-}$ mice (Figure 5a). Apparently, iNOS seems to be the major source of nitric oxide in our model system. This is in line with other findings obtained in different models of inflammation (Virag and Szabo, 2002).

Nitrosative stress is indicated by the formation of protein tyrosine nitration that could be observed in the ears of WT but not PARP-1$^{-/-}$ mice (Figure 5b). Nitrotyrosine staining could be detected in the infiltrating cells and in the keratinocytes, with strongest immunopositivity observed in the microabscesses, in which widespread keratinocyte death has previously been described (Ormerod *et al.*, 1997; Szabo *et al.*, 2001; Cals-Grierson and Ormerod, 2004; Olmos *et al.*, 2007).

We assessed the level of oxidative stress that generally accompanies nitrosative stress. We detected increased lipid, protein, and DNA base oxidation (as shown by protein carbonylation, protein-4-hydroxy-2-nonenal adduct, and 8-OHdG formation) that was all reduced in the PARP-1$^{-/-}$ mice (Figure 6a–c).

Oxidative and nitrosative stress can induce DNA breakage and PARP activation (Virag and Szabo, 2002; Hassa and Hottiger, 2008). Therefore, we set out to investigate DNA strand breakage by TUNEL assay. DNA strand breaks appeared in keratinocytes, endothelial cells, and leukocytes (Figure 6d) in PARP-1$^{+/+}$ mice. There was a high number of TUNEL-positive cells in the microabscesses, suggesting intense oxidative stress (Figure 6d). The number of TUNEL-positive cells was reduced in the PARP-1$^{-/-}$ subjects. DNA strand breaks led to PARP-1 activation, resulting in the formation of PAR (Virag and Szabo, 2002; Hassa and Hottiger, 2008). A nuclear PAR signal could be detected in the PARP-1$^{+/+}$ mice that was absent in the PARP-1$^{-/-}$ animals (Figure 6e). PAR was present in all cell types in the ear.

Our data show that PARP-1 is a regulator of inflammation in CHS; however, other members of the PARP family (except for PARP-2) might also be implicated. The group of macroPARPs (PARP-9/Bal1, PARP-14/Bal2, and PARP-15/Bal3) also possess immunological roles (reviewed in Hakme *et al.*, 2008), suggesting that their involvement cannot be excluded in cutaneous inflammatory processes. However, PAR glycohydrolase, which is responsible for PAR degradation, is a more likely candidate for regulating CHS. Despite the opposing biochemical role, PAR glycohydrolase often shares similar transcriptional function with PARP-1 (Frizzell *et al.*, 2009) and it affects inflammatory gene expression (Rapizzi *et al.*, 2004). Tannins are inhibitors of PAR glycohydrolase (Ying and Swanson, 2000), and it is tempting to hypothesize that the effectiveness of the commonly used tannin-containing external products in dermatology may be related to their PAR glycohydrolase inhibitory effects.

These data obtained in PARP-1$^{-/-}$ mice are very similar to previous results obtained with the administration of a PARP inhibitor compound in the elicitation phase of CHS (Bai *et al.*, 2009). It is important to note the important difference between pharmacological PARP inhibition and PARP-1 knockout. On one hand, the pharmacological inhibitor causes general PARP inhibition affecting all PARP isoforms, and on the other, application of pharmacological inhibitor after the sensitization phase allows us to determine the enzymes' role on the elicitation phase. In the knockout study, however, the absence of PARP-1 may affect both the sensitization and the elicitation phase. For example, uptake and presentation of antigens by dendritic cells is a cornerstone of efficient sensitization. As both ATF-2 and NF-κB have important roles in dendritic cell function (Stepnik and Arkusz, 2003; Sasaki and Aiba, 2007), it cannot be excluded that the sensitization phase of CHS is also impaired in the PARP-1$^{-/-}$ mice. This possibility, however, would require further investigation.

In the effector phase, PARP-1 modulates several key steps of inflammation such as: (1) cellular infiltration, (2) expression of chemokines, (3) adhesion molecules, (4) MMPs, and (5) the

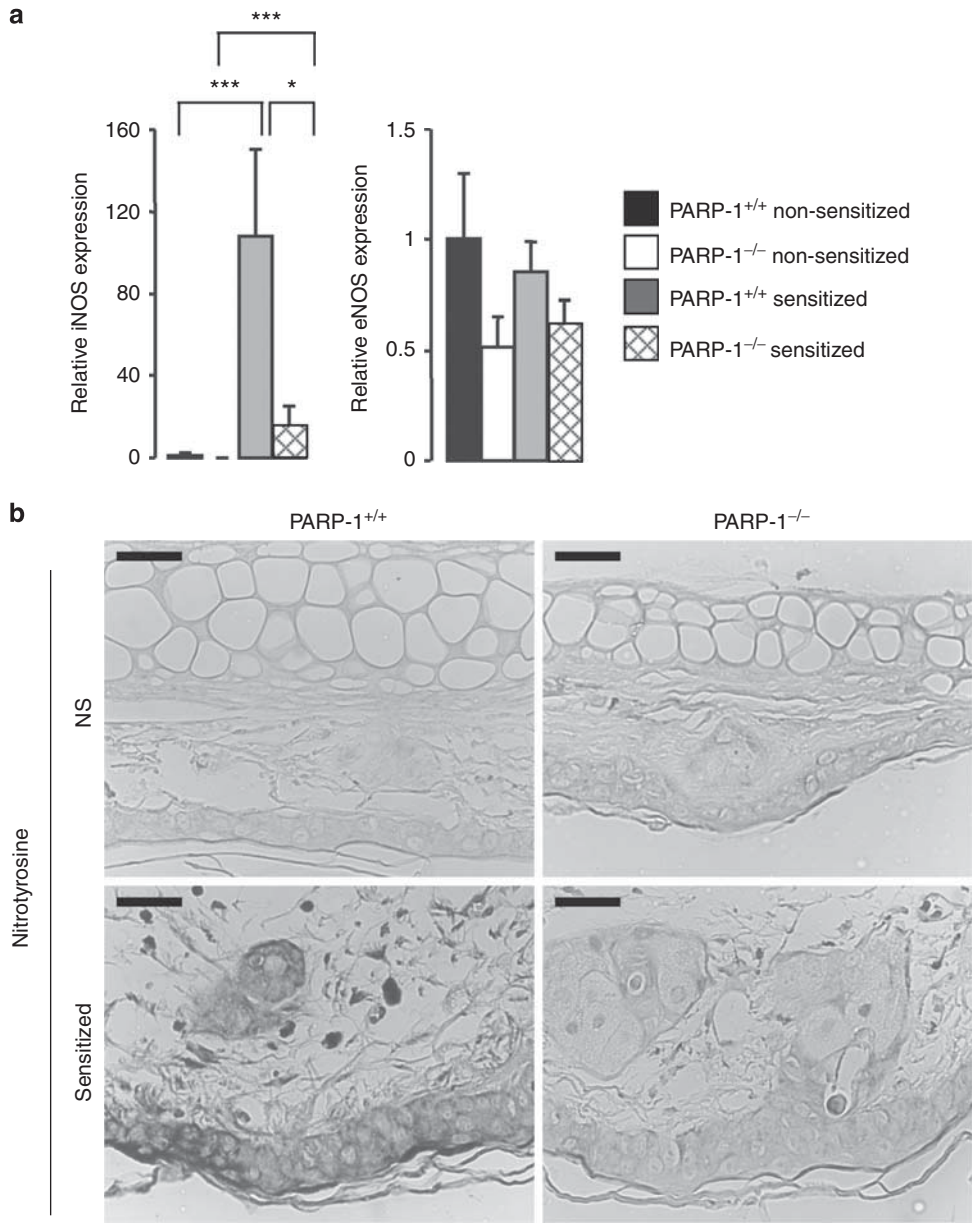

Figure 5. Reduced nitrosative stress in poly(ADP-ribose) polymerase (PARP)-1$^{-/-}$ mice. (**a**) Inducible and endothelial nitric oxide synthase (iNOS and eNOS) expression was determined by quantitative real-time reverse transcriptase PCR (qRT-PCR). (**b**) Nitrotyrosine immunohistochemistry was performed on formalin-fixed, paraffin-embedded tissue sections. NS, nonsensitized. *$P<0,05$; ***$P<0.001$, significant difference between cohorts (linear contrast adjustment was applied on image **b**). Scale bar = 20 μm.

redox-sensitive p65 and ATF-2 transcription factors. In a possible scenario, the increasing level of oxidative/nitrosative stress enhances PARP-1 activation that in turn boosts all the previously described processes, further aggravating oxidative/nitrosative stress and creating a vicious circle. In fact, PARP-1 has a central role in the control of oxidative stress in the elicitation phase of CHS, and its inhibition or genetic deletion disrupts the self-intensifying propagation of inflammation. Altogether, these results provide further support for the possible therapeutic applicability of PARP inhibitors in CHS.

MATERIALS AND METHODS

Materials

OXA and all chemicals were from Sigma-Aldrich (St Louis, MO) unless stated otherwise.

Animal studies

All animal experiments were approved by the local ethical committee (9/2008/DE MÁB) and were performed according to the European Union and national guidelines. Homozygous female PARP-1 and PARP-2 knockout mice and their respective WT littermates on C57/Bl6 background were used (Menissier-de Murcia

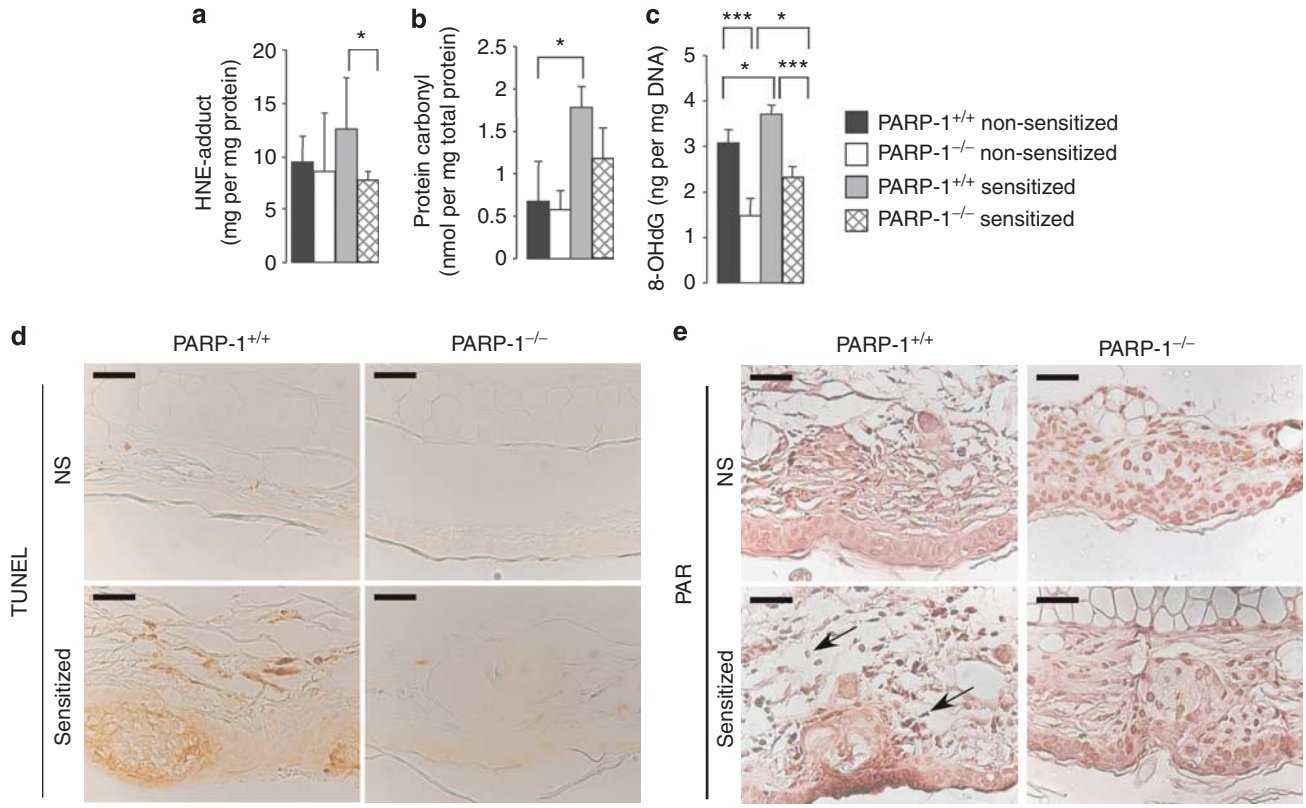

Figure 6. Reduced oxidative stress, DNA damage, and poly(ADP-ribose) polymerase (PARP) activity in PARP-1$^{-/-}$ mice. (**a**) 4-Hydroxy-2-nonenal (HNE), (**b**) protein carbonyl, and (**c**) 8-OHdG were determined using commercial kits. (**d**) TUNEL assay and (**e**) PAR immunohistochemistry were performed on formalin-fixed, paraffin-embedded tissue sections. NS, nonsensitized. The arrows point at PAR-positive nuclei. *P<0,05; ***P<0.001, significant difference between cohorts (linear contrast adjustment was applied on images **d** and **e**). Scale bar = 20 μm.

et al., 1997; Menissier-de Murcia *et al.*, 2003). CHS model was performed as described in Szabo *et al.* (2001), and irritative dermatitis model was performed as described in Bai *et al.* (2009).

Histology and microscopy

Hematoxylin–eosin staining and immunohistochemistry was performed on paraffin-fixed 7 μm tissue sections as described in Szabo *et al.* (2001).

MPO activity measurement

The measurement of MPO activity has been described in Virag *et al.* (2004).

MMP activity measurement

Ear homogenates were incubated with fluorescein-labeled gelatin (Invitrogen, Carlsbad, CA) and then fluorescein fluorescence was determined and normalized for protein content.

Characterization of oxidative stress

Commercial kits from Cell Biolabs (Sand Diego, CA) were used for determining 8-OHdG and 4-hydroxy-2-nonenal. Protein carbonylation was determined using a commercial kit from Cayman Chemicals (Ann Harbor, MI). Samples were processed according to the manufacturer's instructions.

mRNA preparation and reverse transcription and quantitative PCR

Total RNA preparation, and reverse transcription and quantitative PCR were performed as described in Bai *et al.* (2007). Normalized expression values were expressed as fold increase compared with samples from WT nonsensitized mice. Primers are summarized in Supplementary Table S1 online.

Transcription factor transactivation studies

For nuclear protein extraction, the TransFactor Extraction kit (Clontech, Mountain View, CA), and for transactivation studies, TransFactor Inflammatory Profiling-1 kit (Clontech) were used according to the manufacturer's instructions. The results are expressed as fold increase compared to WT non-sensitized samples.

Statistical analysis

Results were expressed as means ± SEM. Statistical significance between groups was determined using Student's *t*-test, and $P<0.05$ was considered as significant. Error bars represent ± SEM.

CONFLICT OF INTEREST

The authors state no conflict of interest.

ACKNOWLEDGMENTS

This work was supported by a Bolyai and SNSF fellowship to PB, a FEBS fellowship to AB, OTKA NNF78498, K73003, K60780, K82009, TAMOP-4.2.2-08/1-2008-0019, NKTH (Baross program), Mecenatura (DE OEC Mec-1/2008), Ambassade de France en Hongrie and Ministère des Affaires Étrangeres, Hungarian Science and Technology Foundation (FR-26/2009), Association pour la Recherche sur le Cancer, Centre National de la Recherche Scientifique, Université de Strasbourg, and Agence Nationale de la Recherche. We acknowledge the help of Mrs Erzsébet

Herbály in processing histology samples and Mrs Júlia Hunyadi for technical assistance.

SUPPLEMENTARY MATERIAL

Supplementary material is linked to the online version of the paper at http://www.nature.com/jid

REFERENCES

Ame JC, Rolli V, Schreiber V *et al.* (1999) PARP-2, a novel mammalian DNA damage-dependent poly(ADP-ribose) polymerase. *J Biol Chem* 274:17860–8

Bai P, Hegedus C, Szabo E *et al.* (2009) Poly(ADP-ribose) polymerase mediates inflammation in a mouse model of contact hypersensitivity. *J Invest Dermatol* 129:234–8

Bai P, Houten SM, Huber A *et al.* (2007) Poly(ADP-ribose) polymerase-2 controls adipocyte differentiation and adipose tissue function through the regulation of the activity of the retinoid X receptor/peroxisome proliferator-activated receptor-gamma heterodimer. *J Biol Chem* 282:37738–46

Beckman JS, Koppenol WH (1996) Nitric oxide, superoxide, and peroxynitrite: the good, the bad, and ugly. *Am J Physiol* 271:C1424–37

Biedermann T, Kneilling M, Mailhammer R *et al.* (2000) Mast cells control neutrophil recruitment during T cell-mediated delayed-type hypersensitivity reactions through tumor necrosis factor and macrophage inflammatory protein 2. *J Exp Med* 192:1441–52

Cals-Grierson MM, Ormerod AD (2004) Nitric oxide function in the skin. *Nitric Oxide* 10:179–93

de Murcia G, Menissier-de Murcia J (1994) Poly(ADP-ribose) polymerase: a molecular nick-sensor. *Trends Biochem Sci* 19:172–6

Espinoza LA, Smulson ME, Chen Z (2007) Prolonged poly(ADP-ribose) polymerase-1 activity regulates JP-8-induced sustained cytokine expression in alveolar macrophages. *Free Radic Biol Med* 42:1430–40

Frizzell KM, Gamble MJ, Berrocal JG *et al.* (2009) Global analysis of transcriptional regulation by poly(ADP-ribose) polymerase-1 and poly(ADP-ribose) glycohydrolase in MCF-7 human breast cancer cells. *J Biol Chem* 284:33926–38

Fuchs J, Zollner TM, Kaufmann R *et al.* (2001) Redox-modulated pathways in inflammatory skin diseases. *Free Radic Biol Med* 30:337–53

Grabbe S, Schwarz T (1998) Immunoregulatory mechanisms involved in elicitation of allergic contact hypersensitivity. *Immunol Today* 19:37–44

Grabbe S, Steinert M, Mahnke K *et al.* (1996) Dissection of antigenic and irritative effects of epicutaneously applied haptens in mice. Evidence that not the antigenic component but nonspecific proinflammatory effects of haptens determine the concentration-dependent elicitation of allergic contact dermatitis. *J Clin Invest* 98:1158–64

Ha HC (2004) Defective transcription factor activation for proinflammatory gene expression in poly(ADP-ribose) polymerase 1-deficient glia. *Proc Natl Acad Sci USA* 101:5087–92

Haddad M, Rhinn H, Bloquel C *et al.* (2006) Anti-inflammatory effects of PJ34, a poly(ADP-ribose) polymerase inhibitor, in transient focal cerebral ischemia in mice. *Br J Pharmacol* 149:23–30

Hakme A, Huber A, Dolle P *et al.* (2008) The macroPARP genes Parp-9 and Parp-14 are developmentally and differentially regulated in mouse tissues. *Dev Dyn* 237:209–15

Hassa PO, Hottiger MO (1999) A role of poly (ADP-ribose) polymerase in NF-kappaB transcriptional activation. *Biol Chem* 380:953–9

Hassa PO, Hottiger MO (2008) The diverse biological roles of mammalian PARPS, a small but powerful family of poly-ADP-ribose polymerases. *Front Biosci* 13:3046–82

Homey B, Assmann T, Vohr HW *et al.* (1998) Topical FK506 suppresses cytokine and costimulatory molecule expression in epidermal and local draining lymph node cells during primary skin immune responses. *J Immunol* 160:5331–40

Kauppinen TM, Swanson RA (2005) Poly(ADP-ribose) polymerase-1 promotes microglial activation, proliferation, and matrix metalloproteinase-9-mediated neuron death. *J Immunol* 174:2288–96

Kelly M, Hwang JM, Kubes P (2007) Modulating leukocyte recruitment in inflammation. *J Allergy Clin Immunol* 120:3–10

Koh SH, Chang DI, Kim HT *et al.* (2005) Effect of 3-aminobenzamide, PARP inhibitor, on matrix metalloproteinase-9 level in plasma and brain of ischemic stroke model. *Toxicology* 214:131–9

Korkina L, Pastore S (2009) The role of redox regulation in the normal physiology and inflammatory diseases of skin. *Front Biosci (Elite Ed)* 1:123–41

Le NT, Xue M, Castelnoble LA *et al.* (2007) The dual personalities of matrix metalloproteinases in inflammation. *Front Biosci* 12:1475–87

Lim YM, Moon SJ, An SS *et al.* (2008) Suitability of macrophage inflammatory protein-1beta production by THP-1 cells in differentiating skin sensitizers from irritant chemicals. *Contact Dermatitis* 58:193–8

McHale JF, Harari OA, Marshall D *et al.* (1999a) TNF-alpha and IL-1 sequentially induce endothelial ICAM-1 and VCAM-1 expression in MRL/lpr lupus-prone mice. *J Immunol* 163:3993–4000

McHale JF, Harari OA, Marshall D *et al.* (1999b) Vascular endothelial cell expression of ICAM-1 and VCAM-1 at the onset of eliciting contact hypersensitivity in mice: evidence for a dominant role of TNF-alpha. *J Immunol* 162:1648–55

Menissier-de Murcia J, Niedergang C, Trucco C *et al.* (1997) Requirement of poly(ADP-ribose) polymerase in recovery from DNA damage in mice and in cells. *Proc Natl Acad Sci USA* 94:7303–7

Menissier-de Murcia J, Ricoul M, Tartier L *et al.* (2003) Functional interaction between PARP-1 and PARP-2 in chromosome stability and embryonic development in mouse. *EMBO J* 22:2255–63

Morita H, Hori M, Kitano Y (1996) Modulation of picryl chloride-induced contact hypersensitivity reaction in mice by nitric oxide. *J Invest Dermatol* 107:549–52

Oliver FJ, Menissier-de Murcia J, Nacci C *et al.* (1999) Resistance to endotoxic shock as a consequence of defective NF-kappaB activation in poly (ADP-ribose) polymerase-1 deficient mice. *EMBO J* 18:4446–54

Olmos A, Giner RM, Recio MC *et al.* (2007) Effects of plant alkylphenols on cytokine production, tyrosine nitration and inflammatory damage in the efferent phase of contact hypersensitivity. *Br J Pharmacol* 152:366–73

Ormerod AD, Dwyer CM, Reid A *et al.* (1997) Inducible nitric oxide synthase demonstrated in allergic and irritant contact dermatitis. *Acta Derm Venereol* 77:436–40

Oumouna-Benachour K, Hans CP, Suzuki Y *et al.* (2007) Poly(ADP-ribose) polymerase inhibition reduces atherosclerotic plaque size and promotes factors of plaque stability in apolipoprotein E-deficient mice: effects on macrophage recruitment, nuclear factor-kappaB nuclear translocation, and foam cell death. *Circulation* 115:2442–50

Quenet D, Gasser V, Fouillen L *et al.* (2008) The histone subcode: poly(ADP-ribose) polymerase-1 (Parp-1) and Parp-2 control cell differentiation by regulating the transcriptional intermediary factor TIF1beta and the heterochromatin protein HP1alpha. *FASEB J* 22:3853–65

Rapizzi E, Fossati S, Moroni F *et al.* (2004) Inhibition of poly(ADP-ribose) glycohydrolase by gallotannin selectively up-regulates expression of proinflammatory genes. *Mol Pharmacol* 66:890–8

Reimold AM, Kim J, Finberg R *et al.* (2001) Decreased immediate inflammatory gene induction in activating transcription factor-2 mutant mice. *Int Immunol* 13:241–8

Rowe A, Farrell AM, Bunker CB (1997) Constitutive endothelial and inducible nitric oxide synthase in inflammatory dermatoses. *Br J Dermatol* 136:18–23

Saint-Mezard P, Rosieres A, Krasteva M *et al.* (2004) Allergic contact dermatitis. *Eur J Dermatol* 14:284–95

Sasaki Y, Aiba S (2007) Dendritic cells and contact dermatitis. *Clin Rev Allergy Immunol* 33:27–34

Schraufstatter IU, Hinshaw DB, Hyslop PA *et al.* (1986) Oxidant injury of cells. DNA strand-breaks activate polyadenosine diphosphate-ribose polymerase and lead to depletion of nicotinamide adenine dinucleotide. *J Clin Invest* 77:1312–20

Schreiber V, Dantzer F, Ame JC *et al.* (2006) Poly(ADP-ribose): novel functions for an old molecule. *Nat Rev Mol Cell Biol* 7:517–28

Shieh WM, Ame JC, Wilson MV *et al.* (1998) Poly(ADP-ribose) polymerase null mouse cells synthesize ADP-ribose polymers. *J Biol Chem* 273:30069–72

Stepnik M, Arkusz J (2003) Molecular events associated with dendritic cells activation by contact sensitizers. *Int J Occup Med Environ Health* 16:191–9

Szabo E, Virag L, Bakondi E *et al.* (2001) Peroxynitrite production, DNA breakage, and poly(ADP-ribose) polymerase activation in a mouse model of oxazolone-induced contact hypersensitivity. *J Invest Dermatol* 117:74–80

Virag L, Bai P, Bak I *et al.* (2004) Effects of poly(ADP-ribose) polymerase inhibition on inflammatory cell migration in a murine model of asthma. *Med Sci Monit* 10:BR77–83

Virag L, Szabo C (2002) The therapeutic potential of poly(ADP-ribose) polymerase inhibitors. *Pharmacol Rev* 54:375–429

Yelamos J, Monreal Y, Saenz L *et al.* (2006) PARP-2 deficiency affects the survival of CD4+CD8+ double-positive thymocytes. *EMBO J* 25:4350–60

Yelamos J, Schreiber V, Dantzer F (2008) Toward specific functions of poly(ADP-ribose) polymerase-2. *Trends Mol Med* 14:169–78

Ying W, Swanson RA (2000) The poly(ADP-ribose) glycohydrolase inhibitor gallotannin blocks oxidative astrocyte death. *NeuroReport* 11:1385–8

Zingarelli B, Hake PW, Burroughs TJ *et al.* (2004) Activator protein-1 signalling pathway and apoptosis are modulated by poly(ADP-ribose) polymerase-1 in experimental colitis. *Immunology* 113:509–17

Zingarelli B, Szabo C, Salzman AL (1999) Blockade of poly(ADP-ribose) synthetase inhibits neutrophil recruitment, oxidant generation, and mucosal injury in murine colitis. *Gastroenterology* 116:335–45

Supplementary material to Brunyánszki et al. "Genetic ablation of PARP-1 protects against oxazolone-induced contact hypersensitivity by modulating oxidative stress"

Materials

Oxazolone and all chemicals were from *Sigma-Aldrich* (St. Louis, MO, USA) unless stated otherwise.

Animal studies

All animal experiments were approved by the local ethical committee (9/2008/DE MÁB) and were performed according to EU and national guidelines.

Homozygous PARP-1 and PARP-2 knockout (KO) mice and their respective wild-type (WT) littermates on C57/Bl6 backgorund were used in our experiments (Menissier-de Murcia et al., 1997; Menissier-de Murcia et al., 2003). Female mice were randomized into four groups (WT non-sensitized (n=6), WT-sensitized (n=6), KO non-sensitized (n=7), KO sensitized (n=9)) and were sensitized and challenged as described previously (Szabo et al., 2001).

PMA–induced irritative dermatitis model was performed as described in (Bai et al., 2009). Briefly, PMA (10 ml, 0.05% w/v) was smeared onto both sides of the ears of female mice (6 animals per group), ear swelling was determined together with all other biochemical measurements 24 hours later.

Histology and microscopy

Haematoxylin-eosine (HE) histochemistry was performed as described in (Szabo et al., 2001). Immunohistochemistry was performed using anti-nitrotyrosine (*Sigma*), CD-3 (*Millipore-Upstate*, Billerica, MA, USA), CD-68 (*Serotec*, Raleigh, NC, USA), neutrophil elastase (*Santa Cruz*, Santa Cruz, CA, USA) rabbit polyclonal antibodies and anti-PAR murine monoclonal antibody (*BD Biosciences*, San Jose, CA, USA) on paraffin-fixed 7 μm tissue sections as described in (Szabo et al., 2001).

Myeloperoxidase activity measurement

The measurement of myeloperoxidase (MPO) activity has been described in (Virag et al., 2004). MPO activity was expressed as the percentage of the MPO activity determined in the samples of WT non-sensitized animals.

MMP activity measurement

Ears were homogenized in DQ buffer (50 mM Tris pH 7.6, 150 mM NaCl, 5 mM $CaCl_2$) buffer by Ultra Turrax, then homogenate was cleared by centrifugation. To 100 µl supernatant and 80 µl DQ buffer 20 µl of fluorescein-conjugated gelatin (DQ gelatine, *Invitrogen*, Carlsbad, CA, USA) was added, samples were incubated at room temperature 30 minutes and fluorescein fluorescence was determined using a Victor V3 fluorimeter (*Beckton-Dickinson*, Franklin Lakes, NJ, USA). Fluorescence values were normalized for protein content.

8-OHdG determination

8-OHdG determination was performed using a commercial kit from *Cell Biolabs* (San Diego, CA, USA) according to the manufacturer's instructions.

Protein carbanoylation assay

Protein carbanoylation was assessed using a commercial kit (*Cayman Chemicals*, Ann Harbor, MI, USA) according to the manufacturer's instructions.

Lipid peroxidation assay

Lipid peroxidation was measured using a commercial kit to detect HNE-protein adducts from Cell Biolabs (San Diego, CA, USA) according to the manufacturer's instructions.

mRNA preparation, reverse transcription and qPCR

Total RNA was prepared using TRIzol (*Invitrogen*) according to the manufacturer's instructions. RNA was treated with DNase, and 2 µg of RNA was used for reverse transcription (RT). cDNA was purified on QIAquick PCR cleanup columns (*Qiagen*, Valencia, CA, USA). 10X diluted cDNA was used for quantitative PCR (qPCR) reactions. The qPCR reactions were performed using an ABI 7500 thermal cycler (*Applied Biosciences*, Foster City, CA, USA) and qPCR Supermix (*Applied Bioscience*) with the primers summarized in Supplementary Table 1. Expression values were normalized to the geometric mean of the expression of three control genes (18S, 36B4 and cyclophyllin) (Bai et al., 2007). mRNA expression levels were expressed as fold increase compared to samples from WT non-sensitized mice.

Transcription factor transactivation studies

For nuclear protein extraction the Transfactor Extraction kit (*Clontech*, Mountain View, CA, USA) was used according to the manufacturer's instructions as described bellow.

Ears were frozen in liquid nitrogen and were ground into fine powder in a mortar cooled in liquid nitrogen. All further procedures were performed on ice with ice-cold reagents and equipment. The powdered sample was re-suspended in a small volume of ice-cold PBS and was consequently centrifuged at 450 g for 5 min at 4^{o}C. The pellet was resuspended in lysis buffer (10 mM HEPES (pH 7.9), 1.5 mM $MgCl_2$, 10 mM KCl, 1 mM DTT and protease inhibitor cocktail) and was disrupted repeatedly pressing through a syringe fitted with a No. 27 gauge needle (10 times each). The disrupted tissue lysate was then centrifuged at 11,000 g for 20 min, the supernatant removed and the nuclear pellet resuspended in extraction buffer (20 mM HEPES (pH 7.9), 1.5 mM $MgCl_2$, 0.42 M NaCl, 0.2 mM EDTA, 25% (v/v) glycerol, 1 mM DTT and protease inhibitor cocktail). The nuclei were then disrupted with a syringe fitted with a No. 27 gauge needle (10 times each) and centrifuged for 5 min at 21,000 g. Protein concentration of the supernatant (nuclear extract) was measured with Bradford protein assay.

For the quantification of transcription factor transactivation, the TransFactor Inflammatory Profiling-1 kit was utilized (*Clontech*). The kit enables the colorimetric determination of the DNA binding of the active transcription factors using an ELISA-based technique. 10 μg ear nuclear extract was loaded into each well and the measurement was performed according to the Manufacturer's instructions. The results are expressed as fold increase of the WT non-sensitized control samples.

Statistical analysis

Results were expressed as means ±SEM. Statistical significance between groups was determined by Student's t-test, $p<0.05$ was considered as significant. Error bars represent +/- SEM.

Supplementary Table 1. List of primers

Gene name	Primers
18S	GGG AGC CTG AGA AAC GGC GGG TCG GGA GTG GGT AAT TTT
36B4	AGA TTC GGG ATA TGC TGT TGG AAA GCC TGG AAG AAG GAG GTC
Cyclophyllin	TGG AGA GCA CCA AGA CAG ACA TGC CGG AGT CGA CAA TGAT
eNOS	GCA ATC TTC GTT CAG CCA TCA C AGA GCT CAG TGA TCT CCA CGT TG
iNOS	GAAGTGCAAAGTCTCAGACATGG GATTCTGGAACATTCTGTGCTGTC
E-Selectin	GGCAGAGTGAGATTTGAAGGATG GGACTTCAGCGTCACTTTGGTAG
IL-1β	CAA CCA ACA AGT GAT ATT CTC CAT G GAT CCA CAC TCT CCA GCT GCA
I-CAM	CTT TCG ATC TTC CAG CTA CCA TC CTG CTG TTT GTG CTC TCC TG
MCP-1	CTC AGC CAG ATG CAG TTA ACG CTC TCT CTT GAG CTT GGT GAC A
MIP-1α	CTC TGC AAC CAA GTC TTC TCA GC AAG GCT GCT GGT TTC AAA ATA GTC
MIP-2	CTC CAG CCA CAC TTC AGC CTA G CGT CAC ACT CAA GCT CTG GAT G
MMP-9	CAT TCG CGT GGA TAA GGA GT ACC TGG TTC ACC TCA TGG TC
TIMP-2	CGT TTC TTT GGG GTT TCT GA TTT ATC ACT AAC AAT ATA GAC AGC CAC TCT
TNFα	CAT CTT CTC AAA ATT CGA GTG ACA A TGG GAG TAG ACA AGG TAC AAC CC
V-Cam	TAC CAG CTC CCA AAA TCC TG TCT GCT AAT TCC AGC CTC GT

References

Bai P, Hegedus C, Szabo E, Gyure L, Bakondi E, Brunyanszki A, Gergely S, Szabo C and Virag L (2009). Poly(ADP-ribose) polymerase mediates inflammation in a mouse model of contact hypersensitivity. *J Invest Dermatol.* 129: 234-8. Epub 2008 Jul 17.

Bai P, Houten SM, Huber A, Schreiber V, Watanabe M, Kiss B, de Murcia G, Auwerx J and Menissier-de Murcia J (2007). Poly(ADP-ribose) polymerase-2 controls adipocyte differentiation and adipose tissue function through the regulation of the activity of the retinoid X receptor/peroxisome proliferator-activated receptor-gamma heterodimer. *J.Biol.Chem.* 282: 37738-46.

Menissier-de Murcia J, Niedergang C, Trucco C, Ricoul M, Dutrillaux B, Mark M, Oliver FJ, Masson M, Dierich A, LeMeur M, Walztinger C, Chambon P and de Murcia G (1997). Requirement of poly(ADP-ribose) polymerase in recovery from DNA damage in mice and in cells. *Proc.Natl.Acad.Sci.U.S.A.* 94: 7303-7.

Menissier-de Murcia J, Ricoul M, Tartier L, Niedergang C, Huber A, Dantzer F, Schreiber V, Ame JC, Dierich A, LeMeur M, Sabatier L, Chambon P and de Murcia G (2003). Functional interaction between PARP-1 and PARP-2 in chromosome stability and embryonic development in mouse. *EMBO J.* 22: 2255-63.

Szabo E, Virag L, Bakondi E, Gyure L, Hasko G, Bai P, Hunyadi J, Gergely P and Szabo C (2001). Peroxynitrite production, DNA breakage, and poly(ADP-ribose) polymerase activation in a mouse model of oxazolone-induced contact hypersensitivity. *J.Invest Dermatol.* 117: 74-80.

Virag L, Bai P, Bak I, Pacher P, Mabley JG, Liaudet L, Bakondi E, Gergely P, Kollai M and Szabo C (2004). Effects of poly(ADP-ribose) polymerase inhibition on inflammatory cell migration in a murine model of asthma. *Med.Sci.Monit.* 10: BR77-BR83.

Cell Metabolism
Short Article

PARP-1 Inhibition Increases Mitochondrial Metabolism through SIRT1 Activation

Péter Bai,[1,2] Carles Cantó,[3] Hugues Oudart,[4] Attila Brunyánszki,[2] Yana Cen,[5] Charles Thomas,[3] Hiroyasu Yamamoto,[3] Aline Huber,[1] Borbála Kiss,[1] Riekelt H. Houtkooper,[3] Kristina Schoonjans,[3] Valérie Schreiber,[1] Anthony A. Sauve,[5] Josiane Menissier-de Murcia,[1] and Johan Auwerx[3,*]
[1]Biotechnologie et Signalisation Cellulaire, UMR7242 CNRS, Université de Strasbourg, ESBS, Illkirch, France
[2]Department of Medical Chemistry, University of Debrecen, Debrecen, Hungary
[3]Laboratory of Integrative and Systems Physiology, École Polytechnique Fédérale de Lausanne, Switzerland
[4]CEPE, CNRS UPR9010, Strasbourg, France
[5]Department of Pharmacology, Weill Cornell Medical College, New York, NY 10021, USA
*Correspondence: admin.auwerx@epfl.ch
DOI 10.1016/j.cmet.2011.03.004

SUMMARY

SIRT1 regulates energy homeostasis by controlling the acetylation status and activity of a number of enzymes and transcriptional regulators. The fact that NAD^+ levels control SIRT1 activity confers a hypothetical basis for the design of new strategies to activate SIRT1 by increasing NAD^+ availability. Here we show that the deletion of the poly(ADP-ribose) polymerase-1 (*PARP-1*) gene, encoding a major NAD^+-consuming enzyme, increases NAD^+ content and SIRT1 activity in brown adipose tissue and muscle. *PARP-1*$^{-/-}$ mice phenocopied many aspects of SIRT1 activation, such as a higher mitochondrial content, increased energy expenditure, and protection against metabolic disease. Also, the pharmacologic inhibition of PARP in vitro and in vivo increased NAD^+ content and SIRT1 activity and enhanced oxidative metabolism. These data show how PARP-1 inhibition has strong metabolic implications through the modulation of SIRT1 activity, a property that could be useful in the management not only of metabolic diseases, but also of cancer.

INTRODUCTION

Intracellular NAD^+ levels control the activity of the type III deacetylase SIRT1, allowing it to act both as a metabolic sensor and effector (Yu and Auwerx, 2009). Overexpression studies indicated how activation of SIRT1 or of its orthologs extends life span in lower eukaryotes and protects against high-fat-diet (HFD)-induced metabolic disease in mice (Yu and Auwerx, 2009). These attractive properties spurred a quest to identify small-molecule SIRT1 agonists that could be used in situations of metabolic stress and damage. This strategy identified compounds like resveratrol or SRT1720 (Howitz et al., 2003; Milne et al., 2007), whose ability to directly interact with and activate SIRT1 is, however, debated (Pacholec et al., 2010). Therefore, a strong interest exists to develop alternative strategies to activate SIRT1. Given the NAD^+ dependency of SIRT1, another potential way to activate it is by increasing NAD^+ availability. This could be achieved by specifically inhibiting other NAD^+-consuming activities.

Poly(ADP-ribose) polymerase (PARP)-1 is a major cellular NAD^+ consumer (Sims et al., 1981). PARP-1 is activated upon binding to damaged or abnormal DNA (Durkacz et al., 1980) and catalyzes the formation of poly(ADP-ribose) polymers (PAR) onto different acceptor proteins, including PARP-1 itself (autoPARylation), using NAD^+ as substrate (Adamietz, 1987). PARP-1 activation depletes cellular NAD^+ levels, using it to form PAR (Sims et al., 1981). This led us to test the influence of PARP-1 on SIRT1 activity and metabolic homeostasis. Our results show how a reduction/ablation of PARP-1 activity boosts NAD^+ levels and SIRT1 activity, which in turn enhances mitochondrial content and function, culminating in a solid protection against metabolic disease.

RESULTS

PARP-1$^{-/-}$ Mice Are Leaner and Have Increased Energy Expenditure

Chow-fed *PARP-1*$^{-/-}$ mice (de Murcia et al., 1997) weighed less (Figure 1A) and accumulated less fat than *PARP-1*$^{+/+}$ littermates upon aging (Figure 1B), despite eating significantly more (Figure 1C). During indirect calorimetry, *PARP-1*$^{-/-}$ mice consumed more O_2 (Figure 1D), suggestive of higher energy expenditure (EE). Resting EE was not different (Figure S1A), indicating that the increase was due to changes at night, when mice are active. Accordingly, *PARP-1*$^{-/-}$ mice were more active at night (Figure S1B). In addition, the respiratory quotient was also higher in *PARP-1*$^{-/-}$ mice during the dark phase, indicating enhanced glucose oxidation during the feeding period (Figure 1E). *PARP-1*$^{-/-}$ mice also maintained a higher body temperature upon cold exposure (Figure 1F), were more glucose tolerant (Figure 1G), and had a trend toward lower fasting blood glucose levels (4.30 ± 0.17 mM in *PARP-1*$^{+/+}$ mice versus 3.98 ± 0.18 mM in *PARP-1*$^{-/-}$ mice; $p = 0.058$), despite similar insulin levels (data not shown). During euglycemic-hyperinsulinemic clamp, glucose infusion rates or hepatic glucose production were similar to *PARP-1*$^{+/+}$ mice,

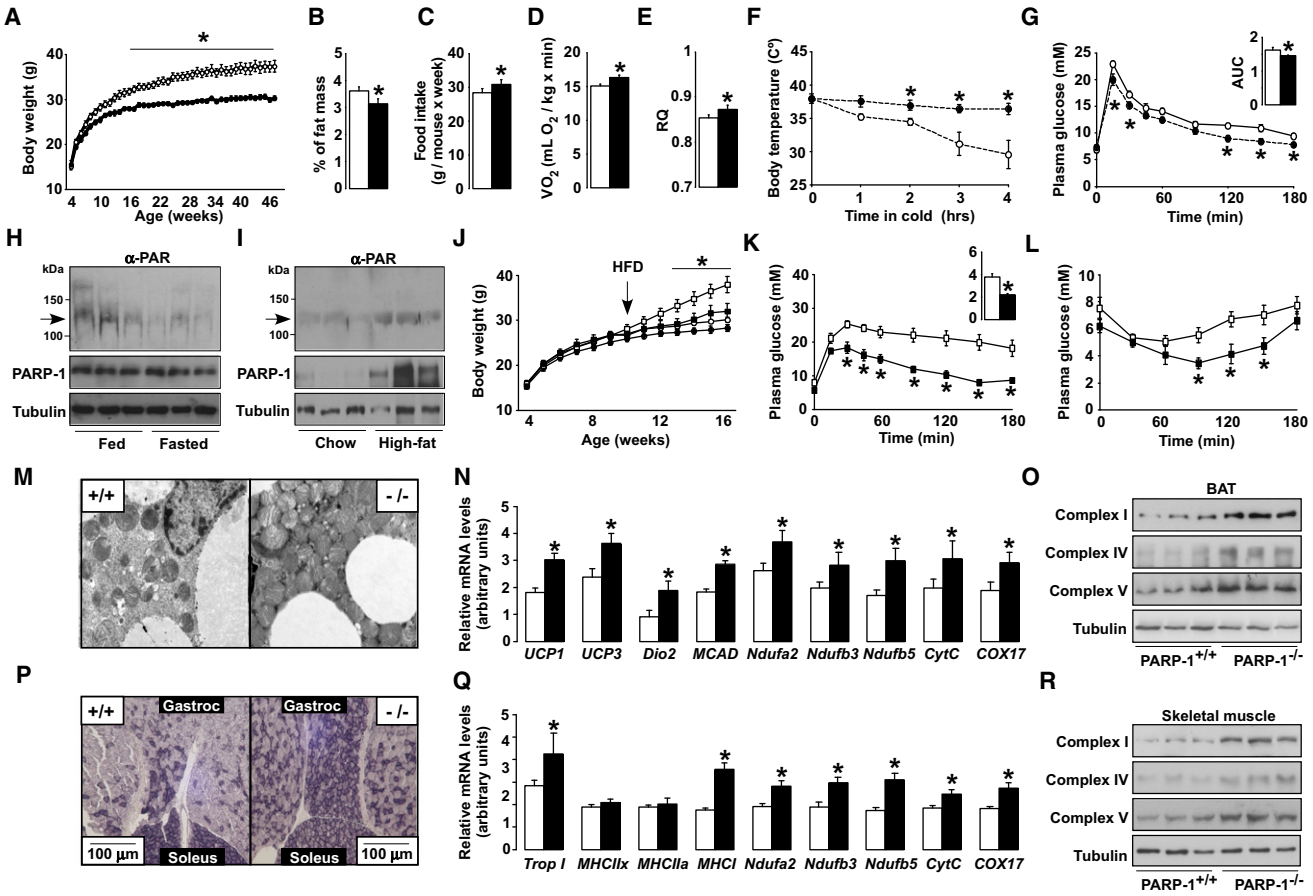

Figure 1. Phenotyping the PARP-1$^{-/-}$ Mice

(A) Body weight (BW) evolution in *PARP-1*$^{+/+}$ and $^{-/-}$ mice (n = 8/9).

(B) Epididymal white adipose tissue mass.

(C) Average food consumption.

(D and E) O_2 consumption (D) and respiratory quotient (RQ) (E) of *PARP-1*$^{+/+}$ and $^{-/-}$ mice (n = 9/9) determined by indirect calorimetry.

(F) Body temperature after exposure to 4°C (n = 6/5).

(G) Oral glucose tolerance test (OGTT) (n = 5/5) and the area under curve (AUC).

(H) PARP-1 autoPARylation (arrow), analyzed in 100 µg of protein extract from gastrocnemius muscles of 16-week-old mice fed ad libitum or fasted (24 hr). PARP-1 and tubulin levels were checked using 50 µg of protein extract.

(I) Gastrocnemius from mice on chow diet (CD) or HFD (12 weeks) were analyzed as in (H).

(J) BW evolution in *PARP-1*$^{+/+}$ and $^{-/-}$ mice (n = 10/10) fed a CD (circles) or HFD (squares) from 8 weeks of age.

(K and L) OGTT (K) and an insulin tolerance test (L) in HFD-fed *PARP-1*$^{+/+}$ and $^{-/-}$ mice at 16 weeks of age (n = 10/10). The AUC of the OGTT is shown on the top right.

(M–O) BAT from *PARP-1*$^{+/+}$ and $^{-/-}$ mice on CD was extracted and mitochondrial biogenesis was analyzed by transmission electron microscopy (M), mRNA expression of the genes indicated (N), and the abundance of mitochondrial complexes (O) in 25 µg of total protein extracts.

(P) SDH staining of sections from gastrocnemius and soleus of *PARP-1*$^{+/+}$ and $^{-/-}$ mice on CD.

(Q and R) Gastrocnemius was also used to analyze mRNA levels of the indicated genes (Q) and the abundance of mitochondrial complexes in 25 µg of total protein extracts (R). White bars represent *PARP-1*$^{+/+}$ mice; black bars represent *PARP1*$^{-/-}$ mice. Values are expressed as mean ± SEM unless otherwise stated. * indicates statistical difference versus *PARP-1*$^{+/+}$ mice at $p < 0.05$. For abbreviations, see Table S1.

but supporting the idea of their better glucose tolerance, glucose uptake in *PARP-1*$^{-/-}$ muscle trended up (Figures S1C–S1E). In line with the lower fat mass and improved glucose tolerance, serum triglycerides (1.04 ± 0.07 mM in *PARP-1*$^{+/+}$ versus 0.84 ± 0.05 mM in *PARP-1*$^{-/-}$ mice; p = 0.048) and free fatty acids (FFA) (0.93 ± 0.09 mEq/l in *PARP-1*$^{+/+}$ versus 0.72 ± 0.03 mEq/l in *PARP-1*$^{-/-}$ mice; p = 0.040) were reduced in *PARP-1*$^{-/-}$ mice.

PARP-1 Is Induced by Nutrient Availability and Contributes to HFD-Induced Diabesity

The metabolic impact of *PARP-1* deletion made us evaluate whether nutrient scarcity (fasting) or overload (HFD) affects PARP-1 activity. Despite similar PARP-1 protein levels, a 24 hr fast sharply reduced PARP-1 autoPARylation levels, which reflect global PARP activity (Adamietz, 1987), suggesting a lower enzymatic activity (Figure 1H). In contrast, HFD robustly

increased PARP-1 protein levels and activity (Figure 1I), indicating a positive correlation between PARP-1 activity and nutrient availability.

As nutrient availability induces PARP-1 activity and *PARP-1* deletion prompts a leaner phenotype, we next explored how *PARP-1*$^{-/-}$ mice responded to HFD-induced metabolic disease. *PARP-1*$^{-/-}$ mice gained less weight after 2 months of HFD (Figure 1J), due to a lower fat accumulation (Figure S1F). Moreover, *PARP-1*$^{-/-}$ mice on HFD were more glucose tolerant (Figure 1K) insulin sensitized (Figure 1L) and had lower serum FFAs (0.66 ± 0.05 mEq/l versus 0.53 ± 0.03 mEq/l; p = 0.026).

Mitochondrial Activation in Brown Adipose Tissue and Muscle from PARP-1$^{-/-}$ Mice

The above results suggested improved mitochondrial activity in key metabolic tissues of *PARP-1*$^{-/-}$ mice, such as skeletal muscle and brown adipose tissue (BAT). *PARP-1*$^{-/-}$ mice had a relatively higher amount of BAT, with a more intense red appearance (Figure S1G). Transmission electron microscopy revealed higher mitochondrial content in *PARP-1*$^{-/-}$ BAT (Figure 1M), which was further corroborated by the increased mitochondrial DNA content (Figure S1H) and mRNA expression of genes involved in mitochondrial respiration (*Ndufa2*, *Ndufb2*, *Ndufb5*, *Cyt C*, *COX17*), uncoupling (*UCP1*, *UCP3*), fatty acid oxidation (*MCAD*), and thyroid hormone activation (*Dio2*). Mitochondrial biogenesis was also evidenced by the higher protein content of subunits from different respiratory complexes in the BAT from *PARP-1*$^{-/-}$ mice (Figure 1O).

Also, *PARP-1*$^{-/-}$ skeletal muscle had a marked oxidative profile. Succinate dehydrogenase (SDH) staining (Figure 1P) and the expression of muscle fiber isotype genes (*Trop I*, *MHCI*) (Figure 1Q) exposed an increase in oxidative fibers with a high mitochondrial content. As in BAT, the increased mitochondrial content was linked to an induction of the mRNA (Figure 1Q) and protein levels (Figure 1R) of mitochondrial components. In contrast to BAT and muscle, the expression of key metabolic genes was not altered in *PARP-1*$^{-/-}$ livers (Figure S1I), reflecting a minor role of PARP-1 in the liver, probably due to its very low expression (Figure S1J).

Higher NAD$^+$ Content and SIRT1 Activity in BAT and Muscle from PARP-1$^{-/-}$ Mice

The *PARP-1*$^{-/-}$ mice phenocopy many features seen after SIRT1 activation (Yu and Auwerx, 2009). As PARP-1 is a major NAD$^+$ consumer (Sims et al., 1981), we speculated that the lack of PARP-1 activity might increase NAD$^+$ content, in turn activating SIRT1. Illustrating how PARP-1 drives most PARP activity, the ablation of *PARP-1* reduced PARylation in both BAT and muscle (Figure 2A). The expression of the other PARP enzymes was not increased in *PARP-1*$^{-/-}$ BAT and muscle (Figures S2A and S2B), explaining the lack of compensation on PARylation. Confirming previous studies (Allinson et al., 2003; Fong et al., 2009), terminal dUTP nick-end labeling indicated that DNA damage was not increased in *PARP-1*$^{-/-}$ tissues (data not shown). In line with the attenuated NAD$^+$-consuming PARP activity, NAD$^+$ content was robustly increased in *PARP-1*$^{-/-}$ BAT and muscle (Figure 2B), while the levels of nicotinamide (NAM), a NAD$^+$-derived metabolite that inhibits sirtuin activity (Bitterman et al., 2002), remained unaffected (Figure 2C).

We next tested if the increase in NAD$^+$ correlated with SIRT1 activation. Indicative of SIRT1 activation, and supporting the higher mitochondrial content, PGC-1α acetylation levels in BAT and muscle of *PARP-1*$^{-/-}$ mice were reduced by ~40% and ~90%, respectively (Figures 2D and 2E). The acetylation of another SIRT1 target, forkhead box O1 (FOXO1), was also reduced by ~60% in BAT and ~40% in muscle (Figures 2D and 2E), supporting the idea that *PARP-1* deficiency leads to SIRT1 activation. Remarkably, SIRT1 protein was also robustly induced in *PARP-1*$^{-/-}$ BAT and muscle (Figures 2D and 2E), further amplifying SIRT1 activity.

As altered NAD$^+$ levels could also potentially impact other sirtuins, we also tested the activity of SIRT2 and SIRT3, which act as cytoplasmic and mitochondrial sirtuins, respectively. The acetylation level of tubulin, a SIRT2 target (North et al., 2003), was not altered in muscle from *PARP-1*$^{-/-}$ mice (Figure 2F). Likewise, the acetylation of complex I, a target for SIRT3 (Ahn et al., 2008), even showed a slight tendency to increase in *PARP-1*$^{-/-}$ muscles (Figure 2G). These results indicate that not all sirtuins are activated in *PARP-1*$^{-/-}$ tissues.

Reduced PARP-1 Activity in Cellular Models Enhances Oxidative Metabolism

Next, we knocked down *PARP-1* in HEK293T cells to evaluate whether an acute reduction in PARP-1 activity enhances oxidative metabolism. In these conditions, PARP-1 protein levels were reduced by ~80%, and the low PARP-1 autoPARylation demonstrated that PARP activity was largely blunted (Figure 3A). The reduced PARP activity was associated with enhanced NAD$^+$ content and SIRT1 function, as illustrated by decreased PGC-1α acetylation (Figures 3B and 3C). Importantly, this happened despite unchanged SIRT1 protein levels (Figure 3C) or changes in the activity of SIRT2 or SIRT3, as manifested in tubulin, Ndufa9, or total mitochondrial acetylation levels (Figures S3A–S3C). The induction of SIRT1 and PGC-1α activity culminated in a robust increase in mitochondrial DNA content (Figure 3D), mitochondrial-related gene expression (Figure 3E), and O_2 consumption (Figure 3F). Importantly, most of the metabolic effects elicited by PARP-1 depletion were lost when SIRT1 was simultaneously knocked down (Figures 3D–3F).

In line with the results in HEK293T cells, the expression of genes involved in mitochondrial function, mitochondrial DNA content, and O_2 consumption were also induced in *PARP-1*$^{-/-}$ compared to *PARP-1*$^{+/+}$ MEFs (Figures S3D–S3F). Consistent with our observations in tissues from *PARP-1*$^{-/-}$ mice, SIRT1 protein was also induced in *PARP-1*$^{-/-}$ MEFs (Figure S3G).

Pharmacological PARP Inhibition Enhances Oxidative Metabolism via SIRT1

To test the relation between SIRT1 and PARP-1 activities, we exposed C2C12 myotubes to H_2O_2 (500 μM, 6 hr), a well-known inducer of PARP-1 activity (Schraufstatter et al., 1986). H_2O_2 treatment vigorously increased PARP-1 (Figure 4A) and global protein PARylation levels (Figure 4B), as manifested by the slow migrating bands, in the absence of changes in PARP-1 levels (Figures 4A and 4B). Importantly, SIRT1 was not PARylated in response to H_2O_2 (Figure 4A), indicating that it is not a PARylation substrate. As reported (Schraufstatter et al., 1986), the H_2O_2-induced increase in PARP-1 activity sharply

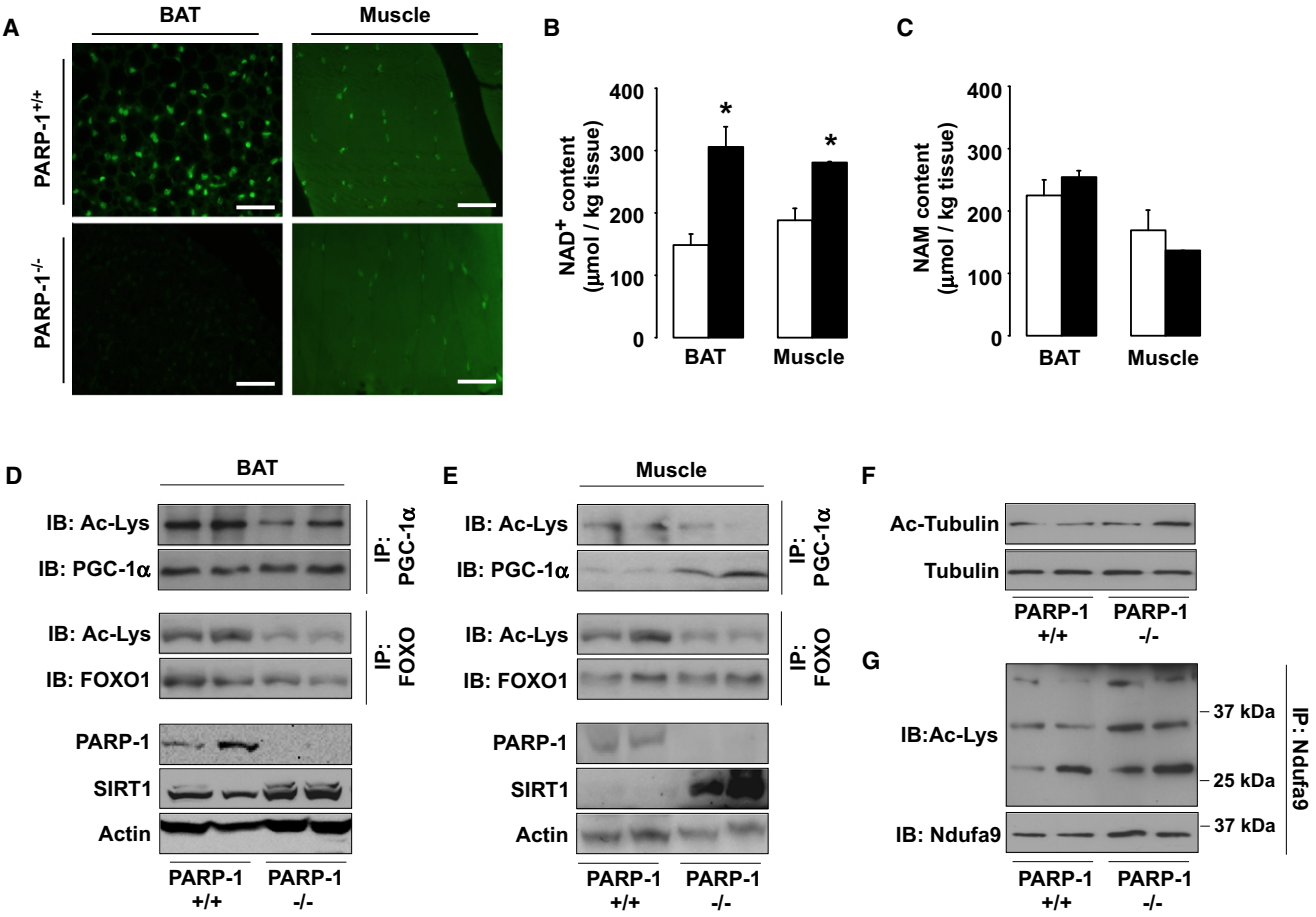

Figure 2. PARP-1 Deletion Raises NAD$^+$ Levels and Activates SIRT1

(A) Protein PARylation determined by α-PAR staining on formalin-fixed 7 μm BAT and muscle tissue sections of *PARP-1*$^{+/+}$ and $^{-/-}$ mice. White bar = 10 μm.

(B and C) NAD$^+$ (B) and NAM (C) levels in BAT and muscle from *PARP-1*$^{+/+}$ (white bars) and *PARP-1*$^{-/-}$ (black bars) mice determined by mass spectrometry.

(D and E) PARP-1, SIRT1, and actin protein content in BAT (D) and muscle (E) were determined by western blot, using 100 μg of protein lysate. PGC-1α and FOXO1 acetylation were examined by immunoprecipitation.

(F) Tubulin and acetylated-tubulin levels were tested in *PARP-1*$^{+/+}$ and $^{-/-}$ gastrocnemius.

(G) The Ndufa9 subunit of mitochondrial complex I was immunoprecipitated from 400 μg of total protein from gastrocnemius, and acetylation levels were analyzed by western blot. Values are expressed as mean ± SEM unless otherwise stated. * indicates statistical difference versus *PARP-1*$^{+/+}$ mice at $p < 0.05$.

depleted NAD$^+$ content (Figure 4C), but did not affect SIRT1 protein levels (Figures 4A and 4B). This lower NAD$^+$ availability limited SIRT1 activity, as reflected in PGC-1α hyperacetylation (Figure 4D). Interestingly, the inhibition of PARP activity with PJ34 (Garcia Soriano et al., 2001) rescued the drop in NAD$^+$ and recovered SIRT1 function during H_2O_2 exposure (Figures 4B–4D). These results indicate that PARP-1 activation restrains SIRT1 activity and that PARP inhibitors relieve this limitation.

PARP-1 activity is not necessarily linked to DNA damage, and it has been shown to fluctuate in a circadian fashion (Asher et al., 2010). Therefore, we wondered whether prolonged PARP inhibition, even in the absence of DNA damage, would favor NAD$^+$ accumulation and, potentially, SIRT1 activity. Supporting this premise, PARP inhibition by PJ34 (Figure 4E) or a structurally unrelated compound, TIQ-A (data not shown), gradually raised NAD$^+$ levels, becoming significant after 24 hr. At that time, PARP activity, but not PARP-1 protein levels, was robustly decreased (Figure 4F). PJ34 increased NAD$^+$ levels dose dependently, in correlation with SIRT1 activity, as illustrated by PGC-1α deacetylation (Figure 4G). Similar effects also happened in vivo, as treatment of mice with PJ34 (10 mg/kg, b.i.d. for 5 days) blunted basal PARP activity in muscle (Figure 4H), while increasing NAD$^+$ and SIRT1 activity (Figure 4I). Despite the short duration of the treatment, serum triglyceride (1.21 ± 0.08 mM vehicle versus 1.11 ± 0.04 mM PJ34; $p = 0.08$) and FFA levels (1.59 ± 0.06 mEq/l vehicle versus 1.44 ± 0.03 mEq/l PJ34; $p = 0.03$) were reduced in PJ34-treated mice. Of note, while compounds like resveratrol impact SIRT1 through AMP-activated protein kinase (AMPK) (Cantó et al., 2010), PJ34 did not alter AMPK activity, as reflected by the unchanged acetyl-CoA carboxylase (ACC) phosphorylation in either C2C12 myotubes (Figure 4J) or gastrocnemius muscle (Figure 4H). PJ34 did not affect SIRT1 protein levels either (Figures 4H and 4J), but robustly induced the expression of mitochondrial and lipid oxidation genes, both in C2C12 myotubes and muscle (Figures 4K and 4L). Consistent with PGC-1α deacetylation and activation,

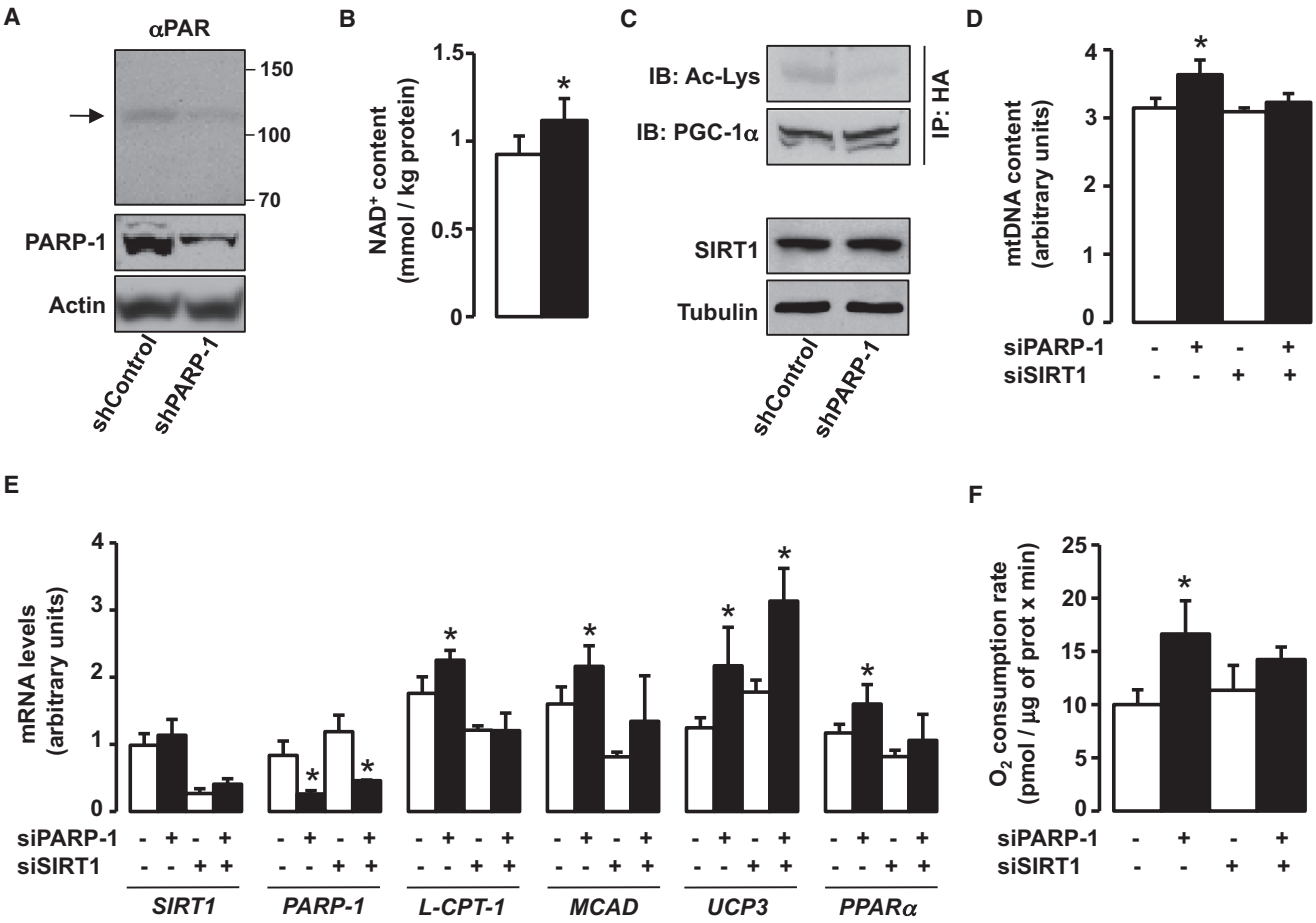

Figure 3. PARP-1 Knockdown Promotes SIRT1 Activity and Oxidative Metabolism

(A–C) HEK293T cells were transfected with either scramble (control) or *PARP-1* shRNA and HA-PGC-1α expression vector for 48 hr. Then, PARP-1 protein levels and autoPARylation (arrowhead) were analyzed in total protein lysates (A). Intracellular NAD^+ was measured on total acid extracts (B). PGC-1α acetylation was analyzed in HA immunoprecipitates (C).

(D–F) HEK293T cells were transfected with either a pool of *PARP-1* siRNAs, a pool of *SIRT1* siRNAs, or different combinations of both using the corresponding scramble siRNAs as control (−). The cells were simultaneously transfected with HA-PGC-1α for 48 hr. Then, relative mitochondrial DNA content (D), mRNA levels of the genes indicated (E), and total O_2 consumption (F) were analyzed. Values are expressed as mean ± SEM unless otherwise stated. * indicates statistical difference versus respective control sh/siRNA-transfected cells at $p < 0.05$.

PJ34 promoted the recruitment of PGC-1α to target gene promoters (e.g., PDK4) (Figure S4A). Finally, the activation of SIRT1/PGC-1α by PJ34 culminated in higher O_2 consumption rates (Figure 4M), testifying for enhanced oxidative metabolism.

The effect of PJ34 on PGC-1α acetylation in C2C12 myotubes was blunted upon *SIRT1* knockdown (Figure 4J). The role of SIRT1 in mediating PJ34-induced PGC-1α deacetylation was further confirmed in *SIRT1*$^{-/-}$ MEFs, where PJ34 was unable to decrease PGC-1α acetylation (Figure S4B). In line with impaired PGC-1α activation, mitochondrial gene expression and O_2 consumption were largely unresponsive to PJ34 upon SIRT1 depletion in C2C12 cells (Figures 4K and 4M) and in *SIRT1*$^{-/-}$ MEFs (Figures S4C and S4D), indicating that SIRT1 is a key mediator of PJ34 action. However, PJ34 also had SIRT1-independent effects, as reflected by the persistent increase in *UCP3* mRNA even after the *SIRT1* knockdown (Figure 4K). This could be explained by the fact that PJ34 does not regulate *UCP3* expression by recruitment of PGC-1α to its promoter (Figure S4A). The pharmacological inhibition of PARP recapitulates the phenotypic characteristics of the *PARP-1*$^{-/-}$ mice and reveals that these effects are largely mediated by SIRT1.

DISCUSSION

The difficulty of identifying compounds that specifically and directly bind and activate SIRT1 led us to test whether the modulation of NAD^+ availability could be an alternative path to activation of SIRT1. Our present work supports this concept by showing how the attenuation of PARP-1, another NAD^+-consuming enzyme, increases intracellular NAD^+ levels and enhances SIRT1 activity. This prompts the deacetylation and activation of key metabolic transcriptional regulators, such as PGC-1α and FOXO1, leading to increased mitochondrial content and metabolism.

Our data suggest that PARP-1 limits NAD^+ availability for SIRT1 activation. This concept originates from the differences

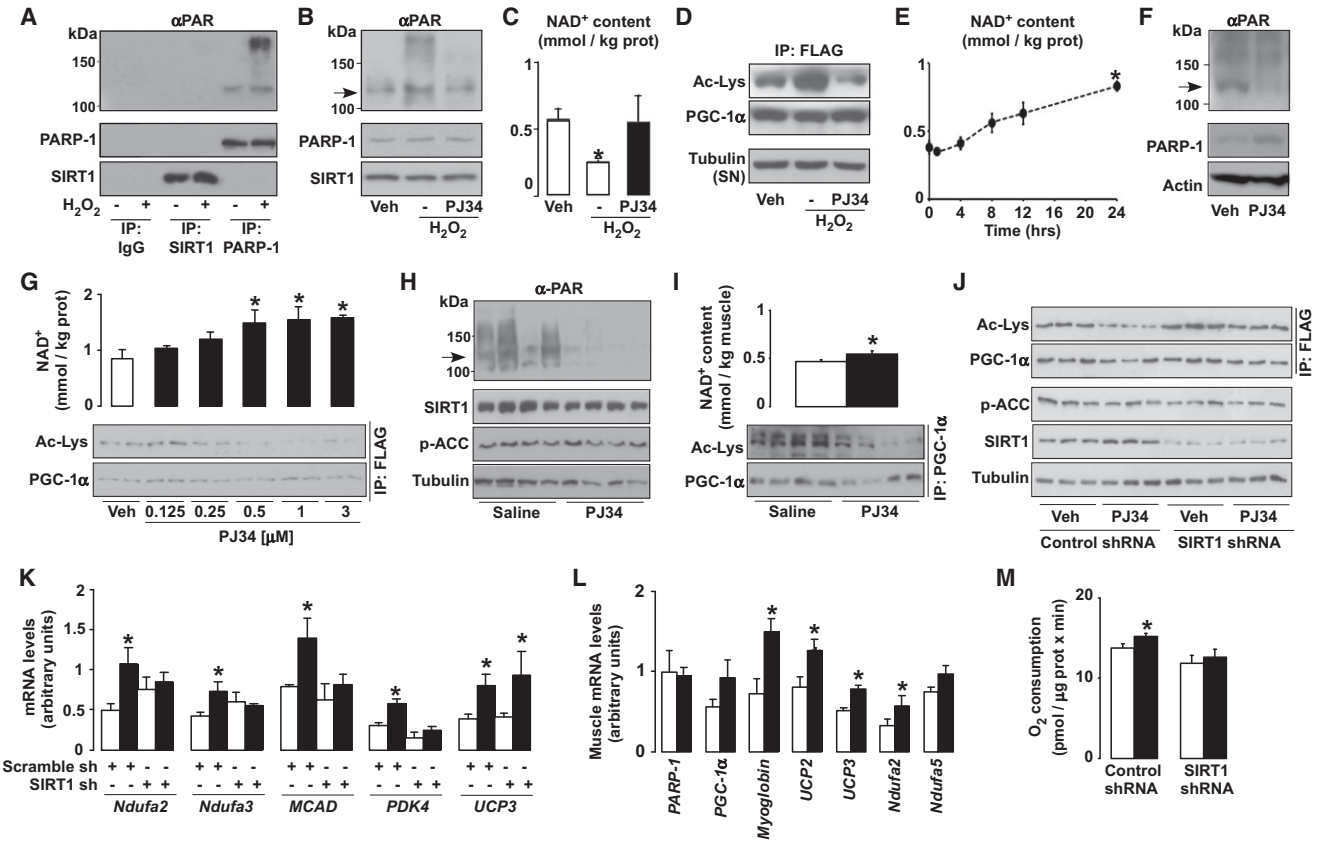

Figure 4. PARP-1 Inhibition Enhances Mitochondrial Function through SIRT1

(A–D) C2C12 myotubes expressing FLAG-HA-PGC-1α were treated for 6 hr with either PBS (vehicle [Veh]), H_2O_2 (500 μM), or H_2O_2 and PJ34 (1 μM). Then, SIRT1, PARP-1, and unspecific IgG immunoprecipitates from 500 μg of protein extracts were used to test PARylation and the proteins indicated (A). Proteins were analyzed in total cell extracts, and the arrow indicates PARP-1 autoPARylation (B). NAD^+ content was measured (C), and PGC-1α acetylation was tested in FLAG immunoprecipitates (D). Tubulin was checked on the supernatants as input.

(E) C2C12 myotubes were treated with PJ34 (1 μM) for the times indicated, and NAD^+ levels were evaluated in acidic extracts.

(F and G) C2C12 myotubes expressing FLAG-HA-PGC-1α were treated for 24 hr with PBS (Veh) or with PJ34 (1 μM, unless stated otherwise). PARP-1 protein and autoPARylation (arrow) were determined by western blot (F), and NAD^+ content and PGC-1α acetylation were measured (G).

(H and I) Ten-week-old mice received PJ34 (10 mg/kg b.i.d, i.p.) or saline (Veh) for 5 days before sacrifice (n = 10/10); then PARP-1 autoPARylation (arrow), p-ACC, and SIRT1 levels were determined in 100 μg of total protein extracts from gastrocnemius (H), and NAD^+ and PGC-1α acetylation were determined (I). PGC-1α was immunoprecipitated using 2 mg of protein from gastrocnemius muscle and 5 μg of antibody.

(J and K) C2C12 myotubes expressing FLAG-HA-PGC-1α and either a control or a SIRT1 shRNA were treated with PJ34 for 48 hr. Then, PGC-1α acetylation levels were quantified in FLAG immunoprecipitates (J), and 50 μg of total protein extracts was used to measure the other markers indicated; mRNA levels of selected genes were quantified (K).

(L) Mice were treated as in (H), and mRNA of selected genes was determined in gastrocnemius.

(M) C2C12 myotubes were treated as in (J), and cellular O_2 consumption was measured. White bars represent Veh; black bars represent PJ34 treatment. Values are expressed as mean ± SEM unless otherwise stated. * indicates statistical difference versus Veh group at $p < 0.05$. For abbreviations, see Table S1.

in the K_M and k_{cat}/K_M of both enzymes for NAD^+, which indicate that PARP-1 is a faster and more efficient NAD^+ consumer than SIRT1 (Knight and Chambers, 2001; Smith et al., 2009). Therefore, it is likely that PARP-1 activity maintains NAD^+ at limiting levels for SIRT1 function. The prediction that *PARP-1* deletion would increase NAD^+ levels and activate SIRT1 is perfectly matched by our data. While previous work already speculated on a link between PARP-1 and sirtuin activities (Kolthur-Seetharam et al., 2006; Pillai et al., 2005), our study expands the consequences of this link to energy homeostasis. In apparent discrepancy, one report (Devalaraja-Narashimha and Padanilam, 2010) suggested that *PARP-1*$^{-/-}$ mice could be more susceptible to HFD-induced obesity. However, that study used mice on an SV129 background, which are less suited for metabolic studies than C57BL/6J mice. The convergent results of our genetic, physiological, pharmacological, and in vitro studies clearly support our conclusions.

Results from our lab indicate that the activation of SIRT1 after a bout of exercise or cold exposure is not linked to decreased PARP-1 activity (data not shown). Rather, only robust and/or protracted changes, such as pharmacological (PJ34) or genetic (knockdown or deletion) PARP-1 inhibition, influence SIRT1 activity. While PARP-1 might not always participate in the physiological modulation of SIRT1 activity, our data suggest that the

interplay between both proteins could be exploited pharmacologically.

Our work illustrates the way in which SIRT1 is a key mediator of the PARP-1-deficient phenotype, but the link between PARP-1 and SIRT1 activities is still unclear. Several models used in this work show that reducing PARP-1 activity controls SIRT1 function, independent of changes in SIRT1 protein levels. In all these cases, the levels of NAD^+, the rate-limiting coenzyme for SIRT1, correlated with SIRT1 activity, suggesting that NAD^+ availability might influence SIRT1 activity. If this were true, boosting NAD^+ content through alternative strategies should elicit similar metabolic phenotypes to those of the *PARP-1*$^{-/-}$ mice. Supporting this notion, deletion of another NAD^+ consumer, CD38, also activates SIRT1 (Aksoy et al., 2006), resulting in protection against HFD-induced obesity (Barbosa et al., 2007). Nutrient scarcity and AMPK activation also lead to increased NAD^+ levels and SIRT1 activation coupled to the induction of oxidative metabolism (Cantó et al., 2009, 2010). This correlative evidence indicates that the increased NAD^+ availability might be a key mechanism by which PARP deficiency activates SIRT1. However, we cannot exclude the possibility that PARP inhibition also impacts SIRT1 via other means, even though our results rule out direct PARylation of SIRT1 as the mechanism (Figure 4A). In addition, SIRT1 content was increased in *PARP-1*$^{-/-}$ tissues and MEFs, further amplifying SIRT1 activity. The reason for this increase in SIRT1 levels remains elusive, but is independent of changes in SIRT1 mRNA (P.B., C.C., and J.A., unpublished data).

Of note, *PARP-1* depletion affects the activity of SIRT1, but not that of SIRT2 and SIRT3, which occupy nonnuclear compartments. If increased SIRT1 activity was mainly driven by changes in NAD^+, the unchanged SIRT2 and SIRT3 activities in *PARP-1*$^{-/-}$ tissues suggest that the increase in NAD^+ is either not enough to enhance SIRT2 and SIRT3 activities or that it only happens in specific cellular compartments, supporting an independent regulation of different subcellular NAD^+ pools (Yang et al., 2007). Alternatively, PARP-1 and SIRT1 activities might not be linked by changes in NAD^+, and some yet unfound mechanism drives the specificity toward this sirtuin.

Some results indicate that the effects of PARP deficiency cannot be completely explained by SIRT1 (Figure 4K). Future research will have to clarify the nature of these SIRT1-independent effects of PARP inhibition on metabolism. It will be interesting to explore whether PARylation can directly modulate the activity of key metabolic transcriptional regulators, as PARP-1 may contribute to nuclear processes other than DNA repair (Krishnakumar and Kraus, 2010).

PARP inhibitors are currently in clinical development as antitumoral drugs (Fong et al., 2009). While our data encourages a possible utilization of PARP inhibitors as therapeutic agents to activate SIRT1 and promote oxidative metabolism, this should be taken cautiously. PARP-1 has key roles in genomic maintenance, and while neither this nor previous studies (Allinson et al., 2003) detected enhanced DNA damage in *PARP-1*$^{-/-}$ mice under basal conditions, it cannot be ignored that *PARP-1*$^{-/-}$ mice are sensitive to ionizing radiation (de Murcia et al.,1997). Hence, it will be important to analyze the impact of aging and metabolic disease on DNA damage to establish the therapeutic potential and limitations of PARP inhibition.

EXPERIMENTAL PROCEDURES

Detailed materials and procedures can be found in the Supplemental Information.

Animal Experiments

Pure C57BL/6J male mice were used for the study. *PARP-1*$^{+/+}$ and *PARP-1*$^{-/-}$ were described (de Murcia et al., 1997). Mice were housed separately, had ad libitum access to water and chow (10 kcal% of fat) (SAFE, Augy, France) or HFD (60 kcal% of fat) (Research Diets, Inc., New Brunswick, NJ), and were kept in a 12 hr dark/light cycle. Animal experiments were carried out according to local, national, and EU ethical guidelines. Animals were sacrificed after 6 hr of fast, and tissues were collected and processed as specified.

NAD^+ and NAM Determination

NAD^+ levels in cultured cells were determined using an enzymatic method (EnzyChrom, BioAssays Systems, Hayward, CA), whereas for tissues (Figure 4), NAD^+ and NAM levels were determined as described (Sauve et al., 2005).

Statistics

All data were verified for normal distribution. Statistical significance was assessed by Student's t test for independent samples. Values are expressed as mean ± SEM unless otherwise stated.

SUPPLEMENTAL INFORMATION

Supplemental Information includes Supplemental Experimental Procedures, Supplemental References, four figures, and three tables and can be found with this article online at doi:10.1016/j.cmet.2011.03.004.

ACKNOWLEDGMENTS

This work was supported by fellowships awarded by Bolyai (P.B.), SNSF (P.B.), EMBO (C.C.), FEBS (A.B.), and NWO (R.H.H.), as well as grants from the NKTH, OTKA (NFF78498, IN80481), Mecenatura (DE OEC Mec-1/2008), the NIH (DK59820 and DK73466), the ERC (2008-AdG-23118), the CNRS, ANR EGIDE (22873YC), and the Ellison Medical Foundation New Scholar in Aging 2007.

Received: April 12, 2010
Revised: May 5, 2010
Accepted: February 24, 2011
Published: April 5, 2011

REFERENCES

Adamietz, P. (1987). Poly(ADP-ribose) synthase is the major endogenous nonhistone acceptor for poly(ADP-ribose) in alkylated rat hepatoma cells. Eur. J. Biochem. *169*, 365–372.

Ahn, B.H., Kim, H.S., Song, S., Lee, I.H., Liu, J., Vassilopoulos, A., Deng, C.X., and Finkel, T. (2008). A role for the mitochondrial deacetylase Sirt3 in regulating energy homeostasis. Proc. Natl. Acad. Sci. USA *105*, 14447–14452.

Aksoy, P., Escande, C., White, T.A., Thompson, M., Soares, S., Benech, J.C., and Chini, E.N. (2006). Regulation of SIRT 1 mediated NAD dependent deacetylation: a novel role for the multifunctional enzyme CD38. Biochem. Biophys. Res. Commun. *349*, 353–359.

Allinson, S.L., Dianova, I.I., and Dianov, G.L. (2003). Poly(ADP-ribose) polymerase in base excision repair: always engaged, but not essential for DNA damage processing. Acta Biochim. Pol. *50*, 169–179.

Asher, G., Reinke, H., Altmeyer, M., Gutierrez-Arcelus, M., Hottiger, M.O., and Schibler, U. (2010). Poly(ADP-ribose) polymerase 1 participates in the phase entrainment of circadian clocks to feeding. Cell *142*, 943–953.

Barbosa, M.T., Soares, S.M., Novak, C.M., Sinclair, D., Levine, J.A., Aksoy, P., and Chini, E.N. (2007). The enzyme CD38 (a NAD glycohydrolase, EC 3.2.2.5) is necessary for the development of diet-induced obesity. FASEB J. *21*, 3629–3639.

Bitterman, K.J., Anderson, R.M., Cohen, H.Y., Latorre-Esteves, M., and Sinclair, D.A. (2002). Inhibition of silencing and accelerated aging by nicotinamide, a putative negative regulator of yeast sir2 and human SIRT1. J. Biol. Chem. *277*, 45099–45107.

Cantó, C., Gerhart-Hines, Z., Feige, J.N., Lagouge, M., Noriega, L., Milne, J.C., Elliott, P.J., Puigserver, P., and Auwerx, J. (2009). AMPK regulates energy expenditure by modulating NAD+ metabolism and SIRT1 activity. Nature *458*, 1056–1060.

Cantó, C., Jiang, L.Q., Deshmukh, A.S., Mataki, C., Coste, A., Lagouge, M., Zierath, J.R., and Auwerx, J. (2010). Interdependence of AMPK and SIRT1 for metabolic adaptation to fasting and exercise in skeletal muscle. Cell Metab. *11*, 213–219.

de Murcia, J.M., Niedergang, C., Trucco, C., Ricoul, M., Dutrillaux, B., Mark, M., Oliver, F.J., Masson, M., Dierich, A., LeMeur, M., et al. (1997). Requirement of poly(ADP-ribose) polymerase in recovery from DNA damage in mice and in cells. Proc. Natl. Acad. Sci. USA *94*, 7303–7307.

Devalaraja-Narashimha, K., and Padanilam, B.J. (2010). PARP1 deficiency exacerbates diet-induced obesity in mice. J. Endocrinol. *205*, 243–252.

Durkacz, B.W., Omidiji, O., Gray, D.A., and Shall, S. (1980). (ADP-ribose)n participates in DNA excision repair. Nature *283*, 593–596.

Fong, P.C., Boss, D.S., Yap, T.A., Tutt, A., Wu, P., Mergui-Roelvink, M., Mortimer, P., Swaisland, H., Lau, A., O'Connor, M.J., et al. (2009). Inhibition of poly(ADP-ribose) polymerase in tumors from BRCA mutation carriers. N. Engl. J. Med. *361*, 123–134.

Garcia Soriano, F., Virág, L., Jagtap, P., Szabó, E., Mabley, J.G., Liaudet, L., Marton, A., Hoyt, D.G., Murthy, K.G., Salzman, A.L., Southan, G.J., and Szabó, C. (2001). Diabetic endothelial dysfunction: the role of poly(ADP-ribose) polymerase activation. Nat. Med. *7*, 108–113.

Howitz, K.T., Bitterman, K.J., Cohen, H.Y., Lamming, D.W., Lavu, S., Wood, J.G., Zipkin, R.E., Chung, P., Kisielewski, A., Zhang, L.L., et al. (2003). Small molecule activators of sirtuins extend Saccharomyces cerevisiae lifespan. Nature *425*, 191–196.

Knight, M.I., and Chambers, P.J. (2001). Production, extraction, and purification of human poly(ADP-ribose) polymerase-1 (PARP-1) with high specific activity. Protein Expr. Purif. *23*, 453–458.

Kolthur-Seetharam, U., Dantzer, F., McBurney, M.W., de Murcia, G., and Sassone-Corsi, P. (2006). Control of AIF-mediated cell death by the functional interplay of SIRT1 and PARP-1 in response to DNA damage. Cell Cycle *5*, 873–877.

Krishnakumar, R., and Kraus, W.L. (2010). The PARP side of the nucleus: molecular actions, physiological outcomes, and clinical targets. Mol. Cell *39*, 8–24.

Milne, J.C., Lambert, P.D., Schenk, S., Carney, D.P., Smith, J.J., Gagne, D.J., Jin, L., Boss, O., Perni, R.B., Vu, C.B., et al. (2007). Small molecule activators of SIRT1 as therapeutics for the treatment of type 2 diabetes. Nature *450*, 712–716.

North, B.J., Marshall, B.L., Borra, M.T., Denu, J.M., and Verdin, E. (2003). The human Sir2 ortholog, SIRT2, is an NAD+-dependent tubulin deacetylase. Mol. Cell *11*, 437–444.

Pacholec, M., Bleasdale, J.E., Chrunyk, B., Cunningham, D., Flynn, D., Garofalo, R.S., Griffith, D., Griffor, M., Loulakis, P., Pabst, B., et al. (2010). SRT1720, SRT2183, SRT1460, and resveratrol are not direct activators of SIRT1. J. Biol. Chem. *285*, 8340–8351.

Pillai, J.B., Isbatan, A., Imai, S., and Gupta, M.P. (2005). Poly(ADP-ribose) polymerase-1-dependent cardiac myocyte cell death during heart failure is mediated by NAD+ depletion and reduced Sir2alpha deacetylase activity. J. Biol. Chem. *280*, 43121–43130.

Sauve, A.A., Moir, R.D., Schramm, V.L., and Willis, I.M. (2005). Chemical activation of Sir2-dependent silencing by relief of nicotinamide inhibition. Mol. Cell *17*, 595–601.

Schraufstatter, I.U., Hinshaw, D.B., Hyslop, P.A., Spragg, R.G., and Cochrane, C.G. (1986). Oxidant injury of cells. DNA strand-breaks activate polyadenosine diphosphate-ribose polymerase and lead to depletion of nicotinamide adenine dinucleotide. J. Clin. Invest. *77*, 1312–1320.

Sims, J.L., Berger, S.J., and Berger, N.A. (1981). Effects of nicotinamide on NAD and poly(ADP-ribose) metabolism in DNA-damaged human lymphocytes. J. Supramol. Struct. Cell. Biochem. *16*, 281–288.

Smith, B.C., Hallows, W.C., and Denu, J.M. (2009). A continuous microplate assay for sirtuins and nicotinamide-producing enzymes. Anal. Biochem. *394*, 101–109.

Yang, H., Yang, T., Baur, J.A., Perez, E., Matsui, T., Carmona, J.J., Lamming, D.W., Souza-Pinto, N.C., Bohr, V.A., Rosenzweig, A., et al. (2007). Nutrient-sensitive mitochondrial NAD+ levels dictate cell survival. Cell *130*, 1095–1107.

Yu, J., and Auwerx, J. (2009). The role of sirtuins in the control of metabolic homeostasis. Ann. N Y Acad. Sci. *1173* (*Suppl 1*), E10–E19.

Supplemental Information

Cell Metabolism, *Volume 13*

PARP-1 Inhibition Increases Mitochondrial Metabolism through SIRT1 Activation

Péter Bai, Carles Cantó, Hugues Oudart, Attila Brunyánszki, Yana Cen, Charles Thomas, Hiroyasu Yamamoto, Aline Huber, Borbála Kiss, Riekelt H. Houtkooper, Kristina Schoonjans, Valérie Schreiber, Anthony A. Sauve, Josiane Menissier-de Murcia, and Johan Auwerx

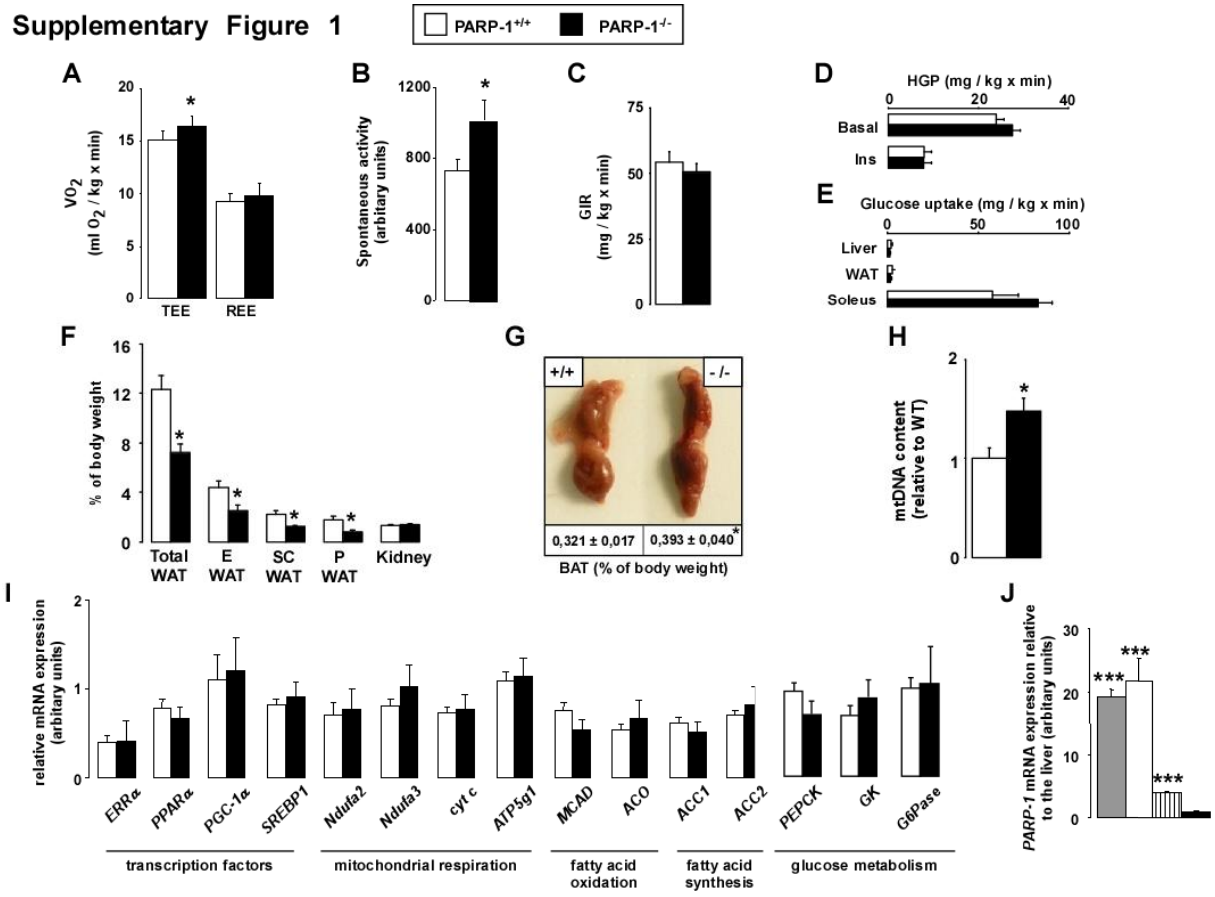

Figure S1, Related to Figure 1. Increased Spontaneous Locomotor Activity and Energy Expenditure in the *PARP-1*$^{-/-}$ Mice during Night

(A) Oxygen consumption was determined in *PARP-1*$^{+/+}$ and $^{-/-}$ male mice (n=6/6) as described in the Materials and Methods. TEE – total energy expenditure, REE – resting energy expenditure.

(B) Spontaneous activity was determined during indirect calorimetry in CLAMS using *PARP-1*$^{+/+}$ and $^{-/-}$ male mice (n=9/9).

(C-E) Peripheral and hepatic insulin responsiveness of *PARP-1*$^{+/+}$ and *PARP-1*$^{-/-}$ male mice was assed by euglycemic-hyperinsulinemic clamp. (C) Glucose infusion rates (GIR), (D) hepatic glucose production (HGP) and (E) glucose uptake in different tissues are all shown as mean +/- SEM.

(F) The total WAT mass, individual WAT depots, and organ weights were determined upon autopsy (E – epididymal, SC – subcutaneous, P – perirenal).

(G) BAT was photographed and weighed after autopsy of *PARP-1*$^{+/+}$ and $^{-/-}$ male mice (11,5 months of age, n=8/9 males). BAT content (relative to total body weight), is shown at the bottom of the image.

(H) BAT mitochondrial DNA (mtDNA) was quantified by qPCR in the BAT.

(I) mRNA expression levels of selected genes were quantified by RT-qPCR reactions in the liver of *PARP-1*$^{+/+}$ and $^{-/-}$ male mice (n=9/9). Abbreviations are listed in the text and in Table S1.

(J) mRNA expression of *PARP-1* were quantified in different metabolic tissues of C57Bl/6J male mice (n=5) (black bar – liver; dashed bar – BAT; white bar – skeletal muscle; grey bar – testis). Asterisks indicate significant difference at * $p<0,05$; *** $p<0.001$.

Supplementary Figure 2

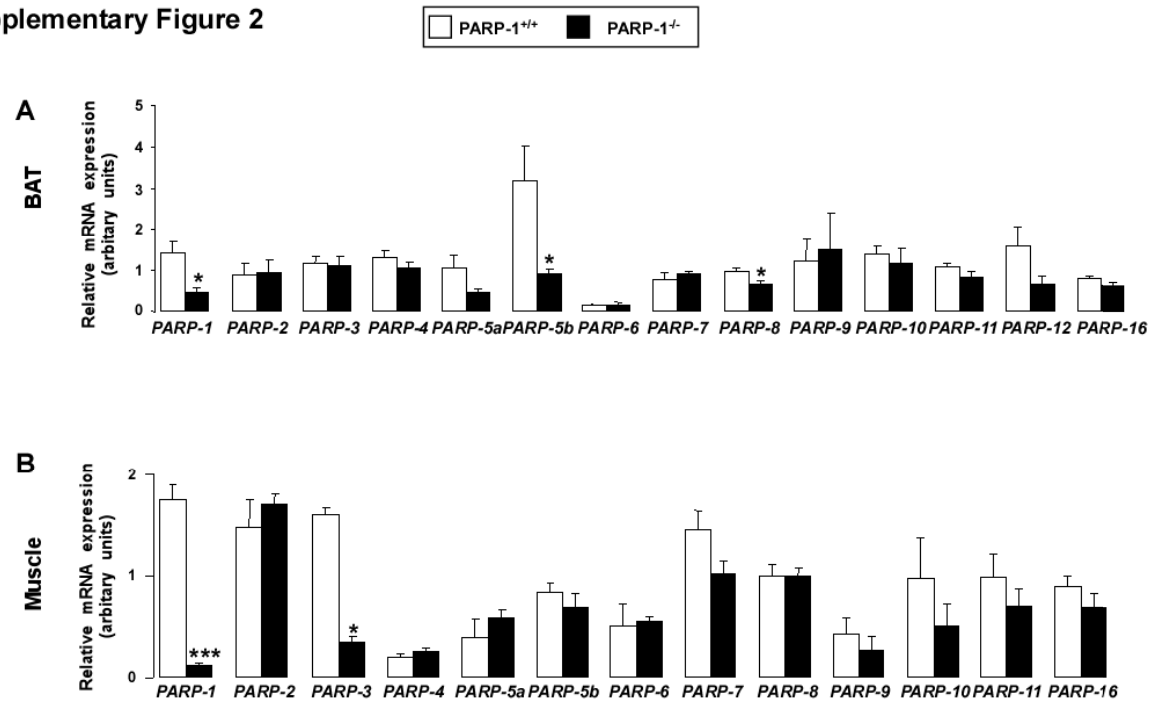

Figure S2, Related to Figure 2. Gene Expression Pattern of the Different Members of the PARP Family in the BAT and Gastrocnemius Muscle

(A-B) RT-qPCR reactions were performed on cDNA populations from the BAT (A) and the gastrocnemius muscle (B) of *PARP-1*$^{+/+}$ and $^{-/-}$ male mice (n=7/5). Asterisks indicate significant difference between cohorts, where * p<0,05; *** p<0.001.

Supplementary Figure 3

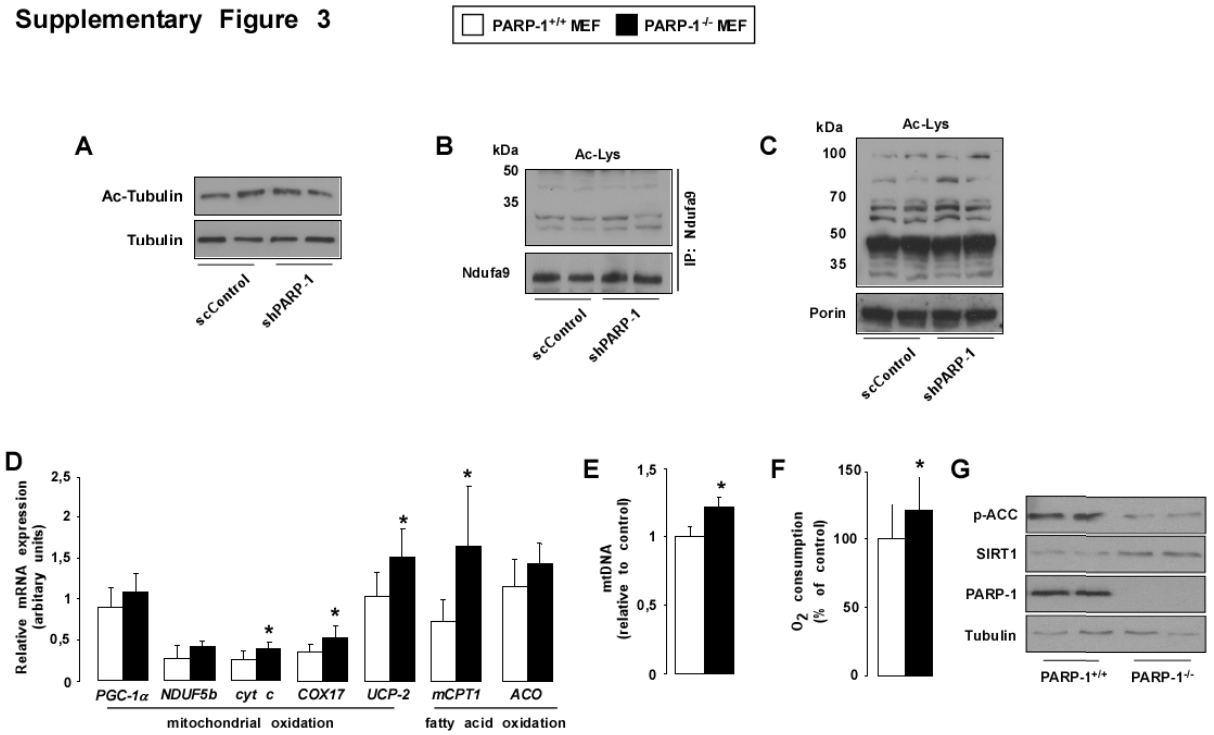

Figure S3, Related to Figure 3. Assessment of Protein Acetylation in HEK293T Cells and Measurement of Mitochondrial Function and Protein Levels in *PARP-1*$^{+/+}$ *and* $^{-/-}$ MEFs

(A-C). HEK293T were transfected with either control or PARP-1 shRNAs. 48 hrs later, total and mitochondrial extracts were obtained.

(A) 50 mg of total extracts were used to test tubulin acetylation levels.

(B) 400 mg of total extracts were used to immunoprecipitate Ndufa9, using 3 mg of antibody, and evaluate lysisne actylation on the immunoprecipitates.

(C) 50 ug of mitochondrial extracts were used to test global lysine acetylation and porin levels (as input).

(D-F) In *PARP-1*$^{+/+}$ and $^{-/-}$ primary MEFs (n=3/3) mRNA expression (D), mitochondrial DNA content (E), oxygen consumption (F) pACC, SIRT1 and PARP-1 protein levels (G) was determined. Abbreviations are listed in the text. Asterisks indicate significant difference between cohorts, where * $p<0,05$, ** $p<0,01$.

Supplementary Figure 4

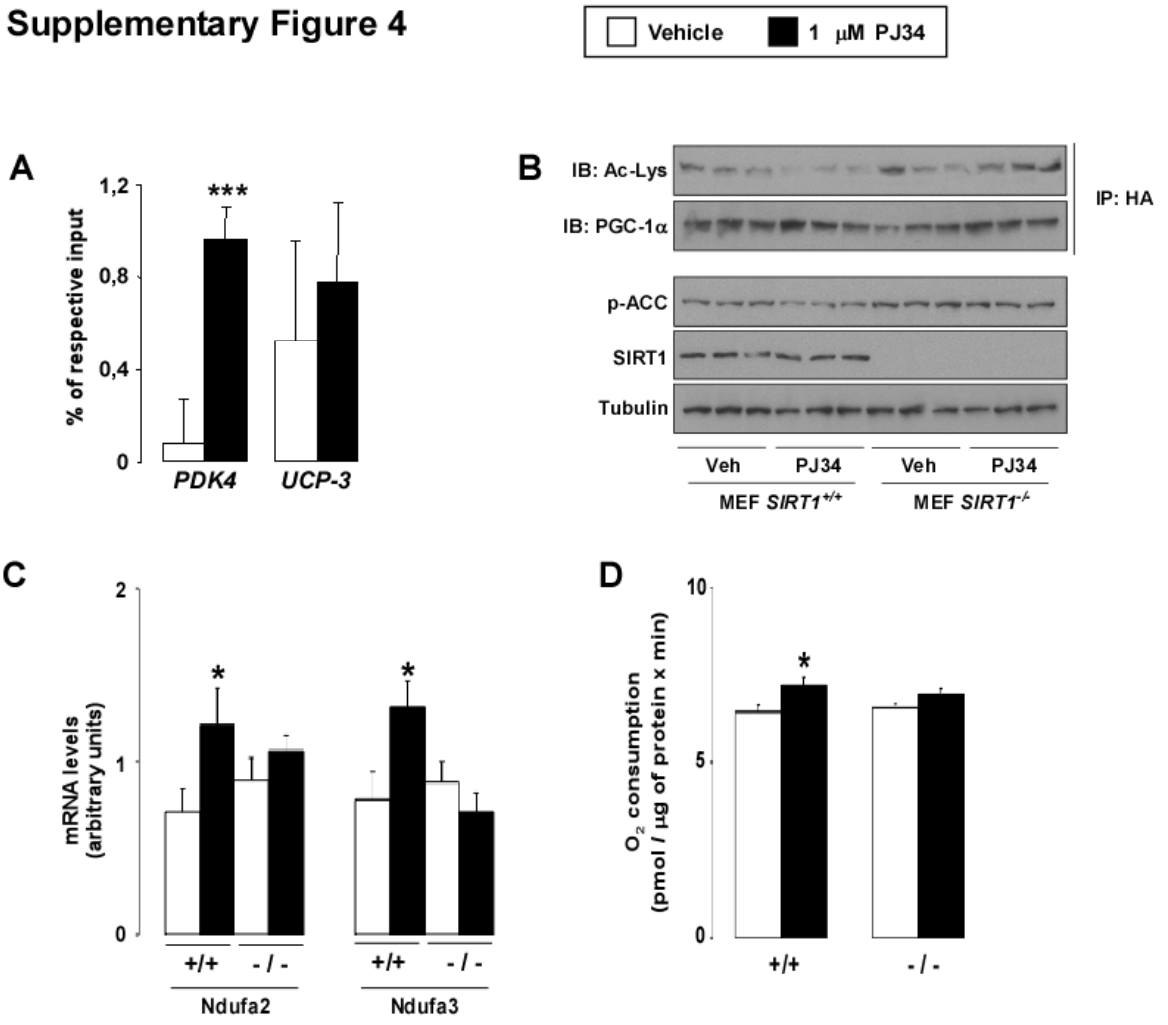

Figure S4, Related to Figure 4. Assessment of Mitochondrial Function upon Pharmacological PARP Inhibition in C2C12 Cells and SIRT1$^{-/-}$ MEFs

(A) Promoter occupancy of PGC-1α was quantified after PJ34 treatment on the *PDK4* and *UCP-3* promoters (1 μM, 48h) (n=3/3).

(B-D) PGC-1α acetylation, ACC phosphorylation, SIRT1 protein levels (B), expression of mitochondrial protein mRNAs (C) and O_2 consumption (D) were determined in *SIRT1*$^{+/+}$ and $^{-/-}$ MEF cells , treated with PBS (Veh) or PJ34 for 48 hrs.

Table S1. qRT-PCR Primers for Quantification of Gene Expression

All primers are designed for murine sequences unless otherwise specified.

Gene	**Primers**
18S (human)	5'-CGG CTA CCA CAT CCA AGG AA-3' 5'-CCT GTA TTG TTA TTT TTC GTC ACT ACC T-3'
ACC1 ***acetyl-CoA carboxylase -1***	5'-GAC AGA CTG ATC GCA GAG AAA G-3' 5'-TGG AGA GCC CCA CAC ACA-3'
ACC2 ***acetyl-CoA carboxylase-2***	5'-CCC AGC CGA GTT TGT CAC T-3' 5'-GGC GAT GAG CAC CTT CTC TA-3'
ACO ***Acyl-CoA oxidase***	5'-CCC AAC TGT GAC TTC CAT T-3' 5'-GGC ATG TAA CCC GTA GCA CT-3'
ATP5g1	5'-GCT GCT TGA GAG ATG GGT TC-3' 5'-AGT TGG TGT GGC TGG ATC A-3'
COX17	5'-CGT GAT GCG TGC ATC ATT GA-3' 5'-CAT TCA CAA AGT AGG CCA CC-3'
Cyclophyllin B	5'-TGG AGA GCA CCA AGA CAG ACA -3' 5'-TGC CGG AGT CGA CAA TGA T-3'
cyt c ***Cytochrome C***	5'-TCC ATC AGG GTA TCC TCT CC-3' 5'-GGA GGC AAG CAT AAG ACT GG-3'
Dio2 ***Deiodinase-2***	5'-GCA CGT CTC CAA TCC TGA AT-3' 5'-TGA ACC AAA GTT GAC CAC CA -3'
ERRα ***estrogen receptor related receptor α***	5'-ACTGCCACTGCAGGATGAG-3' 5'-CACAGCCTCAGCATCTTCAA-3'
GK ***Glucokinase***	5'-ACA TTG TGC GCC GTG CCT GTG AA-3' 5'-AGC CTG CGC ACA CTG GCG TGA AA-3'
G6Pase ***- glucose-6 phosphatase***	5'-CCG GAT CTA CCT TGC TGC TCA CTT T-3' 5'-TAG CAG GTA GAA TCC AAG CGC GAA AC-3'
L-CPT-1 (human) ***Liver Carnitine Palmitoyl Transferase***	5'-CAG GCG AGA ACA CGA TCT TC-3' 5'-GCG GAT GTG GTT TCC AAA G-3'
MCD ***malonyl-CoA decarboxylase***	5'-TGG ATG GCT GAC AGC AGC CTC AA-3' 5'-CTG AGG ATC TGC TCG GAA GCT TTG-3'
MCAD (human) ***Medium chain acyl-coenzyme A dehydrogenase***	5'-AGA ATT GGC TTA TGG ATG TAC AGG-3' 5'-TTT GTT GAT CAT TTC CAG CAA TAA T-3'
MCAD ***Medium chain acyl-coenzyme A dehydrogenase***	5'-GAT CGC AAT GGG TGC TTT TGA TAG AA-3' 5'-AGC TGA TTG GCA ATG TCT CCA GCA AA-3'
mCPT1 ***Carnitine Palmitoyl Transferase-1***	5'-TTG CCC TAC AGC TGG CTC ATT TCC -3' 5'-GCA CCC AGA TGA TTG GGA TAC TGT-3'
MHCI ***Myosin heavy chain 1***	5'-GAG TAG CTC TTG TGC TAC CCA GC -3' 5'-AAT TGC TTT ATT CTG CTT CCA CC -3'
MHCIIA ***Myosin heavy chain 2A***	5'-GCA AGA AGC AGA TCC AGA AAC-3' 5'-GGT CTT CTT CTG TCT GGT AAG TAA GC-3'
MHCIIX ***Myosin heavy chain 2X***	5'-GCA ACA GGA GAT TTC TGA CCT CAC-3' 5'-CCA GAG ATG CCT CTG CTT C-3'
Ndufa2	5'-GCA CAC ATT TCC CCA CAC TG-3' 5'-CCC AAC CTG CCC ATT CTG AT-3'
Ndufb3	5'-TAC CAC AAA CGC AGC AAA CC-3'

	5’-AAG GGA CGC CAT TAG AAA CG-3’
Ndufb5	5’-CTT CGA ACT TCC TGC TCC TT-3’ 5’-GGC CCT GAA AAG AAC TAC G-3’
PARP-1 (human)	5’-GCT CCT GAA CAA TGC AGA CA-3’ 5’-CAT TGT GTG TGG TTG CAT GA-3’
PARP-1	5’-GGA GCT GCT CAT CTT CAA CC-3’ 5’-GCA GTG ACA TCC CCA GTA CA-3’
PARP-2	5’-GGA AGG CGA GTG CTA AAT GAA-3’ 5’-AAG GTC TTC ACA GAG TCT CGA TTG-3’
PARP-3	5’-CCT GCT GAT AAT CGG GTC AT-3’ 5’-TTG TTG TTG TTG CCG ATG TT-3’
PARP-4	5’-GTT AAA TTT TGC ACT CCT GGA G-3’ 5’-AAT GTG AAC ACT GTC AAG AGG AAC A-3’
PARP-5a	5’-TAG AGG CAT CGA AAG CTG GT-3’ 5’-CAG GCA TTG TGA AGG GG-3’
PARP-5b	5’-GGC CCT GCT TAC ACC ATT G-3’ 5’-CGT GCT TGA CCA GAA GTT CA-3’
PARP-6	5’-TTT CCA GCC ATC GAA TAA GG-3’ 5’-ACC ACT TGC CTT GAA CCA AC-3’
PARP-7	5’-AAA ACC CCT GGA AAT CAA CC-3’ 5’-AGA AGG ATG CGC TTC TGG TA-3’
PARP-8	5’-TCC ACC ATT AAA TCG CAC AA-3’ 5’-GCT CCA TTT TCG ATG TCT TG-3’
PARP-9	5’-ACC TGA AGA ATG GCC TAT TAC ATG G-3’ 5’-ACA GCT CAG GGT AGA GAT GC-3’
PARP-10	5’-CAA GAT CCT GCA GAT GCA AA-3’ 5’-TTG GAG AAG CAC ACG TTC TG-3’
PARP-11	5’-CAA TGA GCA GAT GCT ATT TCA TG-3’ 5’-CAC CAA TTA GCA CTC GAG CA-3’
PARP-12	5’-CGG ATC CAG AAC ATG GGC-3’ 5’-GGC ATC TCT CGC AAA GTA GC-3’
PARP-14	5’-GGC AAA CGC AAT GGA ACT AT-3’ 5’-AGC ACG TTC CTA AGC CTT GA-3’
PARP-16	5’-CCG TGT GCC TTA TGG AAA CT-3’ 5’-TGG ATT GTG TCT GGG CAC-3’
PDK4 ***pyruvate dehydrogenase kinase, isoenzyme 4***	5’-AAA GGA CAG GAT GGA AGG AAT CA-3’ 5’-ATT AAC TGG CAG AGT GGC AGG TAA-3’
PEPCK ***Phosphoenolpyruvate carboxykinase***	5’-CCA CAG CTG CTG CAG AAC A-3’ 5’-GAA GGG TCG CAT GGC AAA-3’
PGC-1α ***peroxisome proliferator-activated receptor gamma, coactivator 1α***	5’-AAG TGT GGA ACT CTC TGG AAC TG-3’ 5’-GGG TTA TCT TGG TTG GCT TTA TG-3’
PPARα (human) ***peroxisome proliferator-activated receptor α***	5’-TCA TCA AGA AGA CGA GTC G-3’ 5’-CGG TTA CCT ACA GCT CAG AC-3’
PPARα ***peroxisome proliferator-activated receptor α***	5’-CCT GAA CAT CGA GTG TCG AAT AT-3’ 5’-GGT TCT TCT TCT GAA TCT TGC AGC T-3’
SIRT1 (human)	5’-TAG GCG GCT TGA TGG TAA TC-3’

	5’-TCT GGC ATG TCC CAC TAT CA-3’
SREBP1 ***sterol regulatory element binding transcription factor 1***	5’-GGC CGA GAT GTG CGA ACT-3’ 5’-TTG TTG ATG AGC TGG AGC ATG T-3’
Trop I ***Troponin I***	5’-CCA GCA CCT TCA GCT TCA GGT CCT TGA T-3’ 5’-TGC CGG AAG TTG AGA GGA AAT CCA AGA T-3’
UCP1 ***Uncoupling protein-1***	5’-GGC CCT TGT AAA CAA CAA AAT AC-3’ 5’-GGC AAC AAG AGC TGA CAG TAA AT-3’
UCP2 ***Uncoupling protein-2***	5’-TGG CAG GTA GCA CCA CAG G-3’ 5’-CAT CTG GTC TTG CAG CAA CTC T-3’
UCP3 (human) ***Uncoupling protein-3***	5’-GTG ACC TAC GAC ATC CTC AAG G-3’ 5’-GCT CCA AAG GCA GAG ACA AAG-3’
UCP3 ***Uncoupling protein-3***	5’-ACT CCA GCG TCG CCA TCA GGA TTC T-3’ 5’-TAA ACA GGT GAG ACT CCA GCA ACT T-3’

Table S2. Primers for mtDNA Determination

mtDNA specific (murine)	5’-CCG CAA GGG AAA GAT GAA AGA C-3’ 5’-TCG TTT GGT TTC GGG GTT TC-3’
nuclear specific (murine)	5’-GCC AGC CTC TCC TGA TTT TAG TGT-3’ 5’-GGG AAC ACA AAA GAC CTC TTC TGG-3’
mtDNA specific (human)	5’-CTA TGT CGC AGT ATC TGT CTT TG-3’ 5’-GTT ATG ATG TCT GTG TGG AAA G-3’
nuclear specific (human)	5’-GTT TGT GTG CTA TAG ATG ATA TTT TAA ATT G-3’ 5’-CAT TAA ACA GTC TAC AAA ACA TAT-3’

Table S3. ChIP Primers

PDK4	5’-AAC CCT CCT CCC TCT CAC CCT-3’ 5’-ACA CCA ATC AGC TCA GAG AA-3’
UCP-3	5’-GAA TGT CAG GCC TCT AAG AA-3’ 5’-CAG GAG GTG TGT GAC AGC AT-3’

Supplemental Experimental Procedures

Animal Experiments

To monitor body weight, mice were weighed and the food consumption was measured each week on the same day. In case of PJ34 treatment, mice received each 12h (at 7:00 and 19:00) 10 mg/kg PJ34 by intraperitoneal injection for 5 continuous days. Oral glucose tolerance test, intraperitoneal insulin tolerance test, free fatty acid (FFA) and triglycerides were determined as described (Lagouge et al., 2006). Plasma insulin and was determined in heparinized plasma samples using specific ELISA kits (*Mercodia*). Thermoadaptation was performed as described (Lagouge et al., 2006). We measured O_2 consumption, CO_2 production, and spontaneous locomotor activity in an open-circuit indirect calorimetry system (*Sabre systems*, Las Vegas, NV, USA) over 24-48h as described (Dali-Youcef et al., 2007; Lagouge et al., 2006; Watanabe et al., 2006). Energy expenditure was obtained by using an energy equivalent of 20.1 J / ml O_2. The respiratory quotient was the ratio of CO_2 production over O_2 consumption. During actimetry, beamline crossings were summarized each 15 minutes. The sum of beamline crosses for each 15 min period were plotted against time and AUC was calculated for each mouse that was averaged in each experimental cohort. Euglycemic-hyperinsulinemic clamps were performed in *PARP-1*$^{-/-}$ and $^{+/+}$ male mice (n = 4 mice per genotype; age = 4 months) exactly as previously described (Feige et al., 2008). In all studies animals were killed (at 14:00) either after CO_2 inhalation or cervical dislocation after 6h of fasting (starting at 8:00), and tissues were collected and their weight was expressed relative to the body weight.

Histology and Microscopy

Haematoxylin-eosine (HE) and succinate dehydrogenase (SDH) staining was performed on frozen-section- and paraffin-fixed 7 μm sections, as described (Lagouge et al., 2006). Transmission electron microscopy (TEM) investigation was performed on glutaraldehyde-

fixed, osmium tetroxyde stained ultrafine sections (Watanabe et al., 2006). Aspecific binding of the secondary antibody was controlled on sections where the primary antibody was omitted.

Cell Culture, Transfection, Adenoviral Infection and Mitochondrial Characterization

HEK293T, MEF and C2C12 cells were cultured in DMEM (4,5 g/l glucose, 10% FCS). *PARP-1*$^{+/+}$ and *PARP-1*$^{-/-}$ MEFs were prepared as described in (Menissier-de Murcia et al., 1997). *SIRT1*$^{-/-}$ and *SIRT1*$^{+/+}$ MEFs were kindly provided by Fred Alt (Chua et al., 2005). HEK293T cells were transfected using JetPei reagent (*Polyplus Transfections*, Illkirch, France) according to the manufacturer's instructions. C2C12 cells were differentiated in DMEM (4,5 g/L glucose, 2% horse serum) after reaching confluency for 2 days, followed by 2 days of PJ34 treatment (10 μM). PARP-1 shRNA constructs were described in (Shah et al., 2005). Human PARP-1 and SIRT1 siRNAs were obtained from Dharmacon (Thermo Scientific). The adenovirus encoding for FLAG-HA-PGC-1α, control and SIRT1 shRNAs were a kind gift from Pere Puigserver and were used (MOI = 100) in C2C12 myotubes as described (Canto et al., 2009). DNA strand breaks were quantified by TUNEL assays according to the manufacturer's instructions (*Millipore*).

mRNA and mtDNA Analysis

Total RNA was prepared using TRIzol (*Invitrogen*) according to the manufacturer's instructions. RNA was treated with DNase, and 2 μg of RNA was used for reverse transcription (RT). cDNA was purified on QIAquick PCR cleanup columns (*Qiagen*, Valencia, CA, USA). 50X diluted cDNA was used for RT-quantitative PCR (RT-qPCR) reactions (Bai et al., 2007). The RT-qPCR reactions were preformed using the Light-Cycler system (*Roche Applied Science*) and a qPCR Supermix (*Qiagen*) with the primers summarized in Table S1. mtDNA quantification was performed as described (Lagouge et al., 2006) with the primers indicated in Table S2.

Immunoprecipitation, SDS-PAGE, Western Blotting

Cells were lysed in lysis buffer (50 mM Tris, 100 mM KCl, EDTA 1 mM, NP40 1%, nicotinamide 5 mM, Na-butyrate 1 mM, protease inhibitors pH 7,4). Proteins were separated by SDS-PAGE and transferred onto nitrocellulose membranes. The origin of the primary and secondary antibodies used can be found bellow. Reactions were developed by enhanced chemiluminescence (*Amersham*, Little Chalfont, UK). PGC-1α, FOXO1 and Ndufa9 acetylation levels were analyzed by immunoprecipitation from cellular or nuclear lysates of tissues with anti-PGC-1α (Millipore), anti-FOXO1 (*Cell Signalling*, Danvers, MA, USA) and anti-Ndufa9 (*Abcam*) antibody followed by Western blot using an acetyl-lysine antibody (*Cell Signalling*) that was normalized to total PGC-1α/FOXO1/Ndufa9 levels. In HEK293T cells HA-tagged PGC-1α was overexpressed and was immunoprecipitated using an anti-HA. In C2C12 myotubes, FLAG-HA tagged PGC-1α was introduced through adenoviral delivery 2 days before treatments, then IP was performed using anti-FLAG antibody and samples were processed as described. All blots were quantified by densitometry using ImageJ software.

Antibodies Used for Western Blot Applications

PARP-1 (Erdelyi et al., 2009), PAR (*Alexis*, Lausanne, Switzerland), SIRT1 (*Millipore*), FOXO1 (*Cell Signalling*), haemagglutinin (*Sigma*), p-ACC (*Upstate*), Complex I (Ndufa9) (*Abcam*), Complex IV (COXI) and V (α subunit) (*Molecular probes*), FLAG (*Sigma*), and actin (*Sigma*) were detected using a polyclonal rabbit antibodies. The secondary antibody was IgG-peroxidase conjugate (*Sigma*, 1:10000).

Poly(ADP-Ribose) Detection

PAR was detected either by using a monoclonal anti-PAR antibody (Alexis) and Mouse-on-mouse kit (Vector Laboratories) on 7 μm formalin-fixed tissues using as described in (Garcia et al., 2001) or by Western blotting of total protein lysates (Erdelyi et al., 2009).

Chromatin Immunoprecipitation (ChIP)

ChIP was performed according to (Bai et al., 2007). FLAG-HA-PGC-1α (Rodgers et al., 2005) was introduced by adenoviral transfer into C2C12 myotubes after 48h of differentiation and cells were cultured for an additional 2 days. Cell were then exposed to 1 μM PJ34 in saline for 24h. Thereafter ChIP was performed using anti-FLAG (*Sigma*) and anti-TNF-R1 (*Santa Cruz*) as described (Bai et al., 2007). Pelleted DNA was quantified by qPCR using the primers against PDK4 and UCP-3 promoters flanking the nuclear receptor site (Table S3). The results were normalized for the signal of the respective inputs (vehicle/PJ34–treated) and were expressed as a percentage. The signal of anti-TNF-R1 (non-specific antibody) was subtracted from the anti-FLAG signal (specific) and the specific signal was plotted.

NAD^+ and NAM Determination

NAD^+ levels in cultured cells were determined using a commercial kit (*Enzychrom*, BioAssays Systems, CA). For tissue samples NAD^+ and NAM levels were determined as described in (Sauve et al., 2005). In brief, to a weighed aliquot of frozen pulverized tissue we added as standards, O^{18}-NAD^+ (typically 2,00 nmol) and O^{18}-NAM (typically 2,00 nmol). 70 μL of ice-cold 7% perchloric acid was then added and the sample was vortexed and sonicated three times, then centrifuged. Clear supernatant was removed and neutralized by additions of 3 M NaOH and 1 M phosphate buffer (pH=9), then centrifuged. Clear supernatant was injected onto HPLC C-18 column with 20 mM ammonium acetate eluent to separate NAD^+ and NAM from other cellular components, NAD^+ and NAM peaks (260 nm absorbance) were collected. Collections were lyophilized to dryness and subjected to MALDI-TOF analysis. For NAD^+ measurement, ratio of intensities for m/z = 664 and 666 peaks, corresponding to ^{16}O- and ^{18}O-NAD^+ isotopomers, was multiplied by 2,00 nmol and then divided by tissue weight to determine NAD^+ concentration in the sample. For NAM the ratio of intensities for m/z = 123 and 125 peaks, corresponding to ^{16}O- and ^{18}O-NAM isotopomers, was multiplied by 2,00

nmol and then divided by tissue weight to determine NAM concentration in the sample. Corrections were applied for isotopic abundance.

Oxygen Consumption in Cultured Cells

Cellular O_2 consumption was measured using a Seahorse bioscience XF24 analyzer with thirty biological replicates per condition, in 24 well plates at 37°C, exactly as described (Canto et al., 2009). C2C12 were infected with an adenovirus encoding for FLAG-HA-PGC-1α and either scramble or SIRT1 shRNAs 48h previous to O_2 consumption measurements. Then myotubes were treated with 1 μM PJ34 for 48h.

Supplemental References

Bai, P., Houten, S.M., Huber, A., Schreiber, V., Watanabe, M., Kiss, B., de Murcia, G., Auwerx, J., and Menissier-de Murcia, J. (2007). Poly(ADP-ribose) polymerase-2 controls adipocyte differentiation and adipose tissue function through the regulation of the activity of the retinoid X receptor/peroxisome proliferator-activated receptor-gamma heterodimer. JBiolChem *282*, 37738-37746.

Chua, K.F., Mostoslavsky, R., Lombard, D.B., Pang, W.W., Saito, S., Franco, S., Kaushal, D., Cheng, H.L., Fischer, M.R., Stokes, N.*, et al.* (2005). Mammalian SIRT1 limits replicative life span in response to chronic genotoxic stress. Cell Metab *2*, 67-76.

Dali-Youcef, N., Mataki, C., Coste, A., Messaddeq, N., Giroud, S., Blanc, S., Koehl, C., Champy, M.F., Chambon, P., Fajas, L.*, et al.* (2007). Adipose tissue-specific inactivation of the retinoblastoma protein protects against diabesity because of increased energy expenditure. Proc Natl Acad Sci U S A *104*, 10703-10708.

Erdelyi, K., Bai, P., Kovacs, I., Szabo, E., Mocsar, G., Kakuk, A., Szabo, C., Gergely, P., and Virag, L. (2009). Dual role of poly(ADP-ribose) glycohydrolase in the regulation of cell death in oxidatively stressed A549 cells. Faseb J *23*, 3553-3563.

Feige, J.N., Lagouge, M., Canto, C., Strehle, A., Houten, S.M., Milne, J.C., Lambert, P.D., Mataki, C., Elliott, P.J., and Auwerx, J. (2008). Specific SIRT1 activation mimics low energy levels and protects against diet-induced metabolic disorders by enhancing fat oxidation. Cell Metab *8*, 347-358.

Lagouge, M., Argmann, C., Gerhart-Hines, Z., Meziane, H., Lerin, C., Daussin, F., Messadeq, N., Milne, J., Lambert, P., Elliott, P.*, et al.* (2006). Resveratrol Improves Mitochondrial Function and Protects against Metabolic Disease by Activating SIRT1 and PGC-1alpha. Cell *127*, 1109-1122.

Rodgers, J.T., Lerin, C., Haas, W., Gygi, S.P., Spiegelman, B.M., and Puigserver, P. (2005). Nutrient control of glucose homeostasis through a complex of PGC-1alpha and SIRT1. Nature *434*, 113-118.

Shah, R.G., Ghodgaonkar, M.M., Affar el, B., and Shah, G.M. (2005). DNA vector-based RNAi approach for stable depletion of poly(ADP-ribose) polymerase-1. Biochem Biophys Res Commun *331*, 167-174.

Watanabe, M., Houten, S.M., Mataki, C., Christoffolete, M.A., Kim, B.W., Sato, H., Messaddeq, N., Harney, J.W., Ezaki, O., Kodama, T.*, et al.* (2006). Bile acids induce energy expenditure by promoting intracellular thyroid hormone activation. Nature *439*, 484-489.